

KfK 3608  
November 1983

**GORGON — A Computer Code  
for the Calculation of  
Energy Deposition and the  
Slowing down of Ions in  
Cold Materials and  
Hot Dense Plasmas**

K. A. Long, N. Moritz, N. A. Tahir  
Institut für Neutronenphysik und Reaktortechnik

**Kernforschungszentrum Karlsruhe**



KERNFORSCHUNGSZENTRUM KARLSRUHE

Institut für Neutronenphysik und Reaktortechnik

KfK 3608

GORGON - A Computer Code for the Calculation of  
Energy Deposition and the Slowing down of Ions  
in Cold Materials and Hot Dense Plasmas.

K.A. Long, N.Moritz and N.A.Tahir

Kernforschungszentrum Karlsruhe GmbH, Karlsruhe

Als Manuskript vervielfältigt  
Für diesen Bericht behalten wir uns alle Rechte vor

Kernforschungszentrum Karlsruhe GmbH

## Abstract

The computer code GORGON, which calculates the energy deposition and slowing down of ions in cold materials and hot plasmas is described, and analyzed in this report. This code is in a state of continuous development but an intermediate stage has been reached where it is considered useful to document the "state of the art" at the present time. The GORGON code is an improved version of a code developed by Zinamon et al. as part of a more complex program system for studying the hydrodynamic motion of plane metal targets irradiated by intense beams of protons. The improvements made in the code were necessary to improve its usefulness for problems related to the design and burn of heavy ion beam driven inertial confinement fusion targets.

The report provides a description of what problems the code can solve and discusses the importance of the problem of energy loss of ions to various aspects of ion beam fusion. A review is given of the theory used in the code, relevant to the problem at hand, in particular discussing the Thomas Fermi theory of the state of high density plasmas and the slowing down of ions due to free and bound electrons using the dielectric function theory and the Bethe theory. The improvements made in the code and their importance are discussed in detail and the limitations and future improvements are also briefly discussed. The method of solution of the problem within the code is treated. Detailed descriptions of input data and output of the code are provided as well as a description of the subroutines and variables used in the code. An executed test problem is provided and described.

GORGON - ein Rechenprogramm zur Berechnung der Energiedeposition und der Ionenverlangsamung in kalten Werkstoffen und heißen, dichten Plasmen

---

### Kurzfassung

Im vorliegenden Bericht wird das Rechenprogramm GORGON beschrieben und analysiert, mit dem die Energiedeposition und Ionenverlangsamung in kalten Werkstoffen und heißen Plasmen berechnet werden können. Das Programm befindet sich im Zustand fortschreitender Entwicklung, jedoch ist nun eine Zwischenstufe erreicht, auf der es als nützlich erachtet wird, den derzeitigen Stand zu dokumentieren. Das Programm GORGON stellt eine verbesserte Version eines Rechenprogramms dar, das Zinamon et al. als Teil eines komplexeren Programmsystems entwickelt haben, um die hydrodynamische Bewegung ebener, mit starken Protonenstrahlen bestrahlter Metalltargets zu untersuchen. Die Programmverbesserungen waren erforderlich, um die Eignung des Programms bei der Lösung von Problemen in Zusammenhang mit der Auslegung und dem Abbrennen von Targets in Fusionsanlagen mit Trägheitseinschluß und Schwerionenstrahltriebwerk zu verbessern.

Der Bericht beschreibt, welche Probleme das Rechenprogramm lösen kann. Auch wird die Bedeutung des Problems des Ionenenergieverlusts in Bezug auf verschiedene Aspekte der Ionenstrahlfusion diskutiert. Der Bericht enthält einen Überblick über die im Rechenprogramm benutzte und auf das anstehende Problem bezogene Theorie und insbesondere eine Diskussion der Thomas-Fermi-Theorie des Zustands von Plasmen hoher Dichte und der Verlangsamung von Ionen infolge freier und gebundener Elektronen unter Verwendung der Theorie der dielektrischen Funktion und der Bethe-Theorie. Die Programmverbesserungen und ihre Bedeutung werden ausführlich diskutiert, und die Grenzen und künftige Verbesserungen werden ebenfalls kurz angesprochen. Die Lösungsmethode für das Problem im Rahmen des Rechenprogramms wird behandelt. Der Bericht enthält eine ausführliche Beschreibung der Eingabedaten und der Programmausgabe sowie eine Beschreibung der im Rechenprogramm benutzten Unterprogramme und Variablen. Der Bericht wird ergänzt durch eine ausgeführte Testaufgabe mit Beschreibung.

## Table of Contents

Page

1.	Introduction	5
2.	Problem definition, importance of the problem in ion beam inertial fusion and general theoretical considerations	8
3.	Calculation of the plasma parameters The Thomas Fermi theory	22
3.1	The high density plasma and its character- istic properties.	22
3.2	The free electron Fermi-Dirac gas.	24
3.3	Electron gas in the Coulomb field of the nucleus. The Thomas Fermi model.	25
3.4	A method suitable for numerical solution	27
3.5	Thermodynamic properties of the high density plasma.	30
4.	The stopping power of free electrons.	35
4.1	Derivation of a general formula for the stopping power of free electrons	35
4.2	The calculation and properties of the dielectric function for an interacting electron gas.	40
4.2.1	The Hartree-Fock method and the random phase approximation.	40
4.2.2	The linear response calculation of the dielectric function	45
4.2.3	The evaluation of the dielectric function at zero and finite temperatures.	51
	Properties of the plasma, screening, and plasmons in the dielectric function formalism.	
4.3	The dielectric function theory in the computer code GORGON	60
4.3.1	The dielectric function method for non-degenerate electrons.	60
4.3.2	The linearized Boltzmann-Vlasov equation	61

4.4	The calculation of the dielectric function when collisions are included. Theory with collisions, in the code.	62
4.5	Energy loss using the Thomas-Fermi model and the R.P.A. dielectric function method	64
5.	The stopping power of bound electrons: The Bethe Theory	66
5.1	Calculation of scattering cross sections of electrons and ions by atoms.	66
5.2	Energy loss of charged particles, scattered by atoms, and the Bethe formula.	71
5.3	The Bethe theory as used in the code. The evaluation of the Bethe parameter I.	78
6.	The stopping power due to ions.	81
6.1	Ion-Ion scattering in plasmas.	81
7.	Improvements made to the GORGON code at INR-KfK	84
7.1	Ion-ion scattering	
7.2	The stopping power of degenerate electrons.	87
7.3	The effective charge	89
7.4	Calculation of the range	90
7.5	Bohr minimum impact parameter	90
7.6	Improvements made to the Fortran programming and structure of the program	92
8.	User's and Programmer's Information.	93
8.1	Description of the code.	93
8.1.1	LATMA-INIT	93
8.1.2	DEDX	97
8.2	Version of the code using atomic physics other than the Thomas-Fermi model, DEC31.	103
8.3	Flow charts	109
8.4	Description of subroutines	113
9.	Results of a sample problem	115
9.1	Description of sample problem	115
9.2	Sample problem: Method of operation and physics input	116
9.3	Sample problem: Input for LATMA	118
9.4	Sample problem: Output for LATMA	119
9.5	Sample problem: Input and Output	122

9.6	Discussion of results of test problem	127
10.	Conclusions	129
11.	List of symbols used in report (not including FORTRAN variables used in code)	132
12.	References	142

## 1. Introduction

The GORGON code is designed to calculate the energy loss of any ion, heavy or light in a cold material or plasma of arbitrary density and temperature. The code solves the problem by calculating the basic plasma parameters within the Thomas-Fermi model and then using this solution to divide the electrons into bound and free electrons. The stopping power of the free electrons is then calculated using the dielectric function theory approach, while that due to the bound electrons is calculated using the Bethe theory including a novel approach to the inclusion of shell corrections. The Bethe I parameter which describes all the excitation and ionization processes of the bound electrons and averages their energy over the probability of their occurrence is calculated using the Thomas Fermi model. The scattering due to the charged nuclei is also calculated. The code includes a simple treatment for degenerate electrons, and a simple theory of the effective charge of the ion which is passing through the plasma. The code calculates the stopping power  $\rho^{-1} dE/dx$  as a function of the energy of the ion, and by an iterative procedure can calculate ranges. The main limitation of the code is probably its simple treatment of the effective charge. A more detailed calculation has been given recently / 3,4 / which shows that for light ions this can very drastically reduce the range in hot plasmas, in addition to the range shortening that is obtained using the GORGON code as it is described here. It is also necessary to give an improved treatment of the degeneracy of electrons and its effect on the stopping power especially for  $\alpha$ -particles in DT plasmas found in ICF pellets. There are also much more fundamental questions about the best theoretical treatment of dense plasmas and the way to treat the stopping power in such systems. For instance the inclusion of collisions in the dielectric function used for the stopping power of free electrons may be too simple. However this is a complicated problem on which research is still in progress.

Historically this problem was first treated by Chandrasekhar who used the methods of classical plasma physics to treat the problem of binary Coulomb collisions in the plasma / 5 /. Bohm and Pines / 6 / pointed out the importance of including plasmons in the calculation of the stopping power. This type of theory was used by Bangerter / 7 /, to first describe stopping power problems in ion beam driven inertial fusion. The work by Nardi, Peleg and Zinamon gave the first thorough /1/ discussion of the problem including a detailed treatment of ionization effects, a sophisticated first principles calculation of the Bethe parameter  $I$ , and a dielectric function theory treatment of the free electrons. Later Mehlhorn also treated /8,9/ the same problem. He included some new features such as using the LSS theory (Lindhard et al / 10 /) at low energies, including ion-ion scattering both in the cold material and in the fully ionized plasma. However a simple scaling relation was used for the calculation of  $I$ . The Zinamon theory was developed only for protons, and Mehlhorn included a "cold" effective charge in order to treat heavy and light ions. The improvements made to the GORGON code at KfK have included such effects and since the code is based on a firmer theoretical foundation, the GORGON code is as good as, if not better than any other presently existing code. Other calculations have been done by More / 11 / He discusses the application of two methods. In the first the dielectric function theory is used for both bound and free electrons in the whole Thomas-Fermi pseudoatom, by averaging the finite temperature R.P.A. approximation to the dielectric function over the electron density. In this case the Thomas-Fermi-Dirac theory is used. It is however doubtful if there is much difference between this approach and the approach made in the GORGON code. The approach for the free electrons is the same, and since for high ion velocities the dielectric theory can be shown to be identical / 12 / to the Bethe theory, and since  $I$  is calculated by the Thomas Fermi theory in the GORGON code, the only difference seems to lie in the way one averages over the electron density. The second approach uses the hydrogenic ionization equilibrium model to provide detailed populations and energy levels for the target plasma / 11 /. The Bethe  $I$  is then calculated from this data using the definition of  $I$ , and the rest of the calculation

(presumably) proceeds as in the GORGON code.

The organization of the rest of this report is as follows. In section 2-6 the theory of stopping power relevant directly to the code is discussed. Section 2 gives a more extensive discussion of the problem, applications, and the importance of the problem for ion beam inertial fusion. In Section 3 a description of the Thomas-Fermi theory is given, which is used in the code to calculate the basic plasma parameters. In Section 4, a discussion of the dielectric function theory of the stopping power is given, and the theory used in the code is discussed. In 5 the stopping power of bound electrons is reviewed and the method of calculation of the Bethe I parameter is described. In Section 6 the treatment of the stopping power of ions used in the code is briefly described.

In Section 7 the improvements made to the original version of the code / 2 / made at KfK are described. Section 8 gives the User's and Programmer's Information. Section 9 gives an executed test problem and discusses a few typical results obtained with the code. Section 10 discusses the desirable future improvements which are intended to be made to the GORGON code and describes the conclusions drawn from this work.

## 2. Problem Definition, Importance of the problem in Ion Beam Inertial Fusion and general theoretical considerations

The problem of the energy loss of fast particles in matter has occupied the minds of some of this century's best physicists, Thompson / 13 /, Rutherford / 14 /, Bohr /15,16/, Bethe / 17,18/, Mott / 19 /, Bloch / 20/, Fermi / 21 / and Landau / 22/. In fact the theoretical and experimental investigation of this problem has played a very important part in the development of modern physics. The distinction between large and small angle Coulomb scattering led to the discovery of the nuclear atom. The way in which  $\alpha$  and  $\beta$  rays slowed down in matter allowed their identification as fully ionized Helium and energetic electrons. Particle track detectors have been responsible for the discovery of most known elementary particles. Many different fields such as astrophysics, nuclear physics, atomic physics, molecular physics, biophysics and many others rely on a good theoretical and experimental knowledge of the slowing down of charged particles in matter.

The problem of the stopping power of ions in matter is also very important in a number of research and development programmes. For instance it plays a significant role in the development and application of heavy ion beam accelerators / 14 /, the interpretation of cosmic ray results / 14/, and as a means of treating cancer / 14 /. Recently another very exciting application has been discovered in heavy and light ion beam inertial confinement fusion /20, 23, 24, 25, 26, 28/ which is discussed in more detail below.

The computer program GORGON described here, calculates the stopping power of any given ion with any charge state in a cold material or hot plasma over the very considerable ranges of temperature and density, which are of importance for ion beam driven inertial confinement fusion. The problem of the stopping power in cold materials has been studied very extensively since 1903, but the problem of the slowing down in hot plasmas has not been

studied until recently. A similar problem was treated by Chandrasekhar in connection with problems in astrophysics /5/, by the conventional theory of gravitational scattering. However the problem of the slowing down of ions in very dense hot plasmas is relatively new and has only assumed importance since the advent of ion beam driven Inertial fusion. These effects were first discussed by Bangerter /7/. Zinamon et al. gave the first thorough discussion of the problem for protons /1/.

The GORGON code was written in its original form by Nardi, Peleg and Zinamon, and is based on the work done for protons. Some extensions and improvements have been made at the Institute for Neutron Physics and Reactor Technology at the Nuclear Research Centre, Karlsruhe, in order to facilitate the codes use in pellet design for heavy and light ion beam fusion. Since the theory in the code is thoroughly discussed in this report we very briefly describe the model. The theory used by Nardi, Peleg and Zinamon divides the electrons in the plasma into free and bound electrons as calculated using the Thomas Fermi model. The contribution of the free electrons is then calculated using the dielectric function theory and that of the bound electrons using the Bethe theory. The basic plasma parameters are calculated using the Thomas Fermi model.

More recently Mehlhorn has also treated this problem /8,9/. His approach is to use the Bethe theory including shell corrections for the stopping power of the bound electrons. At lower energies where this version of the Bethe theory breaks down it is replaced by the LSS theory developed by Linhard and his group /10/. This makes use of a Thomas-Fermi description of the electron cloud around each ion and gives contributions to the stopping power due not only the excitation and ionization, but also due to elastic Coulomb collisions of the ion and the nucleus of the target atom. A suitable empirical formula for the effective charge on the ion is used. At finite temperature the Saha equation is used to find the equilibrium charge  $Z_B$  of the target material as a function of temperature and density. A scaling relation depending on  $Z_B^2$  is used to calculate the value of I. This model is clearly rather crude.

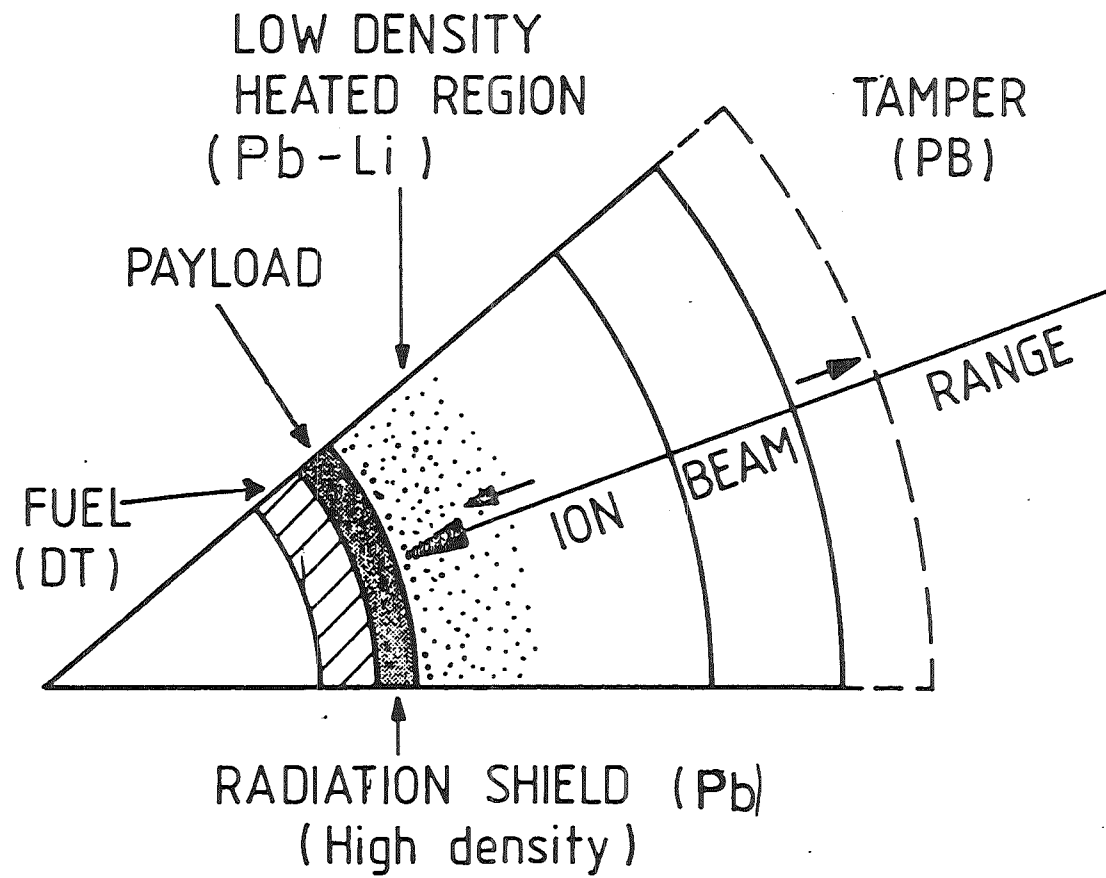


Fig.1 :Target in its imploding configuration.

An empirical formula derived for cold materials is used for the effective charge  $Z_{\text{eff}}$  on the ion as it passes through the plasma /29 /. The velocity is taken as the square root of the sum of the ion velocity squared plus the thermal electron velocity squared. This raises the value of  $Z_{\text{eff}}$  especially at lower energies in hot plasmas. It simulates the greater degree of collisional ionization. The modification occurs mostly at lower energies. A dielectric function theory was used for the free electrons as described in section /4.3 /, and was compared to a theory in which binary collisions and collective plasma wave excitation outside the Debye radius was applied. The latter theory is actually used in the code for both the electron and ion plasma contribution to the stopping power. The possibility of Debye shielding of the remaining bound electrons by the plasma electrons is also considered in Mehlhorn's code. The theory used by Moore /11/ is described elsewhere in this report so will not be considered again here (4.5).

We will now consider in detail the problem of the importance of ion beam energy deposition for ion beam driven inertial confinement fusion. From cold stopping power data it was recognized that / 7 / MeV protons or GEV heavy ions would have the "correct" range needed to drive typical size ICF targets. The ranges of such ions is of the order of  $3 \cdot 10^{-2}$  cms, i.e. less than 1 mm in normal uncompressed matter, e.g. lead. It was also realized that one can tailor ionic species, accelerator voltage, mass etc. to the problem at hand. Heavy ions can naturally carry much more energy/ion than light ions, because the stopping power of heavy ions is much greater since the effective charge is much larger and the energy deposition is proportional to  $Z_{\text{eff}}^2 M$  (where M is the mass of the ion), when the velocity of the ion is greater than the thermal electron velocity. Further the energy loss of both heavy and light ions is expected to be classical and not to involve that because of the highly collisional nature of the plasma, for instance, two stream instability is not likely to occur.

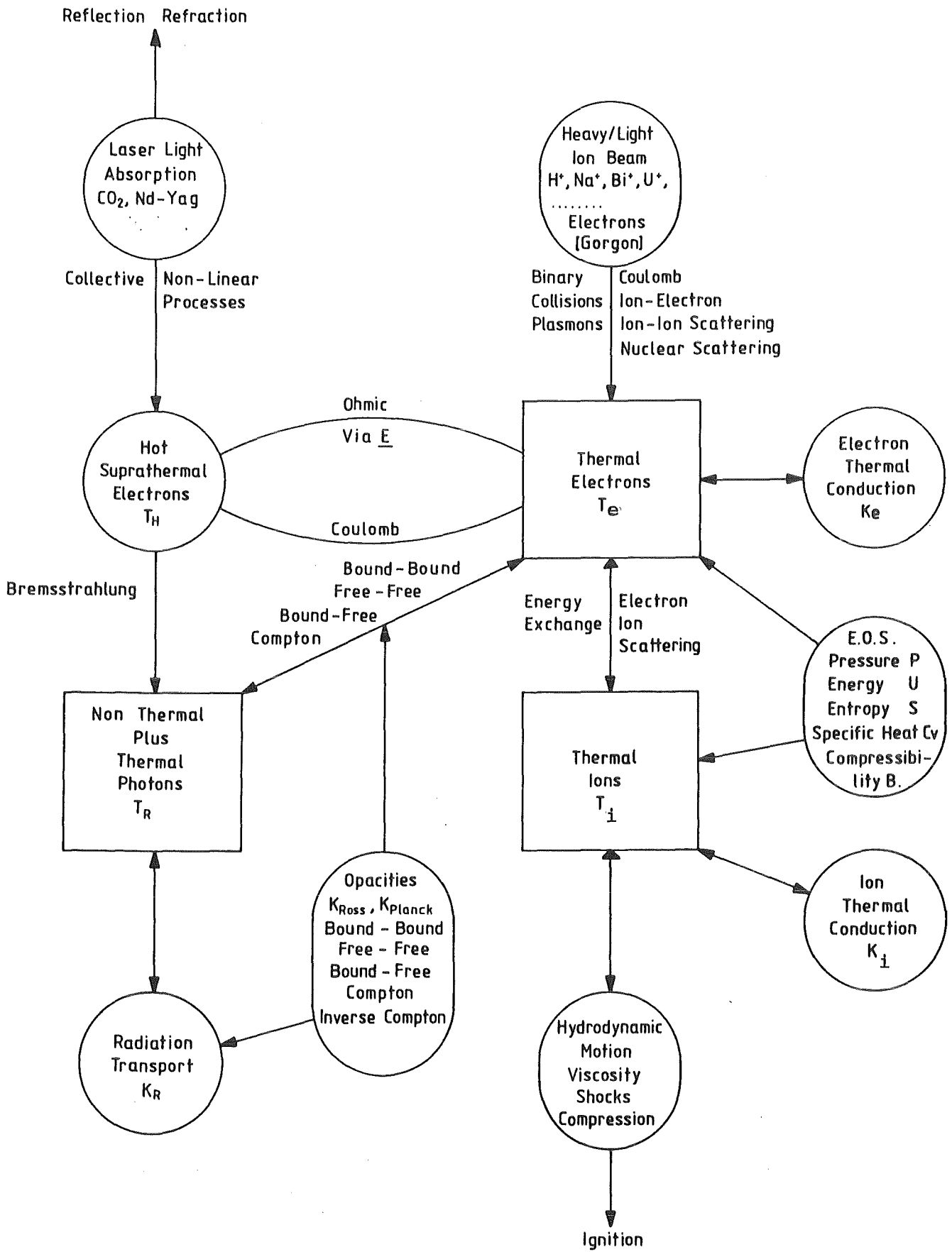


Fig.2 The important physical processes in the implosion phase of ICF Targets.

This is because a plasma wave is damped out by collisions before another ion passes the point where the plasma wave was generated. A good and accurate knowledge of energy deposition of ions in hot plasmas and cold materials is necessary in order to optimize beam generation, calculate target beam coupling efficiencies and to design targets in general. It is also very important in the interpretation of experiments. For coupling into a hydrodynamic code, the energy deposition routine must naturally be not too time consuming.

The type of ion beam target used in the HIBALL reactor /26,2,33,34/ study is shown in Fig.1. This target works in the following way Fig. 2,3. 10 GeV  $\text{Bi}^+$  ions impinge on the outside surface of the lead shell, and because of their high energy they pass through the lead shell, heating it up as they go by binary collisions, and excitation of plasma waves, and go deep into the lithium shell Fig.3. The energy deposition per gm of material by the beam is roughly the same in the lead as in the lithium region but the specific heat/gm of the lithium region is about 5x smaller than the lead region because ionization effects are much more dominant in the lead. The temperature in the lead rises to about 100 eV and that in the lithium to about 500 eV. It should be noted as the lead and lithium plasmas heat up the range of the ions shortens Figs.3 4 and 5. This effect is about 30% of the cold range or about 50% of the hot range (Figs. 4+5). An increase of the ion energy during the course of the implosion or the effect of radiation transport could compensate for this effect. If this is not done then the beam fuel target efficiency may drop to too low a level and ignition will not be achieved /30/. It is therefore very important to be able to accurately calculate this range shortening effect /3/. If the ionization of the ion by electron collisions in the hot plasma is included range shortening is likely to be an even more drastic phenomena , especially for light ions, than that calculated using this code /3, 4/. At the end of the ion beam range the lithium for  $R < R_0$  (where  $R_0$  is the range) is very hot and the lithium-lead beyond the end of the range  $R > R_0$ , is very cold. Hence the thermal pressure of the electrons and ions plus the radiation pressure pushes the shell of cold lithium-lead plus DT (payload)

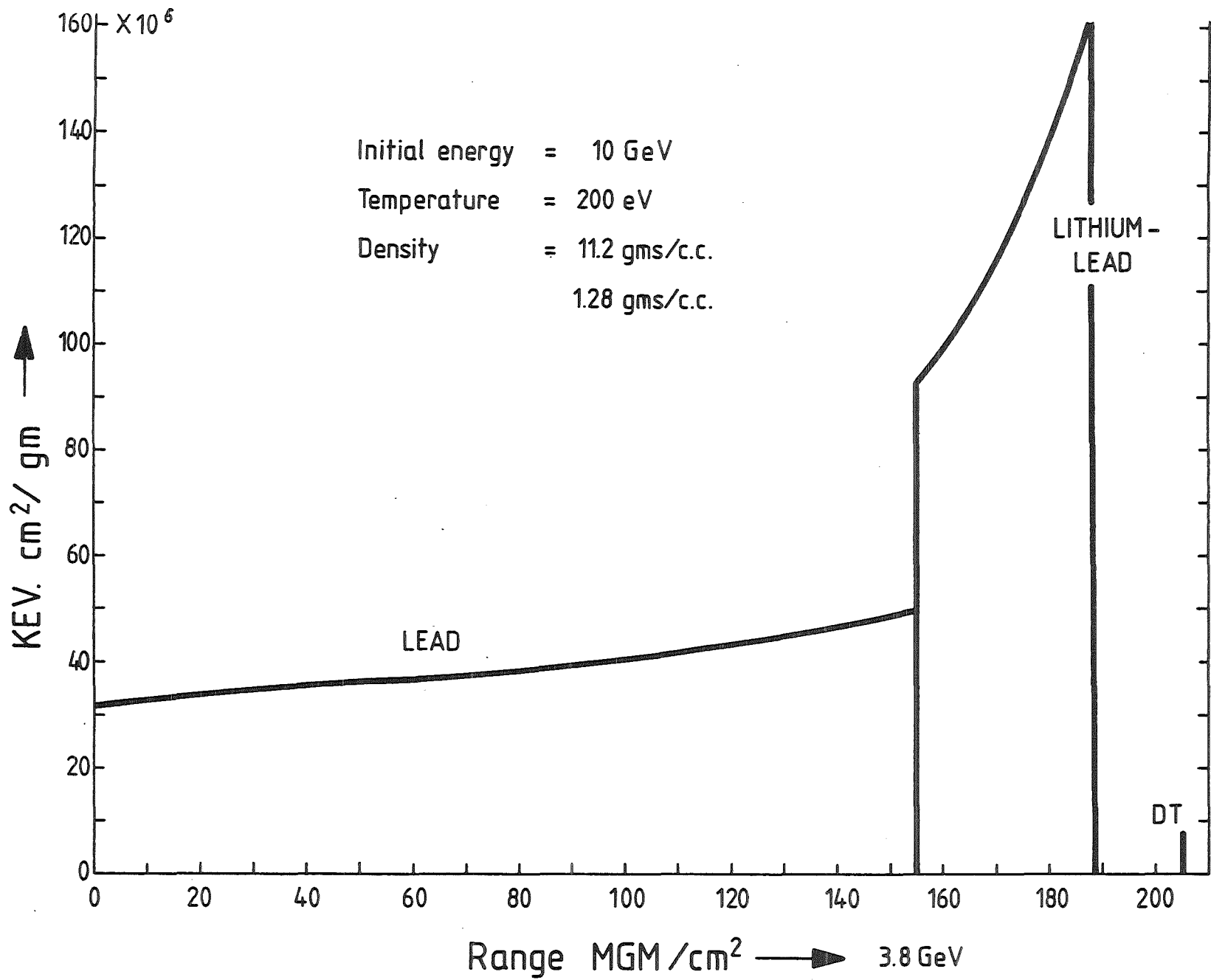


Fig. 3: Bismuth ions on lead and lithium - lead

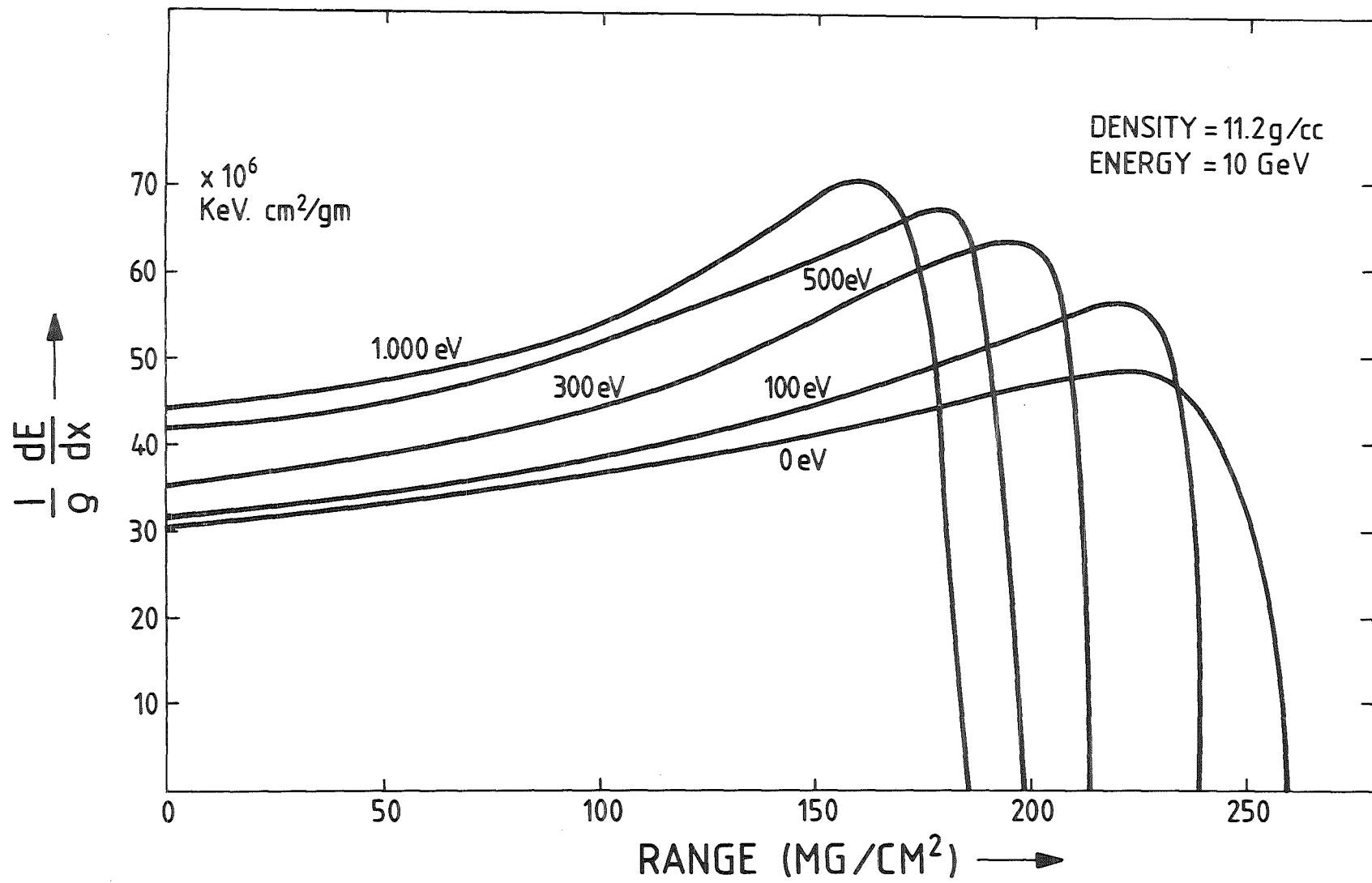
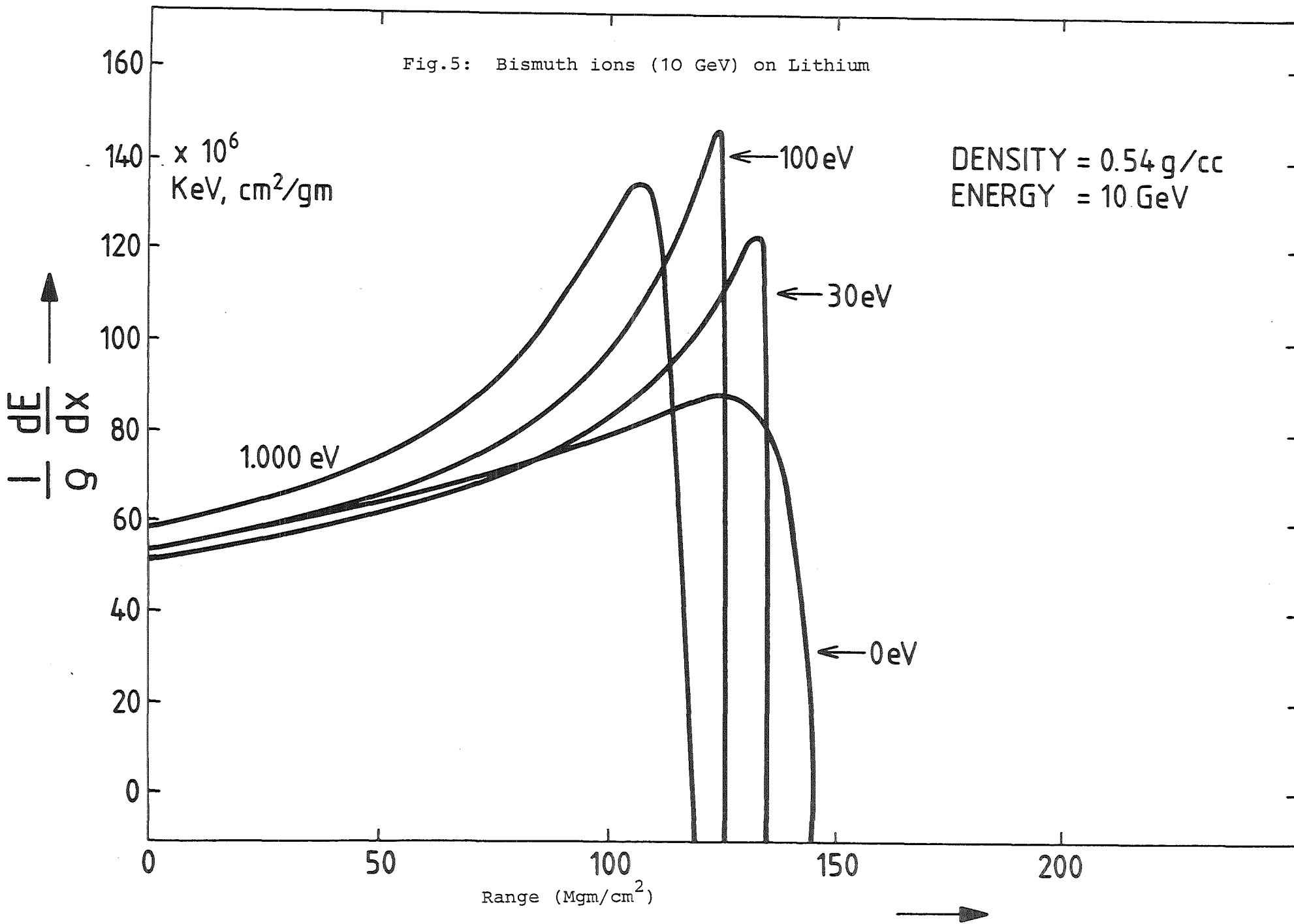


Fig.4: ENERGY LOSS OF BISMUTH IONS IN LEAD

Fig.5: Bismuth ions (10 GeV) on Lithium



inwards while the lead shell moves outwards. The payload part of the shell is the part imploded to ignition. The lead-lithium layer needs to be thick enough to reduce radiation preheat to a minimum (i.e. at least to prevent the Marshak wave reaching the fuel) and to prevent the break up of the shell by Rayleigh-Taylor instabilities. Here another problem arises for which energy deposition calculations are needed. Elastic collisions will occur between the heavy Bismuth ions and <sup>32</sup>/the light lithium ions. This will cause "knock on" Lithium ions with a spectrum of energies less than the remaining energy of the incoming ion. Since  $dE/dX$  is proportional to  $Z_{eff}^2 M$ , the stopping power of the lithium ions is considerably less than the Bi ions of equivalent-energy. Therefore these knock-on lithium ions may have enough energy to penetrate into the fuel pre-heating it and thus degrading the compression and possibly hindering ignition. It should be noted that in the outer layers densities from  $\rho_0$  (solid density) to  $\rho_0/100$  and temperatures from zero to 1 KeV are achieved and the code must at least work in these ranges. Energy deposition calculations are also of great importance during the burn of ICF targets, Figs. 6, 7 and 8. The  $\alpha$ -particles play a crucial role during the ignition phase and dominate the phenomenon of burn propagation. In central ignition only a small central region of the fuel is shock heated to ignition while the rest of the fuel is kept cold on a low adiabat<sup>2,33,34/</sup>. In order for the burn to propagate more energy must be redeposited in the hot spot then is lost by Bremsstrahlung radiation <sup>34,35,33,30,60/</sup>. When the range of the  $\alpha$ -particles is equal to the radius of the sphere about 40% of the energy escapes the burning region. It is this escaping energy which sets the burn propagation on its way. In fact the burn propagation is a self-regulating phenomenon in which if the DT gets too hot, too much  $\alpha$ -particle energy escapes so it cools, whereas if it gets too cool, the range becomes so short that little  $\alpha$ -particle energy escapes so that it heats up again. Therefore both the temperature of the burn and the rate of burn propagation is strongly influenced by  $\alpha$ -particle energy deposition in the DT plasma. The rate of burn

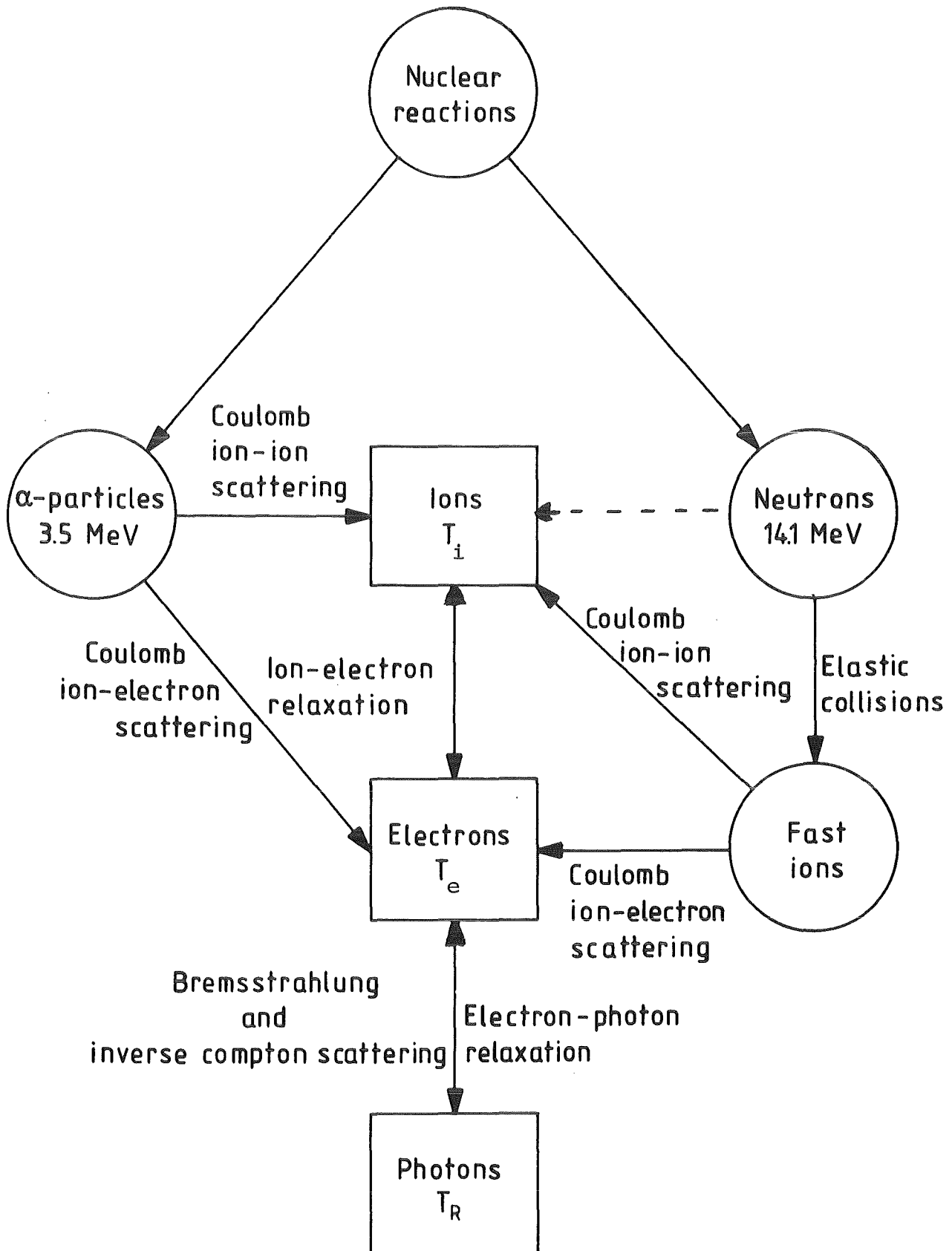


Fig.6:

The important physical processes in the burn of an ICF pellet.

propagation is of course given by the flux of  $\alpha$ -particles coming out of the burning region, their residual energy and the range over which this is deposited. The  $\alpha$ -particle  $dE/dX$  and range are strongly dependent on the temperature. Deposition is to both ions and electrons with a cross over temperature of about 20 KeV. Above this temperature energy loss to ions is dominant, below this energy loss to electrons is dominant. Another interesting place where energy deposition calculations become very important is in the calculation of energy deposition of "knock-on" neutron induced, fast ions, during the burn. Neutrons are born during the nuclear reactions and these have a m.f.p. till the first collision of  $\rho R = 4.75 \text{ g/cm}^2$ , i.e.  $\lambda = \frac{4.75}{\rho} \text{ cms} / 36 /$ . These neutrons collide with  $D^+$  and  $T^+$  ions and because of the spin part of the interaction, the "elastic" scattering is anisotropic /36/. These  $D^+$  and  $T^+$  ions then lose energy in the DT plasma. Because their velocity is less than the thermal electron velocity  $dE/dX \propto \frac{\sqrt{E}}{\sqrt{M}} \cdot Z_{\text{eff}}^2$  where  $M$  is the mass of the  $D^+, T^+$  ion and  $E$  their energy. Scattering to the ions goes as  $dE/dX \propto (M/E) \cdot Z_{\text{eff}}^2$ . Ion scattering is hence much more reduced from the  $\alpha$ -particle case than loss of energy to electrons. Therefore the cross over temperature is much greater. Therefore these ions also have much longer ranges than the  $\alpha$ -particles. Therefore besides  $\alpha$ -particle energy deposition and neutron transport, the transport and energy deposition of neutron induced knock-on  $D^+$  and  $T^+$  ions should be considered. Finally it should be noted in this section that first experiments indicate a confirmation of range shortening of deuterons in hot plasmas /38/.

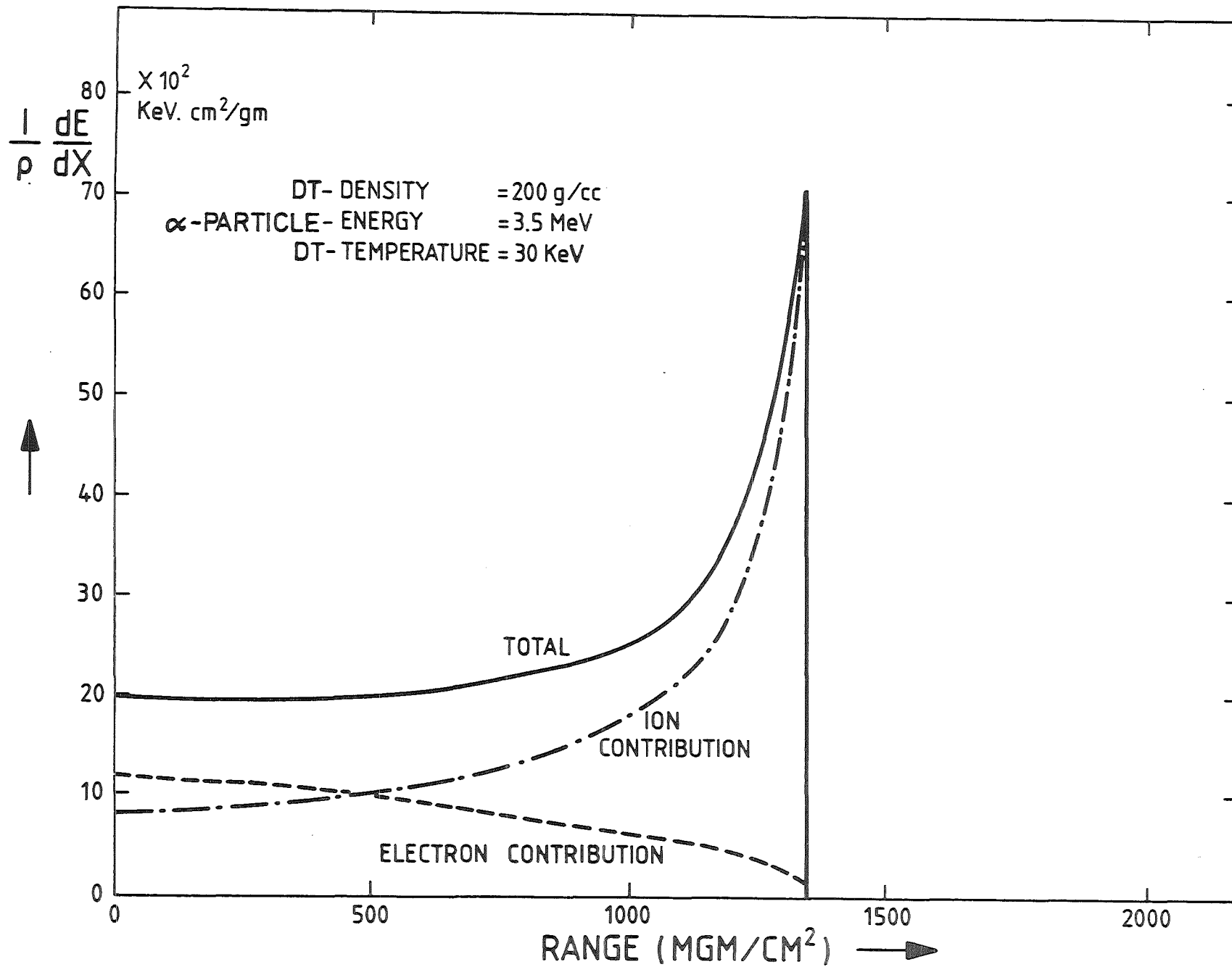


Fig. 7 : SLOWING DOWN OF α-PARTICLES IN DT AT 30 KeV

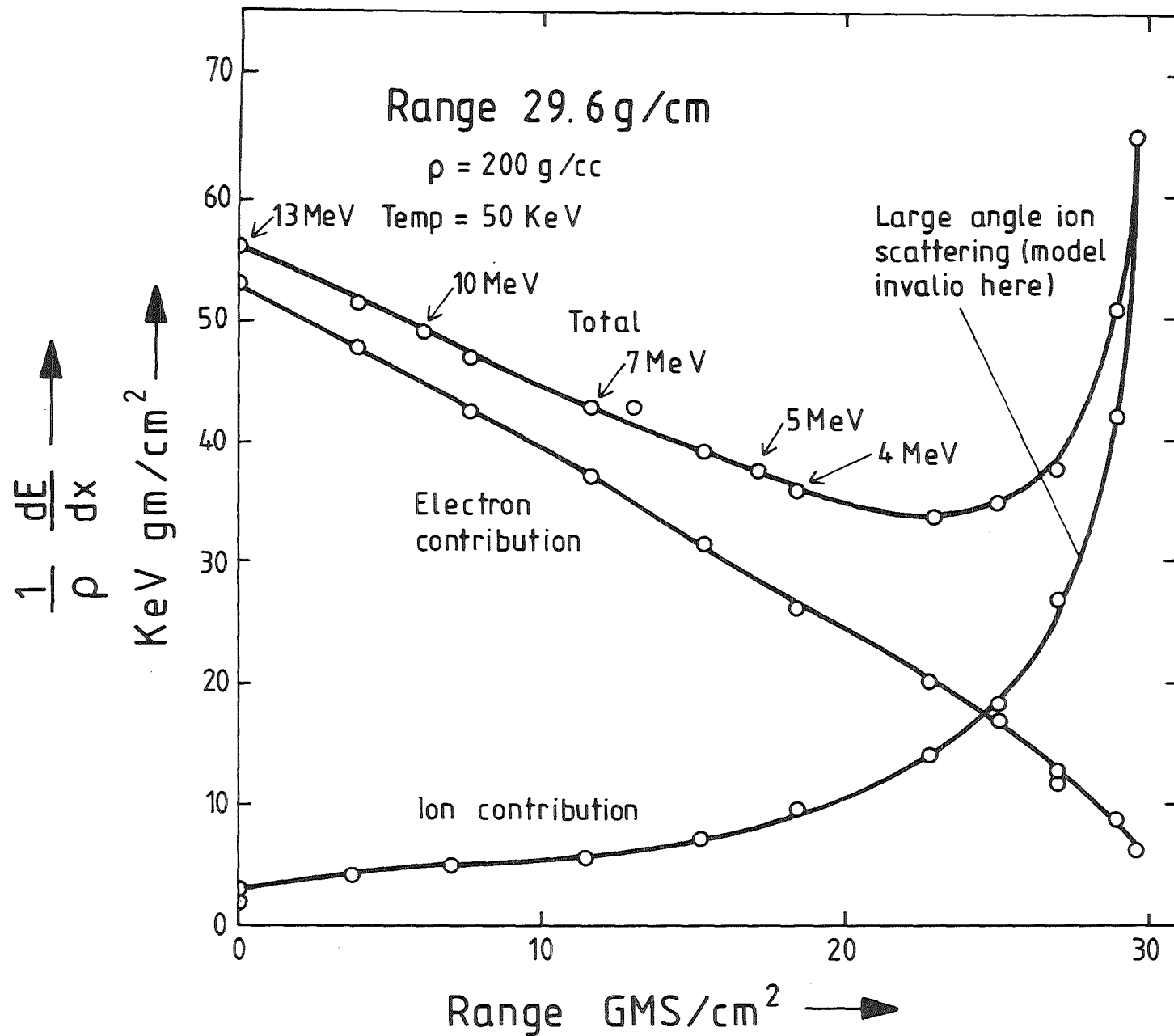


FIG. 8: D<sup>+</sup> Ion (13MeV) slowing down in a DT plasma. D<sup>+</sup> is neutron induced fast ion

3. Calculation of the Plasma Parameters  
The Thomas-Fermi theory

3.1 The high density plasma and its characteristic properties.

When a plasma is in a highly compressed state due to say a very high pressure, such that the average separation between the ions is of the same order or less than the atomic radii, then one has a high density plasma. This kind of plasma can not be treated by the methods used in classical plasma theory which often assumes point particles and that one can neglect the Coulomb interaction energy. In these high density plasmas the Saha equation is not applicable and the equation of state is very different from that of a classical plasma.

It is known experimentally that as the pressure rises the ionization potential is lowered and the lines of the atomic spectra are broadened. In general the line spectrum of a plasma becomes very similar to a continuum spectrum as for energy bands in metals. This means that the outer bound electrons and even deep core levels become very similar to free electrons as the pressure rises. In effect one has a cascade of insulator-metal transitions for all the shells in the atoms /39/. In a high density plasma it is thus somewhat questionable as to whether one should distinguish between free and bound electrons. The actual distinction used in the code within the Thomas Fermi model is of a somewhat technical nature. An exact calculation of the electron distribution as a solution of the quantum mechanical many body problem is from a practical point of view not possible. Therefore it is unfortunately necessary to use simpler models. Since one has already noticed that the distinction between free electrons, valence electrons, and bound electrons is in the case of high pressure somewhat hazy, one usually only distinguishes between ions and electrons. The totality of the electrons

is then treated as a statistical Fermi gas system moving in the field of the nucleus, including the Coulomb interaction energy, the exchange energy, and the correlation energy between the electrons. The Thomas Fermi model of the atom is such a model and in spite of it neglecting the details of the atomic shell structure is a suitable approximation for material under high pressure / 40 /.

The electron density of the electrons is very large in the region of the nuclei. Therefore here the electrons are strongly degenerate. Further away from the nucleus the degree of degeneracy is reduced. Each ion or nucleus is surrounded by an electron cloud and is therefore strongly screened from its neighbouring ions. The ions on the other hand are considered to be non-degenerate and to be treatable as an ideal gas.

The electron distribution is the same around each nucleus apart from statistical fluctuations. One can therefore define a quasiatom which consists of a nucleus plus a surrounding cloud of  $Z$  electrons. On average such a quasi-atom has a volume given by,

$$v = \frac{1}{\bar{n}} \quad ( 3.1 )$$

where  $\bar{n}$  is the nuclei density. Regarding this volume as being a sphere one defines,

$$r_0 = \left( \frac{3}{4\pi} \frac{1}{\bar{n}} \right)^{1/3} \quad ( 3.2 )$$

More exact calculations using an extended Debye-Hückel theory which includes the effect of the thermal transport of ions and electrons on the charge distribution have confirmed the validity of this model. In particular it has been shown that at the radius  $r_0$ , the electrical potential is more or less zero. This means that within a sphere of radius  $r_0$  one really does find  $Z$  electrons.

The material of a high density plasma can be considered to consist of such quasiatoms with a continuous electron density within them. The quasiatoms are always in contact with each other, whereas the ions move within the plasma. This type of model has many similarities to a fluid, in that the motion of the

individual quasiatoms are highly correlated, i.e. the structure factor for the ions contains oscillations .

### 3.2 The free electron Fermi-Dirac gas

In very dense material, the contribution of the electrons to the total pressure and energy is much greater than that of the nuclei. There are two reasons for this namely firstly that the electrons are degenerate with energy/electron  $\sim \frac{3}{5} E_F$ , and secondly in the case of high Z materials that the number of electrons is much greater than that of the nuclei. To fix notation we give briefly here the solution to the Fermi-Dirac electron gas, for N electrons on a volume V. The Fermi-Dirac distribution function is given by,

$$f(\epsilon) = \frac{1}{(\exp((\epsilon - \mu)/kT) + 1)} \quad (3.3)$$

where  $\epsilon$  is the electron energy,  $\mu$  is the chemical potential and T is the temperature.

$$N = \int f(\epsilon) \cdot 2 \frac{d\bar{\tau}}{h^3} \quad U_E = \int \epsilon f(\epsilon) \cdot 2 \frac{d\bar{\tau}}{h^3} \quad (3.4)$$

where  $U_E$  is the total electron energy and where the integral is taken over phase space (momentum).

Each electron of one spin occupies a volume of  $h^3$  in momentum space.

Two electrons of opposite spin can occupy this volume.

In a large volume with no interactions,  $\epsilon = P^2/2m$ .

$$\frac{N}{V} = n_E = \frac{[2\pi mkT]^{3/2}}{h^3} \chi'(\alpha) \quad (3.5)$$

$$U_{E/V} = \frac{3}{2} \frac{kT}{h^2} \left( \frac{2\pi mkT}{h^2} \right)^{3/2} \chi(\alpha) \quad (3.6)$$

where  $\alpha = \mu/kT$ , and

$$\chi(\alpha) = \frac{4}{\sqrt{\pi}} \int_0^{\infty} \log(1+e^{-t+\alpha}) \sqrt{t} \cdot dt \quad (3.7)$$

$$\chi'(\alpha) = \frac{d\chi}{d\alpha} = \frac{4}{\sqrt{\pi}} \int_0^{\infty} \frac{\sqrt{t}}{(e^{t-\alpha} + 1)} dt \quad (3.8)$$

### 3.3 Electron gas in the Coulomb field of the nucleus.

#### The Thomas-Fermi model

For a much better calculation of the state of a high density plasma, one must (at least) include the electric field of the nucleus and the electrons. For high Z materials one should also include relativistic effects, and one should include exchange and quantum corrections / 41 /. This is not done here however where we consider the basic Thomas-Fermi theory. Under the action of the electrostatic field the electrons and nuclei order themselves in the form as quasiatoms as discussed above.

These are the building bricks so to say of the very high density plasma. The problem of the state of the plasma is thereby reduced to the calculation of the thermodynamic properties of one quasiatom.

Let the origin of the co-ordinate system lie at the centre of the quasiatom, i.e. where the nucleus is. Then,

$$Z = 4\pi \int_0^{r_0} n_E(r) \cdot r^2 \cdot dr \quad (3.9)$$

where  $r_0$  is the radius of the quasiatom.

The potential  $\psi$  inside the quasiatom consists of two parts namely the electron and nuclear contributions.

$$\psi(r) = \psi_E(r) + \psi_N(r) \quad (3.10)$$

$$\psi_N(r) = Ze/r \quad (3.11)$$

The Poisson equation then reads,

$$\nabla^2 \psi(r) = 4\pi e n_E(r) \quad (3.12)$$

For  $r \rightarrow 0$  the nuclear potential dominates,

$$\lim_{r \rightarrow 0} (r \cdot \psi(r)) = Z \cdot e \quad (3.13)$$

This gives one boundary condition.

At  $r = r_0$  on the boundary of the quasiatom, the electric field and potential must vanish ,

$$\psi'(r_0) = 0 , \quad \psi(r_0) = 0 \quad (3.14)$$

In the electron distribution function  $f(\epsilon)$ , one must now include in  $\epsilon$  a potential energy part,

$$\epsilon = p^2/2m - e \cdot \psi(r) \quad (3.15)$$

Since,

$$n_E(r) = \frac{(2\pi mkT)^{3/2}}{h^3} \chi'(\sigma) \quad (3.16)$$

where one applies the Fermi-Dirac theory to a shell of volume  $\Delta V$  containing  $\Delta N$  electrons at radius  $r$ , where

$$\sigma(r) = \alpha + e/kT \psi(r) \quad (3.17)$$

Combining this with Poisson's equation (3.12), one obtains,

$$1/r^2 \frac{d}{dr} \left( r^2 \cdot \frac{d\psi}{dr} \right) = 4\pi e \left( \frac{2\pi mkT}{h^3} \right)^{3/2} \chi'(\sigma) \quad (3.18)$$

This is the generalized Thomas-Fermi differential equation for the potential  $\psi(r)$ . Once  $\psi(r)$  is determined one can find  $n_E(r)$  from Poisson's equation. Note that the chemical potential  $\mu = \alpha kT$  is found from the value of  $\sigma(r)$  at  $r = r_0$  where  $\psi(r_0) = 0$ .

The solution is found from the differential equation after subjecting it to several transformations by integrating outwards from  $r = 0$ , using the boundary condition at  $r = 0$ , and using trial and error until the boundary condition at  $r = r_0$  is satisfied / 40 /. In the code the method of Latter is used / 42 / which first converts the differential equation to an integral equation and solves this by an iterative procedure.

### 3.4 A method suitable for numerical solution.

Starting from eqn. ( 3.18 ) we change variables,

$$r = \lambda \zeta \quad , \quad \lambda = \lambda(T) = \frac{1}{2\pi e} \left( \frac{h^6}{8\pi m^3 kT} \right)^{1/4} \quad ( 3.19 )$$

and use  $\sigma(\zeta)$  instead of  $\psi(\zeta)$ .

Then we get,

$$\frac{1}{\zeta^2} \frac{d}{d\zeta} \cdot ( \zeta^2 \frac{d\sigma}{d\zeta} ) = \chi'(\sigma) \quad ( 3.20 )$$

The boundary conditions now read

$$\lim_{\zeta \rightarrow 0} \{ \zeta \cdot \sigma(\zeta) \} = K \quad ( 3.21 )$$

$$K(T) = \frac{ze^2}{\lambda kT} \quad ( 3.22 )$$

At the position  $\zeta = \zeta_0 = r_0/\lambda$ , one obtains from ( 3.14) and ( 3.17)

$$\sigma'(\zeta_0) = 0 \quad \sigma(\zeta_0) = \alpha \quad ( 3.23 )$$

Note that

$$\lambda = 1.4 \cdot 10^{-7} T^{-1/4} \quad (\text{cm}) \quad ( 3.24 )$$

$$K = 1.19 \cdot 10^4 \cdot \frac{z}{T^{3/4}} \quad ( 3.25 )$$

where  $T$  is measured in Kelvin.

The function  $\sigma(\zeta)$  is singular at  $\zeta=0$ , so one puts,

$$Y(\zeta) = \zeta \cdot \sigma(\zeta) \quad (3.26)$$

Then,

$$Y'' = \zeta \cdot \chi' \left( \frac{Y}{\zeta} \right) \quad (3.27)$$

$$Y(0) = K, \quad Y'(\zeta_0) = Y(\zeta_0)/\zeta_0 \quad (3.28)$$

$$Y(\zeta_0) = \alpha \zeta_0 \quad (3.29)$$

$$Y'(\zeta_0) = \alpha \quad (3.30)$$

The boundary value problem posed by eqns. (3.27) and (3.30) can, for fixed  $Z$  and given values of  $\zeta_0$  ( $r_0$ ) and  $K(T)$  be solved uniquely. Physically this means that the potential in the inner atom of high density material can be uniquely determined from just the temperature and the density.

A thorough discussion of the differential equation (3.18) would show that each solution  $\sigma(\zeta)$  starting from  $\zeta=0$ , decreases monotonically at first and at a point  $\zeta_0$  reaches a minimum such that  $\sigma'(\zeta_0) = 0$ , and then monotonically increases. It is therefore certain that for a region  $0 \leq \zeta \leq \zeta_0$  the formulated boundary value problem (3.20) to (3.22) or (3.27) to (3.30) always possesses a solution.

In Fig. 9 a schematic diagram is presented of typical solution curves for  $\sigma(\zeta)$  and  $Y(\zeta)/40$ . The boundary value  $Y(0) = K$  is then chosen to be the same for all the curves. For a given value of  $Z$ , the temperatures for all the curves are the same, so that the atomic radius  $r_0$  or equivalently the particle density  $\bar{n}$  is the parameter which labels the curves. The solutions have a physical meaning only in the region  $0 \leq \zeta \leq \zeta_0$ , i.e. left of the minimum of the function  $\sigma(\zeta)$ . The solutions lie above the axis for small  $\zeta_0$ , and below for large  $\zeta_0$ . Since  $\sigma(\zeta)$  is a measure of the local degree of degeneracy of the electrons, this shows that at large densities strong degeneracy is present, and that at low densities there is weak degeneracy.

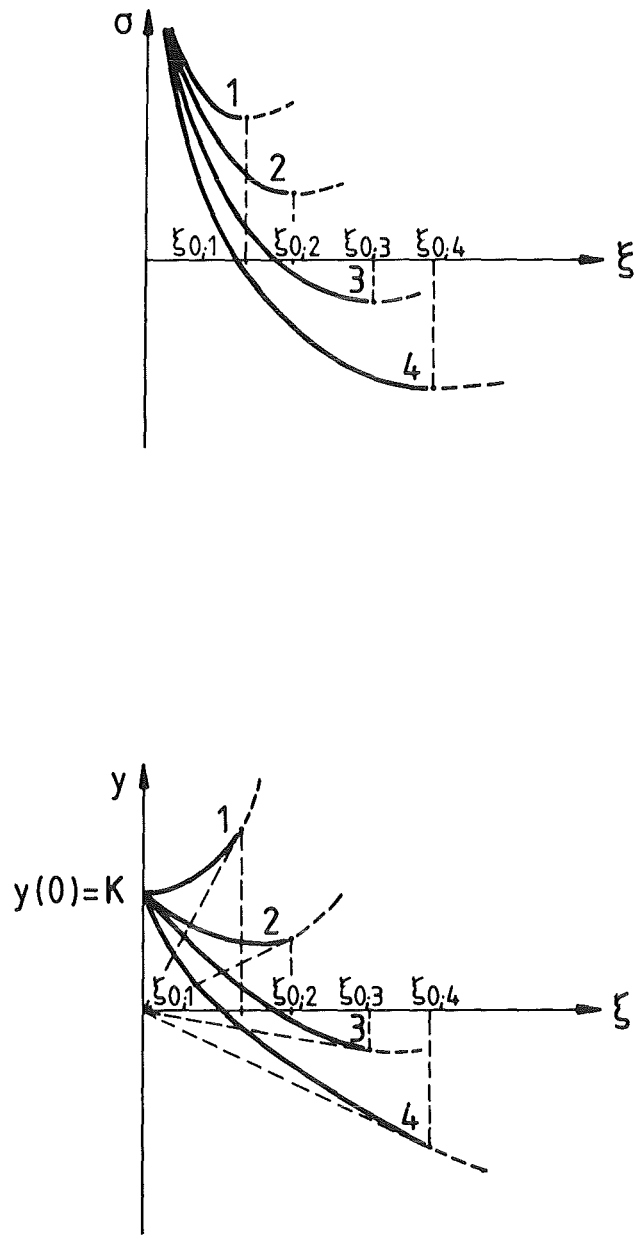


Fig. 9: Types of solutions of the functions  $\sigma(\xi)$  and  $y(\xi)$  for the initial value  $y(0)=K$ . Curves 1 and 2 show strong degeneracy, whereas curves 3 and 4 show weak degeneracy.

The boundary value problem defined by equations (3.27) and (3.28) for the function  $Y(\zeta)$  can be solved as an initial value problem, which significantly reduces the amount of computation / 40 /. In order to integrate (3.27) one starts from  $\zeta=0$  with the boundary value  $Y(0) = K$ , whereas the gradient  $Y'(0)$  is chosen arbitrarily at first. Since  $Y''$  can be seen to be infinite at  $\zeta=0$ , by eqns. (3.27), (3.28), and  $\chi'(\alpha) \sim \alpha^{3/2}$  as  $\alpha \rightarrow \infty$  (3.31) the numerical integration can only be started at a point  $\zeta^* > 0$ . In the interval  $0 \leq \zeta \leq \zeta^*$ ,  $Y(\zeta)$  can be expressed for sufficiently small  $\zeta^*$ , as,

$$Y(\zeta) = Y(0) + Y'(0) \cdot \zeta + \frac{32}{9\sqrt{\pi}} \left[ Y'(0) \right]^{3/2} \zeta^{3/2} \quad (3.32)$$

which can be derived using (3.27), (3.28) and (3.31) by power expansion in  $\zeta^{1/2}$  about  $\zeta=0$ .

The numerical integration proceeds from  $\zeta^*$  to that point  $\zeta = \zeta_0$  at which the condition in (3.28) is fulfilled. The function  $Y(\zeta)$  obtained in this way is the solution one is seeking. Because  $\zeta_0$  (Fig. 9) varies monotonically with  $Y'(0)$ , by varying  $Y'(0)$ , and repeating the integration, one can get to any desired value of  $\zeta_0$ . The Runge-Kutta-Nyström method is a suitable numerical integration method if used with variable integration steps.

### 3.5 Thermodynamic Properties of the High Density Plasma

The energy for the nuclei is,

$$U_K = \frac{3}{2} kT \quad (3.33)$$

The contribution of the electrons, is

$$U_E = U_{E,KIN} + U_{EK} + U_{EE} \quad (3.34)$$

where the first term is the kinetic energy, the second term is the interaction with the nucleus and the third term is the electron-electron interaction energy

$$U_{E,POT} = U_{EK} + U_{EE} \quad (3.35)$$

is the potential energy.

From ( 3.6 ), we have (3.36)

$$dU_{E,KIN} = \frac{3}{2}kT \cdot \frac{(2\pi mkT)^{3/2}}{h^3} \chi(\sigma) \cdot dV \quad (3.36)$$

and it is clear that,

$$dU_{EK} = -en_E \psi_K \cdot dV \quad (3.37)$$

$$dU_{EE} = -en_E \psi_E^* \cdot dV \quad (3.38)$$

where  $\psi_E^*$  excludes the self energy. Using eqns. (3.10), (3.11), (3.16), (3.17), (3.19), and (3.22), one gets,

$$U_{E,KIN} = \frac{3}{2}zkT \cdot \frac{1}{K} \int_0^{\zeta_0} \zeta^2 \chi(\sigma) \cdot d\zeta \quad (3.39)$$

$$U_{EK} = -zkT \int_0^{\zeta_0} \zeta \cdot \chi'(\sigma) d\zeta \quad (3.40)$$

$$U_{EE} = \frac{1}{2}zkT \frac{1}{K} \int_0^{\zeta_0} \zeta^2 \chi'(\sigma) \cdot \left( \frac{K}{\zeta} - \sigma + \alpha \right) d\zeta \quad (3.41)$$

The pressure in the high density plasma can be calculated by evaluating the momentum /second due to the electrons and ions which hit a unit area of a wall. Considering any boundary to be covered by quasiatoms, one can assume that the pressure is the same as that at the boundary of a quasiatom. The distribution function is given by,

$$f(P) \Big|_{r=r_0} = \left[ \exp \left\{ \frac{p^2}{2mkT} - \alpha \right\} - 1 \right]^{-1} \quad (3.42)$$

The number of electrons whose momentum lies between  $P$  and  $P+dP$  is,

$$f(P) \Big|_{r=r_0} \cdot \left(2/h^3\right) 4\pi P^2 \cdot dP = \frac{8\pi}{h^3} \frac{P^2 dP}{\left(\exp\left(\frac{P^2}{2mkT} - \alpha\right) + 1\right)} \quad (3.43)$$

Per second only  $1/6$  of electrons hit the wall, which are in a pipe of length  $P/m$  perpendicular to the wall, each giving an impulse of  $2P$ .

Therefore,

$$P_E = \frac{1}{3m} \cdot \frac{8\pi}{h^3} \int_0^\infty \frac{P^2 \cdot dP}{\left(\exp\left(\frac{P^2}{2mkT} - \alpha\right) + 1\right)} \quad (3.44)$$

$$= kT \cdot \frac{(2\pi mkT)^{3/2}}{h^3} \cdot \chi(\alpha) \quad (3.45)$$

Using eqns.(3.1), (3.2), (3.19) and (3.22), we obtain,

$$P_E = \frac{\zeta_0^3}{3} \frac{Z}{K} \chi(\alpha) \cdot \bar{n}kT \quad (3.46)$$

$$P_K = \bar{n}kT \quad (3.47)$$

$P_K$  is the partial pressure of the nuclei. The total pressure  $P = P_E + P_K$  is then given by,

$$P = \left( \frac{\zeta_0^3}{3} \frac{Z}{K} \cdot \chi(\alpha) + 1 \right) \bar{n}kT. \quad (3.48)$$

One can show that despite the non-linearity of the eqn.(3.18) for the potential, that a virial theorem for the Thomas-Fermi model exists /40/

$$3 \cdot P_E V = 2 \cdot U_{E,KIN} + U_{E,POT} \quad (3.49)$$

Also one has,

$$U_K = \frac{3}{2} p_k V \quad (3.50)$$

$$U_{KIN} = U_{E,KIN} + U_K \quad , \quad U_{POT} = U_{E, POT} \quad (3.51a+b)$$

Therefore,

$$2 \cdot U_{KIN} + U_{POT} = 3 \cdot pV \quad (3.52)$$

The free energy/atom,  $F = F_E + F_K$  (3.53)  
 can be calculated from the thermodynamic relations,

$$P = - \left( \frac{\partial F}{\partial V} \right)_T \quad , \quad U = F - T \left( \frac{\partial F}{\partial T} \right)_V \quad (3.54a+b)$$

One naturally only needs to do this for the electron part.

$$U_E = - T^2 \frac{\partial}{\partial T} \left( \frac{F_E}{T} \right)_V \quad (3.55)$$

$$F_E = - T \cdot \int \frac{U_E}{T^2} dT + T \phi(V) \quad (3.56)$$

where  $\phi(V)$  is undetermined. It can be shown that /40/,

$$\int \frac{U_E}{T^2} \cdot dT = 2/3 \frac{U_{E,KIN}}{T} + \frac{U_{EE}}{T} - Zk\alpha \quad (3.57)$$

Setting this in (3.56), and differentiating by  $V$ ,  
 and comparing to (3.45) for  $p_E$ , one can determine  $\phi(V)$  to  
 be a constant  $C$ . Using Nernst's Theorem one can show that  
 $C = 0$ . Then,

$$F_E = - 2/3 \cdot U_{E,KIN} - U_{EE} + ZkT \cdot \alpha \quad (3.58)$$

Since  $F_E = U_E - T \cdot S_E$ ,

$$S_E = \frac{1}{T} (5/3 U_{E,KIN} + U_{EK} + 2U_{EE}) - Zk\alpha \quad (3.59)$$

$$S_K = k (3/2 \ln T - \ln \bar{n} + c_k + 3/2) \quad (3.60)$$

$$C_k = 47.693 + 3/2 \ln A \quad (3.61)$$

A is the atomic weight.

One can show that, the Gibbs energy is,

$$G_E = \frac{1}{3}(U_{EK} - 2 U_{EE}) + ZkT \cdot \alpha \quad (3.62)$$

and the chemical potential is

$$\mu_E = kT\alpha. \quad (3.63)$$

There  $\mu_E$  is positive or negative when  $\alpha >$  or  $<$  0, i.e. when it is degenerate or non-degenerate.

#### 4. The stopping power of Free Electrons

##### 4.1 Derivation of general formula for the stopping power of free electrons

A fast charged particle, in passing through matter, ionizes the atoms and thereby loses energy. In gases, the ionization losses can be regarded as being due to collisions between the fast particle and the individual atoms. In a solid or liquid medium, however, several atoms interact simultaneously with the particle. The effect of this on the energy loss by the particle can be macroscopically regarded as resulting from the dielectric polarization of the medium by the charge. The derivation of this result is of interest because the method can be extended to other cases.

The dielectric formulation of the energy loss of charged particles in matter can in principle be used for both bound and free electrons. However its use here is confined to use in the free electron case. In this section a general formula is derived relating the stopping power to the generalized dielectric function. This type of macroscopic formulation is valid when,

$$v \gg a\omega_0 \quad \text{and} \quad v > v_0 \quad (4.1)$$

where  $v$  is the ion velocity,  $\omega_0$  is a mean frequency corresponding to the motion of the majority of the electrons,

$a \sim 10^{-8}$  cms, and  $v_0$  is an average electron velocity.

Let us now determine the field produced by a charged particle (charge  $Ze$ ) moving through matter. In the non-relativistic /43/ case it is sufficient to consider only the electric field, defined by the scalar potential  $\phi$ . This potential satisfies Poisson's equation.

$$\hat{\epsilon} \nabla^2 \phi = -Z4\pi e \delta(\underline{r} - \underline{v}t), \quad (4.2)$$

in which the dielectric constant is written as an operator, and the expression on the right-hand side is the charge density due to a point charge moving with constant velocity  $\underline{v}$ . Take the Fourier transform in time and space

$$\phi(\underline{r}, t) = \int_{-\infty}^{+\infty} d^3 \underline{k} \int_{-\infty}^{+\infty} d\omega \phi(\underline{k}, \omega) e^{i\underline{k} \cdot \underline{r}} e^{-i\omega t} \quad (4.3)$$

$$\epsilon(\omega) \phi(\underline{k}, \omega) k^2 = \frac{-eZ}{2\pi^2} \cdot \delta(\omega - \underline{v} \cdot \underline{k}) \quad (4.4)$$

$$\phi(\underline{k}, t) = \frac{eZ}{2\pi^2} \frac{1}{k^2 \epsilon(\underline{k} \cdot \underline{v})} \cdot \exp(-it \underline{v} \cdot \underline{k}) \quad (4.5)$$

From the electric field,  $\underline{E} = -\nabla\phi$  we have,

$$\underline{E}_{\underline{k}}(t) = -i\underline{k}\phi_{\underline{k}}(t) \quad (4.6)$$

$$\underline{E}_{\underline{k}} = \frac{-iZek}{2\pi^2 k^2 \epsilon(\underline{k} \cdot \underline{v})} \exp(-it \underline{v} \cdot \underline{k}) \quad (4.6a)$$

The total field strength is obtained by inverting the Fourier transform.

$$\underline{E}(\underline{r}, t) = \int_{-\infty}^{+\infty} \underline{E}(\underline{k}, t) \exp(i\underline{k} \cdot \underline{r}) d^3 \underline{k} \quad (4.7)$$

The energy loss by the moving particle\* is just the work done by the force  $Ze\underline{E}$  exerted on the particle by the field which is produced. Taking the value of the field at the point occupied by the particle, namely  $\underline{r} = \underline{v}t$ , the force  $\underline{F}$  is given by,

$$\underline{F} = \frac{-iZ^2 e^2}{2\pi^2} \int_{-\infty}^{+\infty} \frac{\underline{k}}{k^2 \epsilon(\underline{k} \cdot \underline{v})} d^3 \underline{k} \quad (4.8)$$

\* We assume that the particle moves in a straight line, and thereby neglect scattering, as is usually permissible in problems of this type, when loss to electrons is dominant.

Note that  $|\underline{F}| dx = dE$ , and therefore

$$dE/dx = |\underline{F}| \quad (4.9)$$

$dE/dx$  or  $|\underline{F}|$  is called the stopping power of the medium.

In order to arrive at the form used in the code /1,2 / we proceed as follows

$$\underline{k} \cdot \underline{v} = |k| |v| \cos \theta = |k| |v| \bar{\mu} \quad (4.10)$$

Further it is evident that the direction of the force  $\underline{F}$  is opposite to that of  $\underline{v}$ . Let this direction be  $\hat{\underline{r}}$  where  $\hat{\underline{r}}$  is a unit vector, along the  $\theta = 0$  axis in spherical co-ordinates

$$\underline{v} \cdot \underline{F} = \frac{-ie^2 Z^2}{2\pi^2} \int \frac{\underline{k} \cdot \underline{v}}{k^2 \epsilon(\underline{k}, \underline{v})} d^3 \underline{k} \quad (4.11)$$

$$|v| dE/dx = \frac{+ie^2 Z^2}{2\pi^2} \int_0^{+\infty} \int_{-1}^{+1} \frac{|k| |v| \bar{\mu} d\bar{\mu} dk \cdot 2\pi}{\epsilon(\underline{k}, w=k\bar{\mu}v)} \quad (4.12)$$

$$\frac{1}{\rho} \frac{dE}{dx} = \frac{ie^2 Z^2}{\rho \pi} \int_0^{+\infty} |k| dk \int_{-1}^{+1} \bar{\mu} d\bar{\mu} \frac{1}{\epsilon(\underline{k}, w=k\bar{\mu}v)} \quad (4.13)$$

Since the  $\text{Re}\epsilon(k, w)$  is even in  $w$ , the real part of the integrand is an odd function of  $\bar{\mu}$  and gives zero.

$$\frac{1}{\rho} \frac{dE}{dx} = \frac{-2.1Z^2 e^2}{\rho \pi} \int_0^{\infty} k dk \int_0^1 \bar{\mu} d\bar{\mu} \text{Im} \left( \frac{1}{\epsilon(\underline{k}, k\bar{\mu}v)} \right) \quad (4.14)$$

If the classical form of the dielectric function is used, an upper cutoff wavenumber  $k_c$  has to be introduced into (4.14), approximately at the de Broglie wavelength. Bethe's suggestion is used

where

$$k_c^{-1} = \frac{e^{-\gamma/\hbar}}{mv_t} \quad (4.15)$$

where  $\gamma = 0.5772$  and  $v_t = \left( \frac{2kT}{m_e} \right)^{1/2}$  is the thermal electron velocity. The use of this upper cut-off can be avoided by using the quantum form of the dielectric function (see section 4.2). Quantum corrections are only important for large wavenumbers, where  $|\epsilon| = 1$  and shielding is of little importance. In the code a simplified quantum form, for non-collisional plasmas is used,

$$\begin{aligned} \text{Im } \epsilon^{-1} &= \text{Im } \epsilon \\ &= \frac{4\pi^{3/2} n e^2}{\hbar k^3 v_t} \exp \left( \frac{-(mq + (\frac{1}{2})\hbar k)^2}{m^2 v_t^2} \right) \\ &\times \left[ \exp \frac{\hbar k q}{kT} - 1 \right] \end{aligned} \quad (4.16)$$

where  $q = \bar{\mu}v - (\hbar k/2m_e)/1$ . This function is matched to  $\text{Im } \epsilon^{-1}$  obtained from (4.119), with  $y = v/kv_t = 0$ , where  $v$  is the collision frequency, at an intermediate value of  $k$  where  $|\epsilon| = 1$  and both classical and quantum forms of the dielectric function are valid. Values of  $1/\rho \, dE/dx$  obtained by this procedure and by the use of the non-collisional version ( $v = 0$ ) of (4.119) for a  $19.0 \text{ g/cm}^3$  gold target are practically equal (to within 0.2%) / 1 /, which supports the cut-off approximation. In view of this good agreement between the quantum and classical cut-off versions, the effect of plasma collisions is calculated only in the classical version of using Bethe's cut-off at  $k_c$ .

The dielectric function in (4.14) is evaluated regarding the plasma ions just as positive charges with no polarizability. In calculating the free electron contribution to the stopping power it should be borne in mind that the electron density is such that in the high density case the plasma is quite collisional / 1 /. The electron collision time is given by / 1 /,

$$\tau = 3m_e^{1/2} (kT)^{3/2} \left[ 4(2\pi)^{1/2} e^4 Z n \ln \Lambda \right]^{-1} \quad (4.17)$$

where  $m_e$  and  $n$  are the electron mass and number density,  $Z$  is the ion charge, and  $\ln \Lambda$  is the Coulomb logarithm. For a  $19.0 \text{ gm/cm}^2$

gold plasma at 1 KeV, this yields a collision time of  $1.8 \cdot 10^{-17}$  secs which is not long compared with the inverse plasma frequency  $\omega_{pi}^{-1} \approx 10^{-17}$  sec.

In the code a simple relaxation model to describe the effect of collisions is used (see section for derivation) for the dielectric function in the classical form /4.4 /.

## 4.2 The calculation and properties of the dielectric function for an interacting electron gas.

### 4.2.1 The Hartree-Fock method and the Random Phase approximation.

The derivation is probably best carried out using Green's function techniques /44/. However in the case of many-body problems of this type one can not hope to obtain exact solutions of the dynamical equations (because there are of the order of  $\sim 10^{23}$  degrees of freedom) and it is necessary to develop suitable methods of approximation. This can not be done purely mathematically but has to be guided by the judicious use of physical intuition, by extracting the important physical behaviour of the system. These can be formulated in terms of the equation of motion approach /45/, in which one devises approximations for breaking off the hierarchy of equations, or one can use the perturbation theory for the Green's function in the many-body system and obtain approximate solutions by summing appropriate (dominant) subsets of diagrams / 46 /.

In two special limiting cases it turns out that one can obtain asymptotically exact solutions of many body problems by the use of approximation methods of the above type. These are: the problem of a system of fermions interacting through long range Coulomb forces in the limit of high density of the particles, and the solution of the superconducting state of a system of fermions interacting through weakly attractive forces, the so called "pairing Hamiltonian" model. In the Coulomb case a particular type of approximation, the "random phase approximation" does the trick, while in the superconducting case a particular version of the Hartree-Fock approximation, the so called B.C.S. approximation /47 / provides a solution.

In the Hartree-Fock approximation to the problem of the interacting electron gas /44 / one does not obtain an adequate account of the properties of the electron gas because it neglects screening. The next level of approximation is the random phase approximation which provides a more satisfactory

description in some cases. /48/.

It turns out that for an electron gas of high density (measured in units of the ratio of the interparticle spacing to the Bohr radius), the effects of the potential energy become relatively weak, compared to the kinetic energy, as the density is increased.

If the gas has  $N$  particles in a volume  $V$ , and let  $r_s$  be the radius of a sphere of volume  $\frac{V}{N}$ ,  $r_s$  measured in units of the Bohr radius

$$\bar{a}_0 = \frac{h^2}{4\pi^2 m e^2} = \frac{\hbar^2}{m e^2} \quad (4.18)$$

Put  $\hbar = 1$ ,

$$\frac{4}{3}\pi (r_s \bar{a}_0)^3 = \frac{V}{N} \quad (4.19)$$

The Fermi momentum  $p_f$  is

$$p_f = \left( \frac{3\pi^2 N}{V} \right)^{\frac{1}{3}} = \left( \frac{9\pi}{4} \right)^{\frac{1}{3}} r_s^{-1} \bar{a}_0 \quad (4.20)$$

The unit of energy is the Rydberg  $\bar{E}_0 = e^2/2\bar{a}_0$

$$\underline{x}' = \underline{x} / \bar{a}_0 r_s \quad \underline{p}' = \bar{a}_0 r_s \underline{p} \quad (4.21)$$

and the Hamiltonian in configuration space is,

$$\begin{aligned} H &= \sum_i \frac{p_i^2}{2m} + \frac{1}{2} \sum_{i \neq j} \frac{e^2}{x_{ij}} \\ &= \frac{\bar{E}_0}{r_s^2} \left\{ \sum_i p_i'^2 + r_s \sum_{i \neq j} \frac{1}{x'_{ij}} \right\} \end{aligned} \quad (4.22)$$

and it is seen that the second term is of higher order in  $r_s$  than the first. Thus as the density is increased ( $r_s \rightarrow 0$ ) the

effects of the potential energy become relatively weak.

In the non-interacting case (except for inclusion of the Pauli principle) the energy per particle is  $3/5 E_F$  (where  $E_F$  is the Fermi energy. In the Hartree-Fock approximation the energy of the individual particle levels ( $\epsilon_p = p^2/2m$  originally) becomes,

$$\begin{aligned} \epsilon_{\underline{p}\sigma}^{\text{HF}} &= \epsilon_{\underline{p}} + V(\underline{q}=0) \sum_{\underline{p}'\sigma'} f_{\underline{p}'\sigma'} \\ &\quad - \sum_{\underline{p}'} V(\underline{p}'-\underline{p}) f_{\underline{p}'\sigma'} \end{aligned}$$

where  $f_{\underline{p}\sigma}$  is the Fermi-Dirac function of spin state  $\sigma$ , and  $V(\underline{q})$  is the Fourier transform of the Coulomb potential.

The first correction term is then,

$$N/V \int V(\underline{x}) d^3\underline{x} \tag{4.24}$$

and represents the infinite self energy of an electron charge distribution of uniform density  $N/V$ . This term can be cancelled out by the introduction of a uniform positive background charge, of the same density; this may be regarded as simulating the static ionic lattice in real metals.

The last term in (4.23) is the exchange term  $\epsilon_p^{\text{ex}}$ . It is easily evaluated for the case of an unscreened Coulomb potential  $V(\underline{x}) = e^2/|\underline{x}|$ , where the Fourier transform is,

$$V(\underline{q}) = \frac{1}{V} \frac{4\pi e^2}{|\underline{q}|^2} \tag{4.25}$$

and replacing the sum over  $p'$  by an integral over the Fermi sphere, we obtain the well known result,

$$\begin{aligned} \epsilon_{\underline{p}}^{\text{ex}} &= \frac{-4\pi e^2}{(2\pi)^3} \int_{|\underline{p}| < p_F} \frac{d^3 p'}{|\underline{p} - \underline{p}'|^2} \\ &= \frac{-e^2 p_F}{\pi} \left\{ 1 + \frac{p_F^2 - p^2}{2pp_F} \log \left| \frac{p_F + p}{p_F - p} \right| \right\} \end{aligned} \quad (4.26)$$

where  $p_F$  is the Fermi momentum.

Then the total exchange contribution is

$$E^{\text{ex}} = 1/2 \sum_{\underline{p}\sigma} f_{\underline{p}\sigma} \epsilon_{\underline{p}}^{\text{ex}} \quad (4.27)$$

On performing the integral over  $p$  this reduces to an energy per particle of, (in the same dimensionless units,  $\hbar = 1$ ),

$$\frac{E^{\text{ex}}}{N} = \frac{-3e^2 p_F}{4\pi} = \frac{-3}{2} \left( \frac{3}{2\pi} \right)^{2/3} \frac{\bar{E}_O}{r_s} \quad (4.28)$$

Since

$$3/5 E_F = 3/5 \left( \frac{9\pi}{4} \right)^{2/3} \frac{1}{r_s^2 \bar{a}_O^2} \frac{1}{2m} \quad (4.29)$$

$$= 3/5 \left( \frac{9\pi}{4} \right)^{2/3} \bar{E}_O \frac{1}{r_s^2} \quad (4.30)$$

the total energy per particle is,

$$E^{\text{TOT}}/N = \frac{3}{5} \left( \frac{9\pi}{4} \right)^{2/3} \frac{\bar{E}_O}{r_s^2} - \frac{3}{2} \left( \frac{3}{2\pi} \right)^{2/3} \frac{\bar{E}_O}{r_s} \quad (4.31)$$

In the limit as  $r_s \rightarrow 0$  (high density limit) it is clear that the kinetic energy (1st term) dominates the second term, the potential energy. The second term is negative because the exclusion principle tends to keep apart particles of parallel spin and thus reduces the effect of the Coulomb potential. However /4.31/ still overestimates the repulsive energy between particles of opposite spin. This is because screening has not been included, so that the effect on the bare Coulomb potential has too long a range /44/.

The next level of approximation is the random phase approximation which provides a more satisfactory description of the interacting electron gas. In the high density limit this may be shown to lead to the next significant correction to the ground state energy after the exchange term /49/.

The R.P.A. was first introduced by Bohm & Pines /48/ in a heuristic manner. They analyzed the possible dynamical degrees of freedom of an interacting electron gas and argued that most of the Coulomb correlation will be absorbed in a plasma mode of collective oscillation which, because of its high zero point energy, will not be excited at low temperatures. The remaining modes can be regarded as electrons, moving in a weak screened potential, which may be described to a good approximation by an independent particle model.

One can obtain the dielectric function by studying the response of the electron gas to an applied external charge density  $\rho_{\text{ext}}(\underline{x}, t)$ . The interaction between the external charge and the electron gas is given by Hamiltonian,

$$H_{\text{ext}} = \int d^3 \underline{x} \int d^3 \underline{x}' \rho(\underline{x}) V(\underline{x} - \underline{x}') \rho_{\text{ext}}(\underline{x}', t) \quad (4.32)$$

where  $\rho(\underline{x})$  is the charge density operator for the electrons. As a result of the perturbation one obtains a non-zero induced charge density  $\rho_{\text{ind}}(\underline{x}, t)$ . This is calculated using linear response theory /50/. The dielectric function is then introduced

by the definition,

$$\langle \rho_{\text{tot}}(\underline{q}, \omega) \rangle = \rho_{\text{ext}}(\underline{q}, \omega) + \langle \rho_{\text{ind}}(\underline{q}, \omega) \rangle \quad (4.33)$$

$$= \frac{\rho_{\text{ext}}(\underline{q}, \omega)}{\epsilon(\underline{q}, \omega)} \quad (4.34)$$

where  $\rho(\underline{q}, \omega)$  is the Fourier transform with respect to space and time of  $\rho(\underline{x}, t)$ . This assumes that  $\rho_{\text{ext}}$  is a weak perturbation, so that only the linear term in  $\rho_{\text{ext}}$  needs to be retained. We thus obtain an expression for  $\epsilon(\underline{q}, \omega)$  in which the Coulomb interactions are still formally included to all orders. The assumption that the linear expansion is possible implies a stability in the system, so that the true ground state of the interacting system evolves continuously from the ground state of the non-interacting gas as the Coulomb interaction increases from zero to its full value. Although the complete evaluation of the expression for  $\epsilon(\underline{q}, \omega)$  of course requires the exact solution of the many-body problem, the formulation in terms of the dielectric response function is useful in that it leads in a natural way to approximations suggested by physical considerations. This formulation also focusses attention on the roots of the equation,

$$\epsilon(\underline{q}, \omega) = 0. \quad (4.35)$$

When this condition is satisfied, we see from (4.34) that  $\rho_{\text{TOT}}$  can be non-zero when  $\rho_{\text{ext}} = 0$ . The free modes (for instance plasmons) of oscillation of the electron gas thus correspond to the frequencies and wave numbers satisfying (4.35).

#### 4.2.2 Linear response calculation of the dielectric function

$$H_{\text{TOT}} = H + H_{\text{ext}} \quad (4.36)$$

where  $H$  is the exact Hamiltonian of the interacting gas.

One has to evaluate the expectation value

$$\langle \rho_{\text{IND}}(\underline{x}, t) \rangle = \langle E(t) | \rho(\underline{x}) | E(t) \rangle \quad (4.37)$$

where  $|E(t)\rangle$  is the state of the system at time  $t$ .

$|E(t)\rangle$  has evolved in time according to both  $H$  and  $H_{\text{ext}}$  from the initial energy state  $|E\rangle$ , which is taken to be the ground state of  $H$ .

To first order in  $H_{\text{ext}}$  one obtains,

$$\langle \rho_{\text{IND}}(\underline{x}, t) \rangle = i \int_0^t dt' \langle [H_{\text{ext}}(t'), \rho(\underline{x}, t)] \rangle \quad (4.38)$$

where in the time development of  $H_{\text{ext}}(t)$ ,  $\rho(\underline{x}, t)$  refers only to the development according to  $H$ . The value of  $H_{\text{ext}}$  is given in (4.32), and thus,

$$\begin{aligned} \langle \rho_{\text{IND}}(\underline{x}, t) \rangle &= \int_{-\infty}^{+\infty} dt' \int d^3 \underline{x} \int d^3 \underline{x}' K(\underline{x} - \underline{x}', t - t') \\ &V(\underline{x}' - \underline{x}'') \rho_{\text{ext}}(\underline{x}'', t) \end{aligned} \quad (4.39)$$

where,

$$K(\underline{x} - \underline{x}', t - t') = -i\theta(t - t') \langle [\rho(\underline{x}, t), \rho(\underline{x}', t')] \rangle \quad (4.40)$$

This result is an example of a Kubo formula.

Introducing a Fourier transform in space,

$$\langle \rho_{\text{IND}}(\underline{q}, t) \rangle = \int_{-\infty}^{+\infty} dt' K(\underline{q}, t - t') V(\underline{q}) \rho_{\text{ext}}(\underline{q}, t) \quad (4.41)$$

where

$$K(\underline{q}, t - t') = -i\theta(t - t') \langle [\rho(\underline{q}, t), \rho(-\underline{q}, t')] \rangle \quad (4.42)$$

and

$$\rho(\underline{q}) = \sum_{\underline{p}} a_{\underline{p} + \underline{q}}^+ a_{\underline{p}} \quad (4.43)$$

is the Fourier transform of the charge density operator, and where  $a_{\underline{p}}$  is a second quantized destruction operator.

for momentum state  $\underline{p}$  /46/. Next taking the Fourier Transform in time, we get

$$\langle \rho_{\text{IND}}(\underline{q}, \omega) = V(\underline{q}) K(\underline{q}, \omega) \rho_{\text{ext}}(\underline{q}, \omega) \quad (4.44)$$

in which  $K(\underline{q}, \omega)$  is the time Fourier transform of (4.42). Finally from (4.44) and (4.34) we obtain the dielectric response function as,

$$\epsilon^{-1}(\underline{q}, \omega) = 1 + V(\underline{q}) K(\underline{q}, \omega) \quad (4.45)$$

The next step is to evaluate,

$$K(\underline{q}, t-t') = -i\theta(t-t') \langle [\rho(\underline{q}, t), \rho(-\underline{q}, t')] \rangle \quad (4.46)$$

This is a so called two particle Green's function. In order to calculate this function, Feynman-Dyson perturbation theory /46, 44/ as generalized by Matsubara to treat finite temperature problems can be used. In this method the classes of diagrams which are of leading order for small  $r_s$  (high density) are picked out and summed. One considers instead of the retarded function, the time ordered form,

$$K^{\text{T}}(\underline{q}, t-t') = -i \langle \hat{\text{T}} [\rho(\underline{q}, t) \rho(-\underline{q}, t')] \rangle \quad (4.47)$$

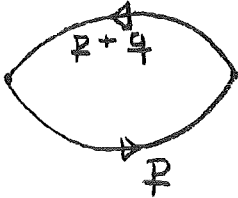
The diagrammatic expansion of  $K^{\text{T}}(\underline{q}, \omega)$  can be obtained by applying rules /46/ derived by perturbation expansion. In the interaction representation one has,

$$K^{\text{T}}(\underline{q}, t-t') = \frac{-i \langle \phi_0 | \hat{\text{T}} [\rho(\underline{q}, t) \rho(-\underline{q}, t')] \hat{\text{S}} | \phi_0 \rangle}{\langle \phi_0 | \hat{\text{S}} | \phi_0 \rangle} \quad (4.48)$$

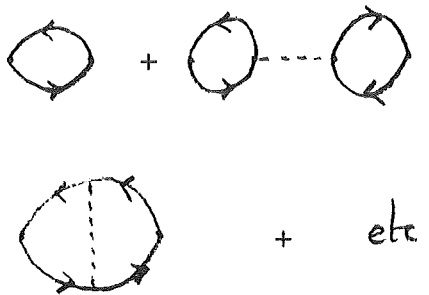
$$\text{where } \hat{\text{S}} = U(\infty, -\infty) = \hat{\text{T}} \exp -i \int_{-\infty}^{+\infty} dt, H, (t,) \quad (4.49)$$

and  $\hat{\text{T}}$  is a time ordering operator.  $\hat{\text{S}}$  is to be expanded in

powers of  $V(\underline{q})$ . It follows from the rules for calculating diagrams in momentum space that the zero-order term in the expansion of  $K^T(\underline{q}, w)$  is,

$$P_0(\underline{q}, w) = \text{Diagram} \quad (4.50)$$


evaluated for fixed  $q = (q, w)$ . The complete perturbation series includes all the higher-order diagrams associated with the diagrams shown above and may be represented as,

$$K^T(\underline{q}, w) = \text{Diagram 1} + \text{Diagram 2} + \dots + \text{Diagram 3} + \text{etc.} \\ + \text{Diagram 4} + \text{etc.} \quad (4.51)$$


where each bubble carries a net 4-momentum  $q$ .

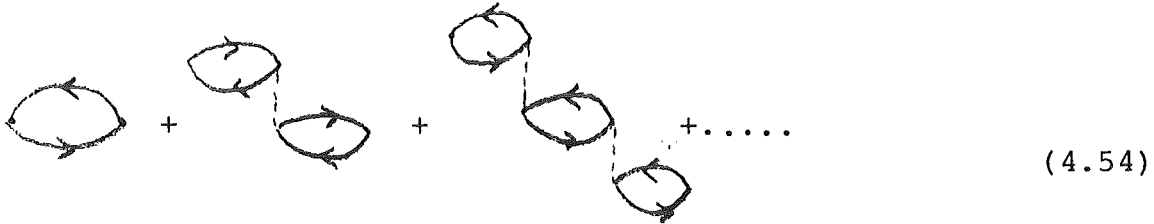
The series can be summed formally by introducing the irreducible polarization propagator  $P(\underline{q}, w)$ , defined as the sum of all the diagrams in (4.51) which can not be divided into two diagrams connected only by a single interaction line carrying a momentum  $\underline{q}$ . In terms of  $P$  the series can be arranged as,

$$K^T(\underline{q}, w) = \bar{P} + \bar{P}V\bar{P} + \bar{P}V\bar{P}V\bar{P} + \dots \\ = \bar{P} + \bar{P}VK^T \quad (4.52)$$

so that,

$$K^T(\underline{q}, w) = \frac{P(\underline{q}, w)}{1 - P(\underline{q}, w)V(\underline{q})} \quad (4.53)$$

If we consider this equation as a power series in  $e^2$ , it may be seen that for small  $q$  the leading terms in each order will be those in which  $V(q)$  occurs to a maximum power. This is because the singularity  $\frac{1}{q^2}$  will be strongest in such terms. Diagrams in which the Coulomb interaction occurs with a momentum different from  $q$ , the input momentum for the response, will be less singular as  $q \rightarrow 0$ . This suggests that the leading corrections in the  $q \rightarrow 0$  limit will be obtained by including only the ring diagrams of the form of (4.50). These are summed exactly by,



These diagrams give the leading contribution on the  $q \rightarrow 0$  limit if  $P(q,w)$  is replaced by the unperturbed electron hole propagator  $P_0(q,w)$ . This sum is usually referred to as the R.P.A. (random phase approximation)

$$P_0(q,w) = 2(-1)i \int \frac{d^4 p}{(2\pi)^4} \cdot G^0(p+q)G^0(p) \quad (4.55)$$

where  $G^0(p,w)$  is the free electron hole propagator.

$$= -2i \int \frac{d^4 p}{(2\pi)^4} \{p_0 + w - \epsilon_{p+q} + i\eta_{p+q}\}^{-1} \cdot \{p_0 - \epsilon_p + i\eta_p\}^{-1} \quad (4.56)$$

Here  $p_0, w$  are the 4-components of the 4-vector momenta,  $p$ ,  $\eta_p$  is an infinitesimal which is positive for  $|p| > p_F$  and negative for  $|p| < p_F$ .

Integration over  $p_0$  yields,

$$P_0(\underline{q}, w) = 2 \int \frac{d^3 p}{(2\pi)^3} f_{\underline{p}}^- f_{\underline{p}+\underline{q}}^+ \{ (w - w_{\underline{q}}(\underline{p}) + i\eta)^{-1} - \{ w - w_{\underline{q}}(\underline{p}) - i\eta \}^{-1} \} \quad (4.57)$$

where  $w_{\underline{q}}(\underline{p}) = \epsilon_{\underline{p}+\underline{q}} - \epsilon_{\underline{p}}$ .

By using the relation between  $K(\underline{q}, w)$  and  $K^T(\underline{q}, w)$  it can be shown /45,46/ that,

$$K(\underline{q}, w) = \frac{P_0^R(\underline{q}, w)}{1 - P_0^R(\underline{q}, w)V(\underline{q})} \quad (4.58)$$

$$P_0^R(\underline{q}, w) = \sum_{\underline{p}} \frac{(f_{\underline{p}}^- - f_{\underline{p}+\underline{q}}^-)}{(w - w_{\underline{q}}(\underline{p}) + i\eta)} \quad (4.59)$$

where  $f_{\underline{p}}$  is the Fermi-Dirac Function.

$$f_{\underline{p}}^- = f(\epsilon_{\underline{p}}) = \left[ \exp \beta(\epsilon_{\underline{p}} - \mu) + 1 \right]^{-1} \quad (4.60)$$

where  $\beta = (kT)^{-1}$ ,  $k$  is Boltzmann's constant,  $T$  is the temperature, and  $\mu$  is the chemical potential.

From equations (4.45) and (4.58)

$$\epsilon^{-1}(\underline{q}, w) = \{ 1 - P_0^R V(\underline{q}) \}^{-1}$$

where  $\epsilon(\underline{q}, w)$  is the dielectric function.

4.2.3 The evaluation of the dielectric function at zero and finite temperatures. Properties of the plasma, screening and plasmons in the dielectric function formalism.

The dielectric function contains in it all the properties of the medium through which the ion moves and with which it interacts. In order to understand the physics of the slowing down formula used in the code for free electrons one has to understand the physics contained in the dielectric function. The simple theory of energy loss from ions treats the problem via Rutherford scattering and uses a maximum impact parameter to avoid a divergence due to the long range nature of the force. However in reality all ions are screened by electrons and all electrons are screened (surrounded to a greater or lesser extent) by ions. Ions and electrons move such that this screening is maintained. This kind of correlated motion is described by the dielectric function. The function  $P_o^R(\underline{q}, \omega)$  can be determined analytically by doing the necessary integrals.

If one introduces the variables for  $T = 0$ ,

$$\bar{z} = \frac{|\underline{q}|}{2P_F}, \quad u = \frac{\omega}{qV_F}, \quad \chi^2 = \frac{e^2}{\pi \hbar V_F} \quad (4.62)$$

where

$$\epsilon_F = \frac{\hbar^2 P_F^2}{2m} = 1/2 m V_F^2 \quad (4.63)$$

is the Fermi energy,  $m$  is the electron mass, and  $V_F$  is the Fermi velocity then, /12/

$$P_o(u, \bar{z}) = 1 + \frac{\chi^2}{\bar{z}^2} \{ f_1(u, \bar{z}) + i f_2(u, \bar{z}) \} \quad (4.64)$$

$$f_1(u, \bar{z}) = \frac{1}{2} + \frac{1}{8\bar{z}} \left( 1 - (\bar{z}-u)^2 \log \left| \frac{\bar{z}-u+1}{\bar{z}-u-1} \right| \right) + \frac{1}{8\bar{z}} \left( 1 - (\bar{z}+u)^2 \log \left| \frac{\bar{z}+u+1}{\bar{z}+u-1} \right| \right) \quad (4.65)$$

The imaginary part is given by,

$$f_2(u, \bar{z}) = \frac{-\pi u}{2} \begin{matrix} | \bar{z}+u | < 1 \\ | \bar{z}-u | < 1 < | \bar{z}+u | \\ | \bar{z}-u | > 1 \end{matrix} \pi / 8 \bar{z} (1 - (\bar{z}-u)^2) \quad (4.66)$$

At finite temperatures the integrals are much harder to carry out. The exact value of the imaginary part was evaluated around 1963 and is also given by Long / 5 /. Long (1974) developed a series expansion method for the real part using Laplace transform techniques using a series expansion for the Fermi function.

Deutsch et al. / 52 /, 1978 also developed series methods and succeeded in collecting all the terms of the real part together in a closed series expansion. The results are given below. Putting,

$$P_0^R(\underline{q}, w) \equiv \chi^0(\underline{q}, w, \beta) \quad (4.67)$$

where  $\beta = (kT)^{-1}$ ,  $T$  is the temperature, we make  $w$  complex, i.e.  $w \equiv \bar{z}$ . Physical values are then obtained by letting  $\bar{z} \rightarrow w + i\eta$  where  $\eta$  is arbitrarily small. Long's method of evaluation is then based on the formula for the expansion of the Fermi-Dirac function,

$$f(E, \beta) = (\exp(\beta(E-\mu)) + 1)^{-1} = \frac{1}{2\pi i} \int_{\bar{c}-i\infty}^{\bar{c}+i\infty} ds \frac{\pi}{\sin\pi s} e^{s\beta(E-\mu)} \quad (4.68)$$

where  $s$  is a complex variable and  $0 < \bar{c} < 1$ .

This can be seen to be true by closing the contour to the left or right depending on whether  $\mu$  is  $> 0$  or  $< 0$ , and picking up the poles of  $\pi/\sin\pi s$  within the closed contour, using Cauchy's theorem, and summing the resulting terms.

The imaginary part can also be evaluated by simpler means namely by integration by parts and can be expressed as,

$$\text{Im}\chi^0(\underline{q}, w, \beta) = \frac{-\mu_0 \pi}{\beta} \log \left( \frac{1 + \exp \beta_1 x_2}{1 + \exp \beta_1 x_1} \right) \quad (4.69)$$

where  $x_1 = \mu_1 + Y_1$ ,  $x_2 = \mu_1 + Y_2$ ,  $\mu_1 = 2m\mu(\beta)$ ,  $\beta_1 = \beta/2m$ ,

$$Y_1 = -\left( \frac{2mw + q^2}{2q} \right)^2 \quad Y_2 = -\left( \frac{2mw - q^2}{2q} \right)^2 \quad (4.70)$$

and  $\mu_0 = \frac{m^2}{n} \frac{1}{4\pi^2}$ ,  $n$  being the electron density.

The next term in the expansion of the real part, which is a term of order  $T^2$  is, given by, /5/

$$\frac{\mu_0}{\beta^2 q} \frac{B_1 \pi^2}{p_F^2} \left( \frac{x_2}{(1-x_2)} - \frac{x_1}{(1-x_1)} \right) \quad (4.71)$$

where  $B_1$  is the first Bernoulli number. Further terms can be obtained in a straight forward way.

Gouedard and Deutsch /52 / have evaluated the real part also using contour integral techniques. This treatment leads to a convergent real part series.

The result is

$$\begin{aligned} \text{Re}\chi^0(\underline{q}, w, \beta) &= \frac{-\bar{\alpha} r_s p_F^2}{\pi^2 e^2} \left( \int_0^\infty dp f(\epsilon_p) \right. \\ &+ \pi Z' \sum_{n=0}^\infty \left\{ \frac{b_n}{r_n^2} - \frac{1}{2\phi'} \left[ \text{Tan}^{-1} \left( \frac{p_+ + a_n}{b_n} \right) \right. \right. \\ &\left. \left. + \text{Tan}^{-1} \left( \frac{p_+ - a_n}{b_n} \right) - \text{Tan}^{-1} \left( \frac{p_- + a_n}{b_n} \right) - \text{Tan}^{-1} \left( \frac{p_- - a_n}{b_n} \right) \right] \right\} \right) \quad (4.72) \end{aligned}$$

where  $Z' = kT/\epsilon_F$ ,  $\phi' = q/p_F$  and  $v' = \frac{\hbar w}{\epsilon_F}$ .

$\gamma = \mu/\epsilon_F$ ,  $p_+ = 2\frac{v'}{\phi'} + \phi'/2$ ,  $p_- = 2\frac{v'}{\phi'} - \phi'/2$ .

The poles of  $f(\epsilon_p)$  are located at,

$$k_n^2 = \gamma + i (2n+1)Z', \quad n = -\infty \dots \dots \dots +\infty \quad (4.73)$$

$$k_n = a_n + ib_n$$

$$a_n = \frac{1}{\sqrt{2}} \left\{ \gamma + (\gamma^2 + (2n+1)^2 \pi^2 Z'^2)^{1/2} \right\}^{1/2} \quad (4.74)$$

$$b_n = \frac{1}{\sqrt{2}} \left\{ -\gamma + (\gamma^2 + (2n+1)^2 \pi^2 Z'^2)^{1/2} \right\}^{1/2} \quad (4.75)$$

$$r_n^2 = a_n^2 + b_n^2, \quad \bar{\alpha} = \left( \frac{9\pi}{4} \right)^{-1/3}$$

and  $r_s$  is the usual dimensionless interelectronic distance. Let us consider the physical interpretation of the dielectric function as this proves important in understanding the physics of the slowing down of ions in matter, especially the difference between the dielectric approach and the classical Chandrasekhar theory / 5 / as for instance given in Spitzer / 53 /.

In the static  $\omega = 0$  limit,  $\epsilon_p(q,0)$  is purely real, with  $V(q) = 4\pi e^2/q^2$  and  $\epsilon_p = p^2/2m$  we have on replacing the sum by an integration,

$$\epsilon^{-1}(q,0) = \left\{ 1 + \frac{4me^2}{\pi^2 q^2} \int_R \frac{d^3p}{2p \cdot q + q^2} \right\}^{-1} \quad (4.76)$$

where the region of integration R is the volume inside the sphere  $|p| = p_F$ , which is exterior to the sphere  $|p+q| = p_F$ . Then

$$\epsilon^{-1}(q,0) = \left[ 1 + \frac{4me^2}{\pi q^2} p_F u(q/2p_F) \right]^{-1} \quad (4.77)$$

$$= \left[ 1 + \left( \frac{4}{9\pi^2} \right)^{1/3} r_s \frac{u(\bar{x})}{\bar{x}^2} \right]^{-1} \quad (4.78)$$

where  $q = |\underline{q}|$ ,  $\bar{x} = q/2p_F$ ,  $r_s$  was defined above, and

$$u(\bar{x}) = \frac{1}{2} \left\{ 1 + \frac{1}{2\bar{x}}(1-\bar{x}^2) \log \left| \frac{1+\bar{x}}{1-\bar{x}} \right| \right\} \quad (4.79)$$

The function  $u(\bar{x})$  decreases from 1 to 0 as  $\bar{x}$  goes from zero to infinity. Thus in the long wavelength limit as  $q \rightarrow 0$ , we have  $u = 1$ , and

$$\begin{aligned} \epsilon(q, 0) &= 1 + \bar{\lambda}^2/q^2, \quad \bar{\lambda} = \left( \frac{4me^2 p_F}{\pi} \right)^{1/2} \\ &= \left( \frac{16}{3\pi^2} \right)^{1/3} r_s^{1/2} p_F \end{aligned} \quad (4.80)$$

This is just the result obtained in the semiclassical Thomas-Fermi approximation. The function  $\epsilon^{-1}(x)$  is shown in Fig.10 for  $\bar{\lambda}/2p_F = 1$  ( $r_s = 6$ ) and compared with the Thomas-Fermi result.

A more correct treatment of this problem has been given by Gouedard & Deutsch / 52 /. They show that the screening charge has at all temperatures a Thomas-Fermi like contribution and a Friedel type oscillatory behaviour. At any temperature the dominant term will be Friedel-like when  $b_0 < p_0$  or Thomas-Fermi like for  $b_0 > p_0$  where

$$p_0^2 = \frac{\bar{\alpha} r_s}{\pi} g_0 = \left( 4\bar{\lambda}^2 p_F^2 \right)^{-1} \quad (4.81)$$

with

$$\lambda = \left( \frac{4}{\pi} me^2 p_F \right)^{1/2}, \quad g_0 = \frac{\pi^2 a_0^2}{16me^2 p_F^2} \quad (4.82)$$

In the  $T \rightarrow 0$  limit,

$$\delta \rho(r)^{T.F.} = -\frac{Z' e p_F^3}{\pi} \cdot \frac{p_0^2}{r g_0} \exp(-2p_0 r) g(ip_0) \quad (4.83)$$

as  $T \rightarrow 0$

$$g(ip_0) \cong \frac{a_0}{2} + \frac{1+p_0^2}{4p_0} \tan^{-1} \frac{2a_0 p_0}{r_0^2 - p_0^2} \quad (4.84)$$

$g(ip_0) \cong 1 + p_0^2/2$  when  $a_0 \sim 1$ ,  $b_0 \ll p_0 \ll a_0$ , where  $a_0$  and  $b_0$  are defined above.

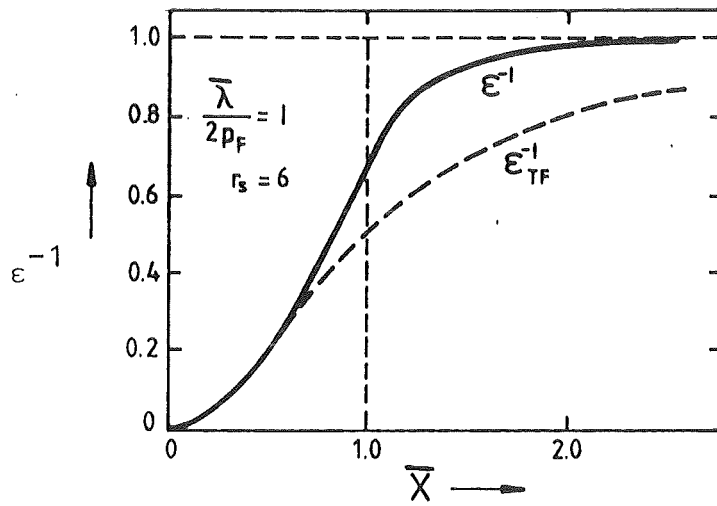


Fig. 10: Static dielectric constant in the r.p.a.  
[The broken curve is the Thomas-Fermi formula]

$$\delta\rho(r) \stackrel{\text{Friedel}}{=} \frac{Z'ep_F^3}{\pi} \cdot \frac{p_0^2}{4g_0} (1+p_0^2)^{-1} \exp(-2b_0r) \frac{\cos 2a_0r}{r^3} \quad (4.85)$$

The relative importance of both contributions is measured by,

$$\frac{\delta\rho(r) \stackrel{\text{Friedel}}{\cdot} \text{TF}}{\delta\rho(r)} \approx \frac{\exp[-2r(b_0-p_0)]}{4(1+p_0^2)r^2} \quad (4.86)$$

which is an increasing function of  $r_s(p_0^2)$ . When  $r_s \rightarrow 0$ , the high density limit, it is clear that the Thomas-Fermi screening dominates. As  $r_s$  increases the Friedel screening becomes more and more important and a Fermi-liquid type behaviour with long range order becomes dominant.

One can use the static dielectric function  $\epsilon(q,0)$  to define an effective potential  $V(q)/\epsilon(q,0)$ . If the above form of  $\epsilon(4.80)$  is assumed to be valid, then one obtains an effective potential  $4\pi e^2/(q^2+\bar{\lambda}^2)$  which is the Fourier transform of the exponentially screened Coulomb potential  $e^{-\lambda x}/x$  in real space, with a constant screening length  $\lambda$ . The more exact formula (4.78) shows that the screening length in fact increases with  $q$ . Thus the electrons are less effective in screening the potential components at shorter wavelengths. Note however that the  $q = 0$  divergence is screened out, which means that any divergence due to the  $r^{-1}$  long range part of the Coulomb potential vanishes.

The physical excitation energies of the system are determined by the condition,

$$\epsilon(\underline{q},w) = 0 \quad (4.87)$$

which implies,  $V(\underline{q})P_0(\underline{q},w) = 1.$  (4.88)

At  $T = 0,$

$$P_0(\underline{q},w) = \int_{\substack{p < p_F \\ |p+q| > p_F}} \{ (w-w_{\underline{q}}(p)+i\eta)^{-1} - (w+w_{\underline{q}}(p)+i\eta)^{-1} \} \quad (4.89)$$

This is the dispersion relation for the eigenfrequencies  $w(\underline{q})$  of the system. The function  $P_o(\underline{q}, w)$  has poles at the unperturbed frequencies  $\pm w_{\underline{q}}(\underline{p})$ , and if one plots  $V(\underline{q})P_o(\underline{q}, w)$  against  $w$  (for fixed  $\underline{q}$ ) one obtains curves as shown in Fig. 11.

The roots of ( 4.87 ) are given by the intersections of these curves with unity. There is only a small shift from the unperturbed frequencies of the particle-hole states. The figure shows however that an additional root  $w = w_{pl}$  has split off from the top of the continuum. This is the collective plasmon mode. If one expands  $P_o(q, w)$  in powers of  $q$ ,

$$P_o(q, w) = \sum_{p < |p_F|} q^2 / mw^2 + O(q^4) \quad (4.90)$$

$$= \frac{q^2 n}{mw^2} + O(q^4) \quad (4.91)$$

where  $n$  is the electron density.

Putting  $V(q) = 4\pi e^2 / q^2$ , for small  $q$ ,

$$\begin{aligned} \epsilon^{-1}(qw) &= \left( 1 - \frac{4\pi n e^2}{mw^2} \right)^{-1} \\ &= \left( 1 - w_{pl}^2 / w^2 \right)^{-1} \end{aligned} \quad (4.92)$$

Therefore

$$w_{pl} = \left( \frac{4\pi n e^2}{m} \right)^{\frac{1}{2}} \quad (4.93)$$

which is the classical plasma frequency. One can now map out the spectrum of poles Fig. 12 of  $\epsilon^{-1}(q, w)$  in the  $w$ - $q$  plane. For each value of  $q$  there will be a continuum of poles from  $w=0$  up to  $qV_F$ , followed by a discrete pole at  $w = w_{pl}$ . The various modes all contribute a  $\delta$  function or with damping a Lorentzian to  $\text{Im}\epsilon^{-1}(q, w)$ . It is this function that appears on the energy loss formula. This formula is then an average over the various ways in which the system can take up energy  $\hbar w$ .

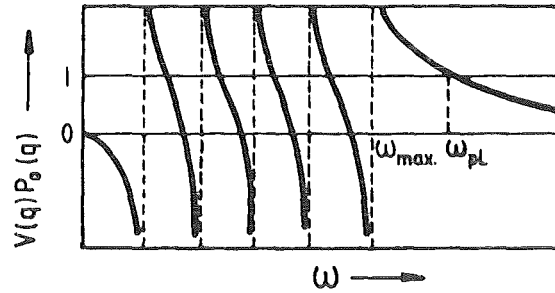


Fig. 11: Eigenfrequencies of electron gas in r. p. a.

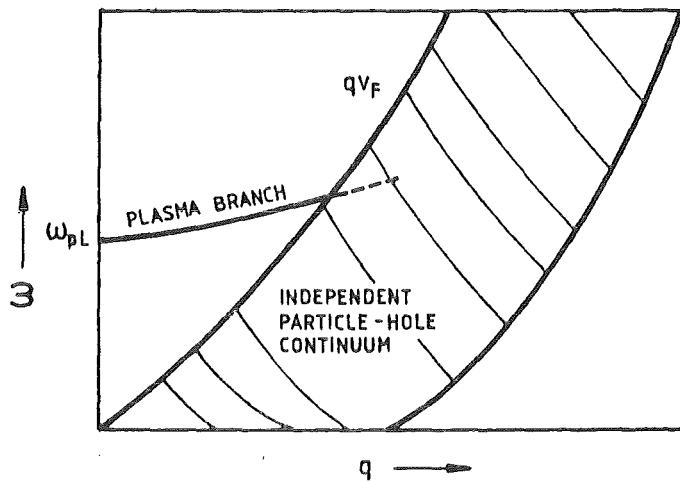


Fig. 12: The spectrum of poles of  $\epsilon^{-1}(q, \omega)$  for the Coulomb gas

4.3 Dielectric function theory in the computer code GORGON

4.3.1 The Dielectric function method for non-degenerate electrons.

The basic formula for the stopping power of free electrons used in the code is,

$$\frac{1}{\rho} \frac{dE}{dx} = \frac{-2e^2}{\rho\pi} \int_0^\infty k dk \int_0^1 \mu d\mu \operatorname{Im} \frac{1}{\epsilon(\underline{k}, w=k\mu v)} \quad (4.94)$$

The original version of the code / 1,2 / assumes that  $kT > \epsilon_F$ , ie that the free electrons are non-degenerate, or in other words that the de Broglie wavelength is less than the interparticle spacing. Now from ( 4.61),

$$\epsilon^{-1}(\underline{q}, w) = \left( 1 - V(\underline{q}) P_0(\underline{q}, w) \right)^{-1} \quad (4.95)$$

$$P_0(\underline{q}, w) = \sum_{\underline{p}} \frac{f(\epsilon_{\underline{p}+\underline{q}}) - f(\epsilon_{\underline{p}})}{\epsilon_{\underline{p}+\underline{q}} - \epsilon_{\underline{p}} - w + i\eta} \quad (4.96)$$

$$\epsilon_{\underline{p}} = \hbar^2 p^2 / 2m$$

The expression is valid for both degenerate and non-degenerate systems. If one takes the classical limit of (4.97) one can assume that  $\hbar \rightarrow 0$ , ie that  $\epsilon_{\underline{p}+\underline{q}} \rightarrow \epsilon_{\underline{p}}$  or that  $\underline{q} \rightarrow 0$ . Expanding in powers of  $\underline{q}$ , neglecting terms in  $\underline{q}^2$ ,

$$P_0(\underline{q}, w) = \sum_{\underline{p}} \frac{\underline{q} \cdot \frac{\delta f}{\delta \epsilon_{\underline{p}}}}{\left( 2m + \frac{\underline{q} \cdot \underline{p}}{m} - w + i\eta \right)} \quad (4.97)$$

$$= \int \frac{d^3 p}{(2\pi)^3} \cdot \frac{\underline{q} \cdot \delta f / \delta \epsilon_{\underline{p}}}{\left( \underline{q} \cdot \underline{p} / m - w + i\eta \right)} \quad (4.98)$$

$$\epsilon(\underline{q}, \omega) = 1 + \frac{w_p^2}{q^2} \int d\underline{v} \frac{1}{(\omega - \underline{q} \cdot \underline{v} + i\nu)} \underline{q} \cdot \frac{\delta f(\underline{v})}{\delta \underline{v}} \quad (4.99)$$

where  $f(\underline{v})$  is now the Maxwell-Boltzmann distribution.

#### 4.3.2 The linearized Boltzmann-Vlasov equation

This formula can also be derived using the linearized Boltzmann-Vlasov equation

$$\delta f_1 / \delta t + \underline{v} \cdot \frac{\delta f_1}{\delta \underline{r}} + \frac{e}{m} \underline{E} \cdot \frac{\delta f_0}{\delta \underline{v}} = \left( \frac{\delta \bar{F}}{\delta t} \right)_{\text{COLL}} \quad (4.100)$$

where  $f(\underline{v})$  is the time independent equilibrium distribution and  $f_1(\underline{r}, \underline{v}, t)$  represents a small perturbation. If the Coulomb interaction is weak compared to the Kinetic energy collisions may be ignored. If one further assumes that

$$f_0(\underline{v}) = \left( \frac{m}{2\pi kT} \right)^{3/2} \exp(-mv^2/2kT) \quad (4.101)$$

at the temperature  $T$ , then

$$\epsilon(\underline{q}, \omega) = 1 - w_{p1}^2 / \omega^2 \phi(x) \quad (4.102)$$

$$x = \frac{\omega}{qv_t} \quad v_t = \sqrt{\frac{2kT}{m}} \quad (4.103)$$

$$\phi(x) = -2x^2 (1 - 2xe^{-x^2} \int_0^x e^{-t^2} dt - i/\pi x e^{-x^2}) \quad (4.104)$$

It is often more useful to express the value of the dielectric coefficient given above in terms of the plasma dispersion function  $Z(\xi)$ . The values of this function are calculated in the code and are tabulated elsewhere / 54 /.

It is defined as follows where  $\xi$  is complex,

$$\sqrt{\pi} \cdot Z(\xi) = \int_{-\infty}^{+\infty} \frac{e^{-t^2}}{(t-\xi)} dt \quad \text{Im}\xi < 0 \quad (4.105)$$

$$= \text{P.P.} \int_{-\infty}^{+\infty} \frac{e^{-t^2}}{(t-\xi)} - i\pi e^{-\xi^2} \quad \text{Im}\xi = 0 \quad (4.106)$$

$$= \int_{-\infty}^{+\infty} \frac{e^{-t^2}}{(t-\xi)} - i2\pi e^{-\xi^2} \quad \text{Im}\xi > 0. \quad (4.107)$$

and  $Z'(\xi) = \frac{dZ}{d\xi} = -2\{1 + \xi Z(\xi)\}$  (4.108)

Then  $\epsilon(q, w) = 1 - (w_{pl}^2/w^2) x^2 Z'(x)$ ,  $\phi(x) = x^2 Z'(x)$  (4.109)  
 where  $x$  is defined above.

4.4 The calculation of the dielectric function when collisions are included. Theory with collisions in the code.

One way to allow for collisions is through the full Boltzmann collision integral (or its equivalent for Coulomb encounters). To carry this through successfully is however very difficult. Also such a perturbation expansion is not necessarily possible because if the interactions become very strong and the potential energy of the plasma is greater or of the order of the kinetic energy, then there does not exist a small parameter in which to expand, and the perturbation series will diverge. This situation is well known for instance in the theory of fluids / 55 / and requires a new approach not based on the non-interacting gas.

A simple approach to treating collisions is the relaxation model.

$$\left( \frac{\delta \bar{F}}{\delta t} \right)_{\text{COLL}} = -\nu(v) \{\bar{F} - f_0\} = -\nu(v) f_1 \quad (4.110)$$

with  $\bar{F} = f_0 + f_1$  and where  $\nu(v)$  is a phenomenological collision frequency which may or may not be a function of the particle speed.

A collision term of this type forces the distribution function to relax upon each collision to the average distribution.

As a result this method does not conserve particles at every position and each instant of time, but it conserves particles only in an averaged sense. A better method is one in which the collision term is artificially chosen so as to give precise particle conservation / 56 /.

$$\left( \frac{\delta \bar{F}}{\delta t} \right)_{\text{COLL}} = -\nu(\underline{v}) \left\{ \bar{F} - f_0 \frac{\int \nu(\underline{v}) \bar{F} d^3 \underline{v}}{\int \nu(\underline{v}) f_0 d^3 \underline{v}} \right\} \quad (4.111)$$

When  $\nu$  is independent of velocity, this becomes,

$$\left( \frac{\delta F}{\delta t} \right)_{\text{COLL}} = -\nu \left\{ f_1 - f \frac{\int f_1 d^3 \underline{v}}{\int f_0 d^3 \underline{v}} \right\} \quad (4.112)$$

Inserting this expression in the R.H.S. of the Boltzmann-Vlasov equation and solving as before using Fourier transform techniques, one obtains for  $\epsilon(q, w)$ ,

$$\epsilon(q, w) = 1 + \frac{w_{pl}^2}{q^2} \left[ \int \frac{q \cdot \delta f(\underline{v}) / \delta \underline{v}}{(w - \underline{k} \cdot \underline{v}) - i\nu} \right] \quad (4.113)$$

$$\times \left[ 1 + i\nu \int \frac{f(\underline{v}) d^3 \underline{v}}{(w - \underline{q} \cdot \underline{v}) - i\nu} \right]^{-1} \quad (4.114)$$

$$\epsilon(\underline{q}, w) = 1 - w_{pl}^2 / w^2 \theta(x, iy) \quad (4.115)$$

$$x = \frac{w}{qV_t}, \quad y = \frac{\nu}{qV_t} \quad (4.116)$$

$$\bar{\theta} = -2x^2 \left[ 1 + \frac{xZ(\xi)}{1 + iyZ(\xi)} \right] \quad (4.117)$$

$$\xi = x + iy.$$

If one uses the relaxation model then

$$\bar{\theta} = -2x^2 \left[ 1 + xZ(\xi) \right] \quad (4.118)$$

and

$$\varepsilon(\underline{q}, w) = \left[ 1 + 2x^2 (1 + xZ(\xi)) \right] \frac{w_{pl}^2}{w^2} \quad (4.119)$$

This is the dielectric function used in the code, with the option that the collisions can be ignored altogether if so desired.

#### 4.5 Energy loss using the Thomas-Fermi model and the R.P.A. dielectric function method.

In the present version of the code the energy loss for bound and free electrons are calculated separately. The dielectric function theory is used to calculate the contribution from the free electrons and the Bethe theory is used to calculate the contribution from those electrons which are not ionized. By use of the Thomas-Fermi theory of the atom it is possible to calculate  $dE/dx$  totally within the dielectric treatment / 11 /. That this can be done is easily realised if one sees that in the T-F-model the electrons are distributed within the atomic potential according to Fermi statistics. Therefore one can use the dielectric function (4.61) for such a system for each set of electrons at a given radius and average over the electron density.

$$\frac{dE}{dx} = - \frac{4\pi Z_{eff}^2 e^4}{mv^2} N \cdot L \quad (4.120)$$

where  $Z_{eff}$  is the current charge on the ions,  $v$  is its velocity,  $m$  is the electron mass and  $N$  is the ion number density in the target plasma.  $L$  is the stopping number per target atom. The important unknown quantities are  $Z$  and  $L$ .

In order to calculate the stopping number per atom,  $L_{atom}$  from the Thomas Fermi model one can use the local-density approximation,

$$L = \int_V n(r) L_0(n(r), T, v_0) \left[ 1 - \frac{Z_{eff} V_1(r)}{E} \right] d^3 \underline{r} \quad (4.121)$$

In this equation  $L_0(n, T, v_0)$  is the stopping power per electron in a uniform electron gas having density  $n$ , temperature  $T$ , where the velocity of the ion is  $v_0$ . The value of  $L_0$  can be calculated from the dielectric function for a degenerate electron gas as given in ( 4.61 ). The electron density  $n(r)$  is calculated within the Thomas Fermi model or the Thomas Fermi Dirac model. The factor in brackets in (4.121 ) is a correction for curved orbits followed by heavy ions traversing the volume of the target, where  $V_1(R)$  is the pair potential and  $E$  is the energy of relative motion of projectile and target ions. It is suggested to use the Bohr minimum impact parameter where appropriate i.e. for heavy ions. However this is only a good idea if one has a good theory of the effective charge which together with the above theory fits the cold experimental data. The empirical effective charge formulae are usually calculated using the Bethe theory so here it would yield wrong results if the Bohr minimum impact parameter is used

5. The stopping power of bound electrons:

The Bethe theory

5.1 Calculation of scattering cross sections of electrons and ions by atoms.

The theory is here developed for fast electrons scattering off atoms / 17 /, and was first given by Bethe /17,18/. The necessary modifications needed to apply the theory to ions is then given and the much used Bethe formula is finally derived. The Bethe treatment is the first quantum mechanical derivation of the stopping power of charged particles in matter. It differs in significant ways from the classical Bohr theory /15,16/, and this difference was clarified by Bloch who gave a modified /20/ quantum treatment which agrees with both formulae in their respective domains of application.

Inelastic collisions between fast electrons (ions) and atoms (nucleus plus atomic electrons) can be considered by means of the Born approximation. The condition for the Born approximation to apply is that the velocity of the incident electron should be large compared to that of the atomic electrons-

The electron may suffer an elastic or inelastic collision with the electrons in the atom. An inelastic collision is accompanied by a change in the internal state of the atom. The atom may go from its normal state into an excited state of the discrete or continuous spectrum, in the latter case the atom becomes ionized. The centre of mass system in this case is one in which the atom is at rest.

Let  $p$  and  $p'$  be the momenta of the incident electron before and after the collision, and  $E_0$  and  $E_n$  the corresponding energies of the atom.

The transition probability is then given by, where Dirac notation is used,

$$dw(n) = \frac{2\pi}{\hbar} \left| \langle E_n, \underline{p}' | U | E_0, \underline{p} \rangle \right|^2 \times \delta \left( \frac{p'^2 - p^2}{2m_e} + E_n - E_0 \right) dp'_x dp'_y dp'_z \quad (5.1)$$

where, 
$$U(\underline{r}) = Ze^2/r - \sum_{a=1}^{\bar{z}_b} e^2/|\underline{r} - \underline{r}_a| \quad (5.2)$$

is the interaction potential,  $\bar{z}_b$  is the number of bound electrons (we are also considering the case where the atom is partially ionized),  $\underline{r}$  is the radius vector of the incident electron and  $\underline{r}_a$  those of the bound electrons,  $m_e$  is the mass of the electron, and the origin is at the nucleus. The wave functions of the electrons are,

$$\psi_{\underline{p}}(\underline{r}) \equiv \langle \underline{r} | \underline{p} \rangle = \exp(i/\hbar \underline{p} \cdot \underline{r}) \cdot \left( \frac{m}{|\underline{p}|} \right)^{1/2} \quad (5.3)$$

$$\psi_{\underline{p}'}(\underline{r}) \equiv \langle \underline{r} | \underline{p}' \rangle = \exp(i/\hbar \underline{p}' \cdot \underline{r}) / (2\pi\hbar)^{3/2} \quad (5.4)$$

where  $\psi_{\underline{p}}(\underline{r})$  is normalized to unit current density.

Then  $d\omega(n)$  is the effective cross section  $d\sigma$  for the collision i.e. the probability of an electron with momentum  $\underline{p}$  scattering into  $d^3\underline{p}'$  around  $\underline{p}'$  while the atom goes from state 0 to state n.

Integration of (5.1) over the absolute magnitude  $|\underline{p}'|$  gives

$$d\sigma(n) = \frac{2\pi m p'}{\hbar} | \langle \underline{p}', n | U | \underline{p}, 0 \rangle |^2 d\sigma' \quad (5.5)$$

$$d\sigma' = 2\pi \sin\theta' d\theta'.$$

where  $|\underline{p}'|$  is determined from the law of conservation of energy:

$$(p^2 - p'^2) / 2m = E_n - E_0 \quad (5.6)$$

Using the wave functions in (5.3), and (5.4), one obtains,

$$d\sigma(n) = \frac{m^2}{4\pi^2\hbar^4} p'/p \left| \iint U(\underline{r}) e^{-i\underline{q} \cdot \underline{r}} \psi_n^*(\underline{r}) \psi_0(\underline{r}) d\tau dV \right|^2 d\sigma \quad (5.7)$$

$$-\hbar\underline{q} = \underline{p} - \underline{p}'$$

where  $d\sigma \equiv d\sigma'$ ,  $\psi_0$  and  $\psi_n$  are the atomic wave functions,  $d\tau$  is an element of configuration space of the  $z$  electrons in the atom

$$= dV_1, dV_2 \dots dV_{z_p}$$

The functions  $\psi_0$  and  $\psi_n$  are orthogonal, so the term in U involving the nuclear potential vanishes identically on integration over  $\tau$ , and one obtains,

$$d\sigma(n) = \frac{m^2}{4\pi^2 \hbar^4} \frac{p'}{p} \sum_{\alpha=1}^z \left| \iiint \frac{e^2}{|\underline{r}-\underline{r}_a|} e^{-i\underline{q}\cdot\underline{r}} \psi_n^* \psi_0 d\tau dV \right|^2 d\sigma \quad (5.8)$$

Carrying out the integration over V by noting that  $1/r$  is a solution of Poisson's equation, one obtains,

$$d\sigma(n) = \left( \frac{e^2 m}{\hbar^2} \right)^2 \frac{4k'}{kq^4} \left| \iiint_a e^{-i\underline{q}\cdot\underline{r}_a} \psi_n^* \psi_0 d\tau \right|^2 d\sigma \quad (5.9)$$

where  $\underline{k}' = \underline{p}'/\hbar$  and  $\underline{k} = \underline{p}/\hbar$ . This formula gives the probability of a collision in which an electron is scattered into a element of solid angle  $d\sigma$  and the atom enters the nth excited state. The vector  $-\hbar\underline{q}$  is the momentum given to the atom in the collision.

Since

$$q^2 = k^2 + k'^2 - 2kk' \cos\theta \quad (5.10)$$

where  $\theta$  is the scattering angle,  
for given  $k$  and  $k'$ ,

$$qdq = kk' \sin\theta d\theta = \left( \frac{kk'}{2\pi} \right) d\sigma \quad (5.11)$$

and,

$$d\sigma(n) = 8\pi \left( \frac{e^2}{\hbar v} \right)^2 \frac{dq}{q^3} \left| \iiint_a e^{-i\underline{q}\cdot\underline{r}_a} \psi_n^* \psi_0 d\tau \right|^2 \quad (5.12)$$

The most important collisions are those which cause scattering through small angles ( $\theta \ll 1$ ), with a transfer of energy which is small in comparison with the energy  $E = \frac{1}{2} mv^2$  of the incident electron (ion) :  $E_n - E_0 \ll E$ . The difference  $k - k'$  is in this case also small ( $k - k' \ll k$ ) and

$$\begin{aligned}
 E_n - E_0 &= \hbar^2(k^2 - k'^2)/2m = \hbar^2 k(k - k')/m \\
 &= \hbar v(k - k') \qquad (5.13)
 \end{aligned}$$

Since  $\theta$  is small, from (6.10) we have,

$$q^2 \cong (k - k')^2 + (k\theta)^2 \qquad (5.14)$$

$$q \cong \sqrt{\left[ \frac{(E_n - E_0)}{\hbar v} \right]^2 + (k\theta)^2} \qquad (5.15)$$

The minimum value of  $q$  is,

$$q_{\min} = (E_n - E_0)/\hbar v \qquad (5.16)$$

In the region of small angles we can further distinguish between different regions depending on the relation between the small quantities  $\theta$  and  $v_0/v$  where  $v_0$  is of the order of the velocity of an atomic electron, (note in code  $v > v_0$  always). If one considers energy transfers of the order of the energy  $\epsilon_0$  of the atomic electrons ( $E_n - E_0 \sim \epsilon_0 \sim mv_0^2$ ) then for  $(v_0/v)^2 \ll \theta \ll 1$ ,

$$q \cong k\theta = (mv/\hbar)\theta \qquad (5.17)$$

In this range of angles therefore,  $q$  is independent of the energy transfer. For  $\theta \ll 1$ ,  $q$  may be either large or small in comparison to  $a_0^{-1}$  (where  $a_0$  is say the Bohr radius). On the same assumption regarding the energy transfer we have,

$$qa_0 \sim 1 \qquad \theta \sim v_0/v \qquad (5.18)$$

Let us now apply the general formula for  $d\sigma(n)$  (5.12) to the case of small  $q$  ( $qa_0 \ll 1$ , i.e.  $\theta \ll v_0/v$ ). In this case one can expand the exponential factors as series of powers of  $q$ :

$$e^{-i\mathbf{q}\cdot\mathbf{r}_a} = 1 - i\mathbf{q}\cdot\mathbf{r}_a + \dots = 1 - iqx_a \quad (5.19)$$

where we have chosen a co-ordinate system with the x-axis lies along the vector  $\mathbf{q}$ . In (5.19) the terms containing  $I$  then give zero (by orthogonality) and one obtains,

$$d\sigma(n) = 8\pi \left(\frac{e}{\hbar v}\right)^2 \frac{dq}{q} |(d_x)_{on}|^2 = \left(\frac{2e}{\hbar v}\right)^2 |(d_x)_{on}|^2 \frac{d\sigma}{\theta^2} \quad (5.20)$$

where  $d_x = e \int_a x_a$  is the x-component of the dipole moment of the atom.

Let us now consider the opposite limiting case of large  $q$  ( $qa_0 \gg 1$ ). If  $q$  is large this means that the atom receives a momentum which is large compared with the original intrinsic momentum of the atomic electrons. It is then clear that we can consider the atomic electrons to be effectively free, and one can consider the collision between the incoming electron and the atomic electron as an elastic collision, the latter being originally at rest. For large  $q$  the integrand contains rapidly oscillating factors  $e^{-i\mathbf{q}\cdot\mathbf{r}_a}$  and the integral is practically zero unless  $\psi_n$  contains similar factors. Such a function  $\psi_n$  corresponds to an ionized atom, with the electron momentum emitted given by  $-\hbar\mathbf{q} = \mathbf{p} - \mathbf{p}'$ . In this case the incident and final electrons may have final velocities which are very similar and so they become indistinguishable, Thus in this case the exchange effect must be taken into account /19 /. Since we are mainly interested in ion scattering we treat this case later when exchange effects are not included.

5.2 Energy loss of charged particles, scattered by atoms, and the Bethe formula.

The energy loss of a charged particle (into a given solid angle), due to collisions can be expressed as,

$$dE(\Omega) = \sum_n (E_n - E_0) d\sigma_n \quad (5.21)$$

If the scattering at the various atoms is independent and the number of atoms / unit volume is N, then the energy lost per unit path length is  $NdE(\Omega)$  which is equal to  $dE/dX$  when integrated over all solid angles. The summation is taken over states of both the discrete and continuous spectrum. Therefore the general formula for the energy loss of fast electrons is,

$$dE(\Omega) = 8\pi \left( \frac{e^2}{\hbar v} \right)^2 \sum_n (E_n - E_0) \left| \sum_a (e^{-i\mathbf{q} \cdot \mathbf{r}_a})_{on} \right|^2 \frac{d\mathbf{q}}{q^3} \quad (5.22)$$

as taken from (5.12). We now exclude from consideration the region of very small angles and assume that  $1 \gg \theta \gg (v_0/v)^2$ . Then  $q$  is independent of the amount of energy transferred, and the sum over  $n$  can be calculated without further approximation. It can be shown that if  $f$  is some operator (in a suitable Hilbert space), and  $\dot{f}$  is its time derivative, that /17/,

$$\sum_n (E_n - E_0) |f_{on}|^2 = \frac{1}{2} i\hbar (\dot{f}f^+ - f^+\dot{f})_{oo} \quad (5.23)$$

where  $f_{on} = (0, f n)$  and  $f^+$  is the adjoint operator to  $f$ . This theorem can now be applied to the operator,

$$f = \sum_a e^{-i\mathbf{q} \cdot \mathbf{r}_a} \quad (5.24)$$

Then,

$$\dot{f} = \frac{-\hbar}{2m} \sum_a \left( e^{-i\mathbf{q} \cdot \mathbf{r}_a} \mathbf{a}(\mathbf{q} \cdot \nabla_a) + (\mathbf{q} \cdot \nabla_a) e^{-i\mathbf{q} \cdot \mathbf{r}_a} \right) \quad (5.25)$$

and the value of  $[\dot{f}, f]$  can be calculated as,

$$\dot{f}f^+ - f^+\dot{f} = \left( \frac{-i\hbar}{m} \right) q^2 Z \quad (5.26)$$

where  $Z$  is the number of electrons in the atom.

Then,

$$\sum_n \frac{2m}{\hbar^2 q^2} (E_n - E_0) \left| \left( \sum_a e^{-i\mathbf{q} \cdot \mathbf{r}_a} \right) \right|^2 = Z \quad (5.27)$$

and

$$dE(\Omega) = \frac{4\pi Z e^4}{mv^2} \frac{dq}{q} = \frac{2Ze^4}{mv^2} \frac{d\sigma}{\theta^2} \quad (5.28)$$

where  $d\sigma = 2\pi \sin\theta d\theta$ .

The range of applicability of this formula is given by the inequality

$$(v_0/v)^2 \ll \theta \ll 1 \quad \text{or} \quad v_0/v \ll a_0 q \ll v/v_0 \quad (5.29)$$

We now determine  $dE(\Omega)$ , the energy loss for all collisions in which the transfer of momentum does not exceed some value  $q_1$  such that  $v_0/v \ll a_0 q_1 \ll v/v_0$ .

$$dE(q_1) = \sum_n \int_{q_{\min}}^{q_1} (E_n - E_0) d\sigma_n \quad (5.30)$$

where  $q_{\min} = (E_n - E_0)/\hbar v$ . The integration and summation signs cannot be transposed since  $q_{\min}$  depends on  $n$ .

Now divide the integration range into two parts, from  $q_{\min}$  to  $q_0$  and from  $q_0$  to  $q_1$  where  $q_0$  is some value such that  $v_0/v \ll q_0 a_0 \ll 1$ . Then over the whole range of integration from  $q_{\min}$  to  $q_1$  can use for  $d\sigma_n$  (5.20).

$$dE(q_0) = 8\pi \left( \frac{e}{\hbar v} \right)^2 \sum_n \left| (d_x)_{on} \right|^2 (E_n - E_0) \int_{q_{\min}}^{q_0} \frac{dq}{q} \quad (5.31)$$

so that

$$dE(q_0) = 8\pi \left( \frac{e}{\hbar v} \right)^2 \sum_n \left| (d_x)_{on} \right|^2 (E_n - E_0) \log \left( \frac{q_0 \hbar v}{E_n - E_0} \right) \quad (5.32)$$

In the range from  $q_0$  to  $q_1$  on the other hand, one can first sum over  $n$  (since  $q$  does not depend on  $n$ ) which yields (5.28) for  $dE(q)$  and then on integrating over  $q$  we have,

$$dE(q_1) - dE(q_0) = 4\pi \left( \frac{Ze^4}{mv^2} \right) \log q_1/q_0 \quad (5.33)$$

In order to transform the above expressions one uses the summation theorem discussed above, using

$$f = d_x / e = \sum_a x_a \quad \dot{f} = 1/m \sum_a p_{x_a} \quad (5.34)$$

Then in this case,

$$f\dot{f} - \dot{f}f = \frac{-i\hbar Z}{m} \quad (5.35)$$

where  $f$  and  $\dot{f}$  are naturally operators, so that

$$\sum_n N_{on} = \sum_n \left( \frac{2m}{e^2 \hbar^2} \right) (E_n - E_0) |d_{xo}|^2 = Z, \quad (5.36)$$

The quantities  $N_{on}$  are called oscillator strengths for the corresponding transitions.

Now one defines  $I$  the Bethe parameter, by

$$\log I = \sum_n N_{on} \log (E_n - E_0) / \sum_n N_{on} \quad (5.37)$$

$$= \frac{1}{Z} \sum_n N_{on} \log (E_n - E_0) \quad (5.38)$$

Then

$$dE(q_0) = \left( \frac{4\pi Ze^4}{mv^2} \right) \log(q_0 \hbar v / I) \quad (5.39)$$

Adding this to ( 5.33 ), one has

$$dE(q_1) = \left( \frac{4\pi Ze^4}{mv^2} \right) \log \left( \frac{q_1 \hbar v}{I} \right) \quad (5.40)$$

Only one constant characterising the atom concerned appears in this formula.

Since  $q_1 = mv\theta_1/\hbar$ , the effective energy loss in scattering through all angles  $\theta \leq \theta_1$ , is given by

$$dE(\theta_1) = \left( \frac{4\pi Ze^4}{mv^2} \right) \log \left( \frac{mv^2 \theta_1}{I} \right) \quad (5.41)$$

### 5.3 Energy loss of heavy particles to atoms.

The condition for the applicability of the Born approximation to collision between heavy particles and atoms, expressed in terms of the velocity of a particle remains the same as for electrons, namely

$$v \gg v_0 \quad (5.42)$$

In a system of co-ordinates in which the centre of mass of the atom and the particle is at rest the effective cross section is given by,

$$d\sigma_n = \frac{m^2}{4\pi^2 \hbar^4} \frac{p'}{p} \left| \iint U e^{-i\mathbf{q} \cdot \mathbf{r}} \psi_n^* \psi_0 d\tau dV \right|^2 d\sigma \quad (5.43)$$

where  $m$  is now the reduced mass of the particle and the atom and not the electron mass. It is however more convenient to consider the collision in a system of co-ordinates in which the atom is at rest before the collision. The general formula for the transition probability for the transition  $\underline{p} \rightarrow \underline{p}'$ , and  $E_0 \rightarrow E_n$  was given as,

$$d\omega_n = \frac{2\pi}{\hbar} \left| U_{E_n p'}^{E_0 p} \right|^2 \delta \left( \frac{p'^2 - p^2}{2m} + E_n - E_0 \right) dp'_x dp'_y dp'_z \quad (5.44)$$

for the case of an electron. In a system of co-ordinates in which the atom is at rest before the collision, the argument

of the  $\delta$  function which expresses the law of conservation of energy is of the form,

$$\frac{1}{2} p'^2/M - \frac{1}{2} p^2/M + \frac{1}{2} (\underline{p}' - \underline{p})^2/M_a + E_n - E_o = 0 \quad (5.45)$$

where  $M$  is the mass of the incident particle and  $M_a$  that of the atom. The third term is the kinetic "recoil" energy of the atom.

In a collision between a fast heavy particle and an atom, the change in the momentum of the particle is almost always small in comparison with its original momentum. If this condition holds, one can neglect the recoil term. Then bearing in mind that the transfer of momentum is supposed small in comparison with the original momentum, i.e.  $p \sim p'$ , then the effective cross section in a system of coordinates in which the atom is at rest before the collision is the same as that for electrons except that  $p$  and  $p'$  cancels and  $m_e$  has to be replaced by  $M$ , namely

$$d\sigma_n = \frac{M^2}{4\pi^2 \hbar^4} \left| \iiint U e^{-i\mathbf{q}\cdot\mathbf{r}} \psi_n^* \psi_o d\tau dV \right|^2 d\sigma \quad (5.46)$$

and taking into account a possible  $Z_1 e$  charge on the ion the general formula for inelastic scattering is, compared to (5.43)

$$d\sigma_n = 8\pi \left( \frac{Z_1 e^2}{\hbar v} \right)^2 \left| \left( \sum_a e^{-i\mathbf{q}\cdot\mathbf{r}_a} \right)_{on} \right|^2 \frac{dq}{q^3} \quad (5.47)$$

This formula does not contain the mass of the particle and hence it follows that all formulae that derive from it remain applicable to collisions with heavy particles, provided that these formulae are expressed in terms of  $v$  and  $q$ .

The scattering angle  $\theta$  is always small in an inelastic collision with a heavy particle. For when the momentum transfer is large (compared with the momenta of the atomic electrons) one can regard the inelastic collision with the atom as an elastic

collision with free electrons in which case the heavy particle hardly changes its direction. An exception is elastic scattering through large angles but this has a very small probability.

Thus over the whole range of angles one can put

$$q = \sqrt{\left[ (E_n - E_o)/V \right]^2 + (Mv\theta)^2} / \hbar \quad (5.48)$$

which in practice reduces to,

$$q\hbar \equiv Mv\theta \quad (5.49)$$

everywhere except for very small angles. When considering electrons we had,

$$q = \sqrt{\left[ (E_n - E_o)^2/V \right]^2 + (mv\theta)^2} / \hbar \quad (5.50)$$

So one can deduce that the formulae that one had for collisions between electrons and atoms, if expressed in terms of velocity and angle of deviation, remain valid on using the substitution,

$$\theta \rightarrow \frac{M\theta}{m} \quad (5.51)$$

including the solid element  $d\sigma = 2\pi \sin\theta d\theta$ ,

the velocity of the incident particle remaining the same.

The total effective energy loss is obtained by substituting the maximum possible momentum transfer  $q_{\max}$  in place of  $q_1$  in (5.40). The value of  $q_{\max}$  is easily expressed in terms of the velocity of the heavy particle (ion) as follows. Since even  $\hbar q_{\max}$  is small compared to  $Mv$ , the momentum of the particle, and the change in its energy is related to the change in momentum by

$$\Delta E = \underline{v} \cdot \hbar \underline{q} \quad (5.52)$$

On the other hand, for a large momentum transfer nearly all this energy is given to one atomic electron, so,

$$\epsilon = \hbar^2 q^2 / 2m = \hbar \underline{v} \cdot \underline{q} \ll \hbar v q \quad (5.53)$$

Hence we have,  $h\nu \leq 2mv$

$$h\nu_{\max} = 2mv \quad \epsilon_{\max} = 2mv^2 \quad (5.54)$$

$$\theta_{\max} = \frac{h\nu_{\max}}{Mv} = \frac{2m}{M} < 10^{-3} \quad (5.55)$$

Substituting this in ( 5.41 ) , we obtain

$$dE(q_{\max}) = \left( \frac{4\pi Z_1^2 Z e^4}{mv^2} \right) \log \left( \frac{2mv^2}{I} \right) \quad (5.56)$$

$$\frac{dE}{dx} = \bar{N} \cdot \left( \frac{4\pi Z_1^2 Z e^4}{mv^2} \right) \log \left( \frac{2mv^2}{I} \right) \quad (5.57)$$

where  $\bar{N}$  is the number of atoms/unit volume in the material.

If  $M_a$  is the mass of an atom in the material,

$$\frac{1}{\rho} \frac{dE}{dx} = \frac{1}{M_a} \left( \frac{4\pi Z_1^2 Z e^4}{mv^2} \right) \log \left( \frac{2mv^2}{I} \right) \quad (5.58)$$

which is the usual form of the Bethe equation.

5.3 The Bethe Theory as used in the code. Calculation of the Bethe parameter I.

The Bethe formula (5.58) contains the parameter I which has to be evaluated for each type of atom, each state of ionization and ideally for each state of atomic excitation. In the code the contribution of the bound electrons to the stopping power is calculated by Bethe's theory, including corrections due to the differences between a plasma ion and a neutral atom, and including shell corrections. The basic physical parameter is the average excitation energy I, defined by

$$\log I = \frac{1}{N_B} \sum_{i=1}^{N_B} \log (hw_i) \quad ( 5.59 )$$

where  $N_B$  is the number of bound electrons participating in the slowing down process and  $hw_i$  are the characteristic excitation energies. In the code these are interpreted as the frequencies of revolution following the Bohr model / 15 /.

In order to calculate I within the framework of the Thomas Fermi model we note that at each radius r a spectrum of revolution frequencies is determined by the Fermi statistics energy distribution at this radius.

$$w(r) = \left[ \left( \frac{2}{m} \right) ( E + eV(r) ) \right]^{1/2} / r \quad ( 5.60 )$$

Here E is the total electron energy, i.e potential plus kinetic energy. The number of electrons per unit frequency having a revolution frequency w is,

$$n(w) = \left( \frac{32\pi^2 w^2 m^2}{h^3} \right) \times \int_0^{r_{\max}(w)} r^5 \left( \exp \left[ \left[ \frac{1}{2}mw^2 r^2 - eV(r) - \alpha \right] / kT \right] + 1 \right)^{-1} dr \quad ( 5.61 )$$

Here  $r_{\max}(w)$  is the radius beyond, which the energy which follows from w yields a free electron i.e.

$$eV (r_{\max}(w)) = -E \quad ( 5.62 )$$

The effective excitation energy is then given, within the framework of our model, by

$$\log I = \frac{1}{N} \int_0^{\infty} n(w) \log(hw) dw \quad (5.63)$$

A shell correction is included in the calculation by eliminating from the integration in equation ( 5.61) those electrons which are moving faster than the ion i.e. for

$$2mv^2 < hw \quad ( 5.64 )$$

where  $v$  is the projectile velocity.

The solution of the Thomas-Fermi described in section 3 provides the values of  $V(r)$ ,  $\alpha$  the chemical potential and  $n(r)$  for the integrations which need to be performed.

An alternative method for calculating  $I$ , which is useful especially when the Thomas-Fermi model is not used, is also provided. According to this method (5.59 ) is directly used for the determination of  $I$ . The average degree of ionization in the plasma has to be calculated by solving the Saha equation. An atomic model has to be used in order to provide the binding energies of the electrons as external data. The excitation energies are then calculated as

$$hw_i = \frac{2E_{bi}}{n} \quad ( 5.65 )$$

where  $E_{bi}$  is the binding energy of the  $i$ -th electron and  $n$  is its principal quantum number. The above equation follows from the definition of the revolution frequency in Bohr's model. Also in this procedure electrons which satisfy condition (5.64 ) are excluded from the summation in (5.59 ). Two alternatives for the use of the Saha equation are provided.

In the first alternative, applicable to single element targets, the Saha equation is solved numerically, using ionization potentials given as input data.

The set of equations,

$$P_{n+1} = P_n 0.515 \left( \frac{kT}{n_e} \right)^{3/2} \exp( E_n/kT ) \quad (5.66)$$

is solved by iterations. Here  $p_n$  is the concentration of ions with degree of ionization  $n$ ,  $kT$  is in eV,  $n_e$  is the free electron density in units of  $10^{22} \text{ cm}^{-3}$ , and  $E_n$  is the  $n$ th ionization energy in eV. From the final value of  $n$  the average number of free electrons per atom  $Z_{\text{free}}$  and the average number of bound electrons ( $Z - Z_{\text{free}}$ ) are determined.

In the second alternative, applicable both for single element targets and compounds such as  $\text{CH}_2$ , previously prepared solutions of the Saha equation are used in analytical fits which give values of the degree of ionization as a function of the target density and temperature. In the case of  $\text{CH}_2$  the degree of ionization of C and H are given separately as functions of the density and temperature. In the  $\bar{Z}, T$  plane ( $\bar{Z}$  is the degree of ionization,  $T$  the temperature) the fit is to linear segments for a given density, the density scaling being logarithmic,

$$\bar{Z} = Z_i + (a_i + b_i \log \frac{\rho}{\rho_0}) (T - T_i) \quad (5.67)$$

Here  $i$  indicates the segment number,  $\rho_0$  is the reference density for each material. The  $\bar{Z}$  segments are chosen according to the target atoms shell structure. The constants  $Z_i, a_i, b_i$  for Al, Cu, Au, C and C in  $\text{CH}_2$  are provided (up to certain degrees of ionization, see description of subroutine IONIZ below).

6. The stopping power due to Ions.

6.1 Ion-Ion scattering in plasmas.

The first theory to be developed in order to calculate non-equilibrium properties of plasmas was developed by Chandrasekhar / 5 / for gravitational forces and transcribed to the case of electrostatic forces by Spitzer / 53 /. The theory can be used to study relaxation phenomena, for instance when electrons and ions have different temperatures, and/or steady state processes such as the transport of electric current or heat. In order to develop the theory one must study the effect of collisions in the plasma. Electrostatic forces have a large range however and so one must consider not so much the effect of close collisions, but more the effect of distant collisions, in which the scattering angle is very small.

If the impact parameter is denoted by  $p$ , and  $u$  is the relative velocity, and  $\chi$  is the deflection angle,

$$\tan \chi = \frac{m_{12} \bar{p} u^2}{z_1 z_2 e^2} \quad (6.1)$$

where  $M$  is the reduced mass,

$$m_{12} = \frac{m_1 m_2}{m_1 + m_2} \quad (6.2)$$

and  $z_1, z_2$  are the charges on the particles.

If one defines a close collision as one in which the deflection is less than  $\pi/2$ , then the impact parameter for this case is

$$\bar{p}_0 = \frac{z_1 z_2 e^2}{m_1 w_1^2} \quad (6.3)$$

$m_1 \ll m_2$ , and the cross section is  $\pi \bar{p}_0^2$ .

The collision time for such collisions is then,

$$t_c = \frac{1}{\pi \bar{n} w_1 p_0^2} \quad (6.4)$$

where  $\bar{n}$  is the density of particles in the plasma. In a gas of charged particles this gives too long a m.f.p. The reason is that since the electrostatic forces decrease weakly with distance, this does not compensate for the increasing cross section due to the increasing impact parameter, and so distant collisions have a large effect. Because the deflections are small and of a random nature they have to be analyzed statistically. One defines statistical averages (over the Maxwell Boltzmann distribution for instance) of the various velocity components, namely  $\langle (\Delta \bar{w}_{//}) \rangle$ ,  $\langle (\Delta \bar{w}_{\perp})^2 \rangle$  and  $\langle (\Delta \bar{w}_{//})^2 \rangle$ , where // means parallel to a beam of test particles moving through the other set of charged particles which have a certain velocity distribution. Then one can show that, / 53 /, for instance,

$$\langle (\Delta \bar{w}_{//}) \rangle = -A_0 l_f^2 \left( 1 + \frac{m_1}{m_2} \right) G(l_f \bar{w}) \quad (6.5)$$

$$A_0 = \frac{8\pi e^4 \bar{n} z_1^2 z_2^2 \ln \Lambda}{m_1^2} \quad (6.6)$$

where

$$\bar{\phi}(X) = \frac{2}{\pi^{1/2}} \int_0^X e^{-y^2} dy \quad (6.7)$$

$$G(X) = \left( \frac{\bar{\phi}(X) - X \bar{\phi}'(X)}{X^2} \right) \quad (6.8)$$

$$l_f = \sqrt{\frac{m_2}{2kT_f}} \quad (6.9)$$

$\bar{n}$  is the density of particles in the plasma,  $T_f$  the temperature,  $Z_f$  the charge, and  $\ln\Lambda$  is the Coulomb logarithm.

$$\Lambda = \frac{3}{2Z_1 Z_2 e^2} \left( \frac{k^3 T_f^3}{\pi n_e} \right)^{\frac{1}{2}} \quad (6.10)$$

where  $n$  is the electron density.

$\langle \Delta \bar{w}_1 \rangle$  is connected to the rate of energy loss and from this the formulae given in section ( 7 ) can be derived for the rate of energy loss of an ion travelling through a plasma due to ions and electrons. These type of formulae are suitable for a fully ionized plasma, but can not of course be used for ion-ion scattering in cold materials.

## 7. Improvements made to the GORGON code at INR/KfK

### 7.1 Ion-Ion-Scattering

The original code was written for protons passing through hot plasmas, mainly metal plasmas, which would be produced if a plane target were irradiated by a powerful ion beam /1/. In this type of plasma and in the plasma formed on the outer layers of ICF pellets, ion-ion scattering is not very important. The reason for this is that in this case the initial ion velocity (of the projectile ion) is very large and usually much larger than the electron thermal velocity. Usually in this case  $dE/dX$  is often roughly constant or rises to a modest peak when the ion velocity is of the order of the electron velocity. Once the ion velocity is less than the thermal electron velocity, then  $dE/dX$  drops very sharply and the projectile ion has virtually lost all its energy. In pellet calculations this is the point (at the end of the range) where the hot plasma pushes the cold part of the pusher. If a  $Bi^+$  ion starts with an energy of 10 GeV at this point it has an energy of 10's of keV which is insignificant so for the purposes considered here this can be considered negligible. However when  $\alpha$ -particles or neutron induced "knock-on"  $D^+$  and  $T^+$  ions pass through burning (very hot) DT a very different situation arises. Here for instance the  $\alpha$ -particle starts off with a velocity which is less than the thermal electron velocity but greater than the thermal ion velocity. The energy loss to ions or electrons in a hot plasma is always greatest when the velocity of the projectile ion is equal to the ion or electron (respectively) thermal velocity (average). Either side of this velocity the stopping power contribution drops off. Now as an  $\alpha$ -particle (3.5 MeV) slows down, the energy loss to the electrons decreases, whereas the energy loss to the plasma ions increases. As the plasma temperature increases, so the loss to the ions becomes more and more important relative to the electrons.

The treatment of ion-ion scattering that we have put in the code follows that of Mehlhorn /8, 9/. For the electron stopping power on the other hand a dielectric function theory approach is used in the code which is more accurate than that used by Mehlhorn. The latter approach uses a simple binary collision model within a Debye radius coupled with interaction with plasma waves outside the Debye sphere.

In this method the ion stopping power is given by,

$$\frac{dE}{dX}_{ion} = \frac{Z_{eff}^2 Z_2 e^2}{\beta^2 c^2 A_2} \frac{m}{m_p} w_{pl}^2 G(y_i) \ln \Lambda_i \quad (7.1)$$

where,

$$y_i = \frac{A_2}{A_1} \frac{E}{kT_i} \quad (7.2)$$

$$G(y_i) = \text{erf}(\sqrt{y_i}) - 2\sqrt{(y_i/\pi)}(\exp(-y_i)) \quad (7.3)$$

where erf(...) is the error function.

$$w_{pl}^2 = \frac{4\pi\rho Z_2 e^2 N_0}{m_e A_2} \quad (7.4)$$

where  $\rho$  is the density,  $E$  the ion energy,  $A_1$  the ion atomic weight,  $A_2$  the atomic weight of a plasma ion,  $T_i$  is the ion temperature,  $Z_{eff}$  is the effective charge (of the ion slowing down),  $\beta = v/c$ ,  $c$  is the velocity of light,  $v$  is the ion velocity,  $m$  is the electron mass,  $m_p$  is the proton mass,  $w_p$  is the plasma frequency. In  $\Lambda_i$  is the ion Coulomb logarithm, and  $e$  is the electronic charge.

$$\Lambda_i = b_{max}/b_{min} \text{ where,}$$

$$b_{max} = \text{Debye Radius} = (kT_e/4\pi n e^2)^{1/2} \quad (7.5)$$

$$b_{min} = \frac{\mu\beta^2}{Z_1 Z_2} \frac{m_p c^2}{e^2}, \quad \mu = \frac{A_1 A_2}{A_1 + A_2} \quad (7.6)$$

where  $T_e$  is the electron temperature, and  $n$  is the electron density.

The corresponding expression used by Mehlhorn /8, 9/ for energy loss to plasma electrons is,

$$\frac{dE}{dX}_{\text{free}} = \frac{w_{pl}^2 z_{\text{eff}}^2 e^2}{c^2 \beta^2} G(y_e) \ln \Lambda_{\text{free}} \quad (7.7)$$

$$y_e = \frac{m c^2 \beta^2}{2kT_e} \quad (7.8)$$

$$\Lambda_{\text{free}} = \frac{0.764 \beta c}{b_{\text{min}} w_{pl}} \quad (7.9)$$

$$b_{\text{min}} = \max \left( \frac{e^2 z_1}{m_{12} \bar{u}^2} ; \frac{h}{2m_{12} \bar{u}} \right) \quad (7.10)$$

where  $m_{12} = m_1 m_2 / (m_1 + m_2)$ ,  $m_1$  is the mass of the incoming ion,  $m_2$  is the mass of the ion in the plasma, and  $N_0$  is the Avagadro's number.  $\bar{z}_2$  is the average number of ionized electrons/atom, and  $\bar{u}$  is the relative speed between the projectile ion and the plasma electrons.

The above expression gives a larger value for  $dE/dX$  than the dielectric funtion theory /1/.

## 7.2 The stopping power of degenerate electrons

When electrons become degenerate the stopping power stops increasing. A full treatment of this problem would involve taking the exact expression for the dielectric function for a degenerate electron gas (at all temperatures, at high temperature it becomes the same as the classical expression without collisions, and putting it into the formula ( 4.14 ) for the stopping power of free electrons and carrying out the integration either numerically or analytically (if this is possible). There are two reasons to treat degenerate electrons. Firstly in a metal at low temperature a few electrons per atom are "free" as band electrons. The free electrons stopping power formula can be applied to this problem in a first approximation. The next approximation would be to use the exact band structure wave functions and energies to calculate the dielectric function. Secondly in ICF pellets the bulk of the DT is compressed on a low adiabat such that the electrons are partially degenerate. So  $\alpha$ -particles and neutron induced "knock-on" fast ions stream out of the expanding burning sphere which is semi-transparent to these ions into the cold degenerate DT. Hence one wants to know the stopping power here. As a first approach in the code, the following scheme has been used (and will be improved upon), as in some respects it has been found not to be satisfactory.

The code calculates this way, only if  $\epsilon_F > kT$ . Then if  $V_F$  is the Fermi velocity  $V$  is the particle velocity, and  $V_t$  is the electron thermal velocity, and  $\epsilon_F$  is the Fermi energy

For  $V > V_F$  and  $V_F > V_t$ , /57/

$$\frac{1}{\rho} \frac{dE}{dX} \Big|_e = \frac{-Z^2 e^2 w_{pl}^2}{\rho V^2} \ln_e \frac{2mV^2}{\hbar w_{pl}} \quad (7.11)$$

where  $w_{pl}$  is the plasma frequency,

If  $V < V_F$  and  $V_F > V_t$ ,

$$\frac{1}{\rho} \frac{dE}{dX} \Big|_e = - \frac{2}{3\pi} Z^2 e^4 \frac{m^2 V}{h^3 \rho} 2 \ln \left( \frac{2mV_F^2}{\sqrt{3}\hbar w_{pl}} \right) \quad (7.12)$$

$$w_{pl}^2 = \frac{4\pi n e^2}{m} \quad (\text{this is for DT}) \quad (7.13)$$

$$V_F = h/m \left( \frac{3}{8\pi} n \right)^{1/3} \quad (7.14)$$

$$V_t = \left( \frac{2kT}{m} \right)^{1/2} \quad (7.15)$$

For  $V < V_F$  it is clear that not all the electrons in the Fermi-sphere can be excited and formulae (7.12) allows for this fact.

### 7.3 The effective charge

When say a Bismuth ion  $\text{Bi}^+$  enters a lead target then collisions with the electrons in the cold material or plasma causes ionization which takes a finite time to occur, comparable to but less than the time the ion takes to reach the end of its range. After a certain time an equilibrium effective charge is attained. This equilibrium effective charge is a function of the ion and its atomic state spectrum and of the electronic properties of the medium through which the ion is moving. In particular the effective charge can be significantly different / 59 / in some cases in a cold material and a hot plasma. Electrons are captured more easily from bound states than from free electron states, so that as the number of free electrons increases so does the effective equilibrium charge. Also as there are more free electrons, there is more collisional ionization.

In the code at the present time an empirical formula is used since the original code was written for protons. The formula was obtained /29 / by comparison between proton data and heavy ion data, by dividing the two stopping powers. One uses,

$$Z_{\text{eff}}(V) = Z_0 (1 - 1.034 \times \exp(-137 V_r' / Z_0^{0.69})) \quad (7.16)$$

$$V_r' = V_r / c$$

where  $Z$  is the nuclear charge on the ion, and  $V_r$  is the relative velocity of the ion to the thermal electrons in the plasma.

$$V_r = \left( v_t^2 + v^2 \right)^{\frac{1}{2}} \quad (7.17)$$

where  $V_t$  is the thermal electron velocity and  $V$  is the ion velocity. This means that in hot plasmas the effective charge stays higher than it would do in cold materials. This shortens the range and at high plasma temperatures the Bragg peak re-appears. The various contributions to  $dE/dX$ , namely free electrons,

bound electron, and ion scattering are all multiplied by  $Z_{\text{eff}}^2$ . The contributions are then summed in order to find the total  $dE/dX$ . The effective charge can not go below the value of the charge of an impurity of the particular type of ion in the material under consideration. If the material is a metal some of the outer electrons of the ion will naturally go into the conduction band. This number may be one for light ions or a few for heavy ions.

#### 7.4 Calculation of the range

The original code calculated one value of  $dE/dX$ . From this it is fairly easy to modify the program to calculate the range. Use of a DO Loop allows one to subtract  $(\frac{1}{\rho} dE/dX) \cdot \rho dX$  from the initial energy. If  $\rho dX$  is called the range factor (gms/cm<sup>2</sup>), this can be set to a given value or is calculated in the code so that about 80 iterations are needed to reach the end of the range. This is done by calculating  $dE/dX$  once and then assuming  $dE/dX$  remains constant and finding the range of an ion with initial energy  $E_0$ , and then dividing this range by 80 to find the range factor. Another facility which is provided is to stop the calculation at a certain energy, i.e. a lower cut -off energy is allowed for.

#### 7.5 Bohr minimum impact parameter

It has been shown in /20,23/ that the Bethe theory is not always valid and that particularly for heavy ions the Bohr theory may well be better. A simple minded way of taking this into account is to use the maximum of the quantum or classical minimum impact parameter. This facility can be used in the code where in both the free electron and bound electron calculations this condition is tested for and used if appropriate. However there exists the following problem of consistency with the effective charge formula. This is evaluated as if the Bethe theory is valid and so is not valid when used with the Bohr theory.

A fully consistent calculation is needed in which the Bohr theory is used with the same shell effect modifications as used in the Bethe theory, together with a first principles calculation of the effective charge in cold material and in the plasma state.

As a first approximation of course one could evaluate the cold effective charge using experimental data and the Bohr theory. Use of the full Bloch formula would be even better because this interpolates between the Bethe and Bloch theories /20,23/.

## 7.6 Improvements made to the Fortran programming and structure of the program

The whole GORGON code was investigated to see whether or not the FORTRAN rules were kept to, and if not the corresponding changes were made. The following changes were made in general

- a) All multiplications were as far as possible replaced by additions.
- b) Divisions and exponentiation operations were replaced by multiplications whenever possible.
- c) If in a given formula there were many constants then they were put together before evaluation
- d) Calculations within a loop which were independent of the index were taken out of the loop.
- e) Subroutines which are only called once were integrated into the program.
- f) In the LATMA program, the error handling facilities were improved and self-explanatory error messages are now printed out.
- g) The input data for the LATMA and DEDX programs were extended.

## 8. User's and Programmer's Information

### 8.1 Description of the Code

Regular version.

The version which is ordinarily used employs the Thomas Fermi model for dealing with the bound electrons and for determining the plasma parameters.

#### 8.1.1 LATMA-INIT

Program LATMA solves the Thomas Fermi model for the given target temperature and density and calculates the chemical potential electron density as function of radius and the degree of ionization.

#### LATMA routines:

MAIN-program: Performs the calculations of the Thomas Fermi model as described in Sec. 3 and controls the service subroutines.

Subroutine INIT: Initializes the Thomas Fermi model integration, following Latter's/42/ procedure. This is required because for the integration the first two points of the mesh are needed. INIT calculates the parameters of the second point, the first (outermost) given by the boundary conditions. The subroutine parameters are:

XMU - The current value in the iteration scheme of the chemical potential.

DU - The mesh step  $U_N - U_{N-1}$ ,  $U = X^{1/2}$ , X the non dimensional distance in the Thomas-Fermi atom.

A - The dimensionless atomic radius in the Thomas Fermi model.

NN - Number of mesh points.

Subroutine ZEFF: Calculates the effective charge Z required for calculations in a mesh cell.

Parameters:

ZEFF - Vector specifying the effective charge up to each mesh point.

AR - Vector of radii of mesh points.

RAV - Average radius in a mesh cell.

ZE - Effective charge to be used in a given mesh cell.

MØN+1 - Number of mesh points + 1

K - Number of mesh points + 2

Subroutine RMAX: Calculates maximum radius for which a given energy implies a bound electron in the Thomas Fermi model.

Parameters:

ZEFF, AR, MØN1, K

Z - Atomic number of target material

E - Electron energy

RM - The required maximum radius.

Important variables:

- XKT - Temperature (keV)
- $R\phi$  - Density ( $\text{g}/\text{cm}^3$ )
- XMU - Chemical potential
- ZEFF - Effective Z as function of radius
- ARR - Radial points in atomic cell
- $R\phi\phi$  - Bound electron density ( $\text{cm}^{-3}$ )
- RXX - Total electron density ( $\text{cm}^{-3}$ )
- ZAVR - Average total charge.

Input description for LATMA

The input for the LATMA-program looks as follows:

1. card	IUMASH	IRECN $\phi$	IMESHP	
N. card	ZO	$R\phi$	XKT	AMU (this card can be repeated N-times)

IUMASH      UNIT-Number of the MASHA-profile (INTEGER)

IRECN $\phi$       Number of records in the MASHA-profile (INTEGER)  
for each input-card with the data 'ZO- $R\phi$ -XKT-AMU'  
3 records are needed in the MASHA-profile,  
1 additional record is needed for the end-record;  
that means  $\text{IRECN}\phi \geq (N-1)*3+1$

IMESHP      Number of meshpoints (INTEGER)

ZO            Target atomic number (double precision)

$R\phi$           Target density in  $\text{g}/\text{cm}^3$  (double precision)

XKT          Target temperature in keV (double precision)

AMU          Target atomic weight(double precision)

Output of Program LATMA

On disk (MASHA profile)

Atomic number, density, temperature (keV), chemical potential (keV)  
(Number of mesh points; maximum 400)

Tables:

- (1) ARR, RXX, ZAVR for the whole cell.
- (2) ARR, R $\phi\phi$  for bound electrons only.

Print:

Total number of electrons  
Number of bound electrons  
Number of free electrons  
Table (2)

Program INIT

Before a LATMA-run can be started, a MASHA-Profile must be created.

This can be done with the program INIT. This job allocates a new MASHA-profile, structures it by the meaning of a 'DEFINE FILE' - command and initializes the first record with the characters 'PROFILE-END'.

### 8.1.2 DEDX

Program DEDX calculates the energy loss of a given ion (atomic mass, charge state and energy) in a given plasma (atomic number, density, temperature) using the Thomas Fermi model according to the procedures described in Secs. 3.2, 3.3, 3.4

#### DEDX routines.

Programm MAIN: reads LATMA-output from disk, calls subroutine DEDX and computes the range.

Subroutine DEDX: control routine, calls routines for calculations required in the determination of  $dE/dX$ .

Subroutine DETRO: Control routine for the calculation of  $dE/dX$ .

Parameters:

- XKT - Temperature
- $R\phi$  - Density
- EK - Projectile energy
- DE - Total energy loss

Subroutine PLDE: calculates free electron contribution to the energy loss as described in Sec. 4.3.

Parameters:

- EK - Projectile energy
- XKT - Temperature
- $R\phi$  - Density
- ZFREE-Number of free electrons per atom
- DEFEL-Energy loss due to free electrons

Subroutine ZFUNC: Calculates the real and imaginary parts of the plasma dispersion function  $Z$  required for the calculation of the dielectric function, as described in Sec. 4.3 and 4.4.

This is now included in PLDE.

Parameters:

U - Variable  $x = \omega/kV_t$  (Sec. 4.4 )

V - Variable  $y = v/kV_t$  (Sec. 4.4 )

XR - Real part of Z

XI - Imaginary part of Z

Subroutine ZPRIME: calculates the plasma dispersion function in the case of non collisional plasma.

Parameters:

XMU - Variable  $\mu = \omega/kV$  (Sec. 2.3)

VDAL - Variable  $v/v_t$  (Sec. 2.3)

ZREAL - Real part of Z

ZIM - Imaginary part of Z

IONP: Calculates excitation energies of bound electrons in Bethe's theory using the Thomas Fermi model as described in Sec. 3.2.

Parameters:

XKT,  $R\phi$

FREEL - Number of free electrons per atom.

ELOSS: Calculates bound electron contribution to  $dE/dX$  as described in Sec. 5.3.

Parameters:

E - Projectile energy

DEDX - bound electrons contribution to  $dE/dX$

Important variables in program DEDX

- XKT - Temperature (keV)
- R $\phi$  - Density (g/cm<sup>3</sup>)
- ZO - Target atomic number
- ZFREE - Number of free electrons per atom
- EK - Projectile kinetic energy
- DEBND - dE/dX by bound electrons (keV/cm<sup>2</sup>/gm)
- DEFEL - dE/dX by free electrons (keV/cm<sup>2</sup>/gm)
- XNW - Atomic frequency spectrum in Thomas Fermi model.
- WTAB - Atomic frequency points in Thomas Fermi model.
- AR - Vector of radii in Thomas Fermi model
- ZEFF - Effective value of charge
- SUMW - Number of bound electrons from oscillator integration
- XI - Bethe's I without shell correction
- AM - Projectile atomic weight
- ZPRJ - Projectile charge number

Input for the program DEDX

- |          |        |              |        |              |   |
|----------|--------|--------------|--------|--------------|---|
| 1. card: | IUMASH | IRECN $\phi$ | IURANG | RFIND        | } the input-cards<br>can be repeated<br>several times |
| 2. card: | IDLEV  | IUTEST       | IDVERS | MAXIT        |   |
| 3. card: | ZPRJ   | AM           | EPRJ   | FREELI ECUTF |   |
| 4. card: | ZO     | R $\phi$     | XKT    | AMU          |   |

This version of the DEDX-program can be started in 2 ways:

- a) with the data of a MASHA-profile, created by a LATMA-job
- b) without LATMA-data

If you use the 1. possibility, a MASHA-profile must be created by the LATMA-program, before a DEDX-job can be started.

If the DEDX-program is started without LATMA-data, 'DE/DX by bound electrons' is set to zero in the subroutine DETR $\phi$ .

### IUMASH - IRECNØ

If a MASHA-profile is needed, the unit-number to which the profile is allocated, must be specified in 'IUMASH' and the number of records of the profile must be specified in 'IRECNØ' (both are INTEGER-values)

### IURANG - RFIND

Another feature in this version of the DEDX-program is the computation of the range. Therefore, in 'IURANG' you have to specify a unit-number of an output-dataset, which will contain the data of the range.

To compute the range, a range-factor, which can be specified in 'RFIND', is needed.

If the value of 'RFIND' is positive, the range-factor is computed as

$$\text{range factor} = \frac{\text{projectile initial energy}}{\text{DE/DX by total electrons} * \text{'RFIND'}}$$

If the value of 'RFIND' is negative, the amount of 'RFIND' is the range-factor.

At the end of the computations the range is determined as

$$\text{range} = (\text{number of iterations} - 1) * \text{range-factor}$$

'IURANG' is INTEGER and 'RFIND' is DOUBLE PRECISION

### IDLEV - IUTEST

In the case of wrong results, you have the possibility to run the program on a test level, that means, some test-printout is produced. The testlevel is specified with 'IDLEV'.

IDLEV = 0 → no testprintout

      = 1 → test-printout on unit 'IUTEST'.

(both are INTEGER-variables)

IDVERS

With the variable 'IDVERS' you can specify the version, with which the calculations should be done.

IDVERS = 1 → standard-version (with data of a masha profile)  
          = 2 → version without LATMA-data  
( 'IDVERS' is INTEGER)

MAXIT

If you choose an unfavourable range-factor, you can get a lot of iterations. This can be prevented with the variable 'MAXIT', which specifies the max-number of iterations to be executed.  
( 'MAXIT' is INTEGER)

ZPRJ - AM - EPRJ - FREELI

ZPRJ is the projectile charge state  
AM is the projectile atomic weight  
EPRJ is the projectile initial energy in keV  
FREELI is the number of free electrons/atom (this value is only needed, if IDVERS=2 is chosen, otherwise you have to specify 0.0D+0)

(all values are DOUBLE PRECISIONS)

ECUTF

To compute a cut-energy, a factor is needed, which is specified in 'ECUTF'. Then the cut-energy is computed as

$$ECUT = EPRJ/ECUTF.$$

After each iteration,  $\Delta E$  is computed as

$$\Delta E = DE/DX \text{ by total electrons } * \text{ range-factor}$$

Then the new projectile initial energy is determined as

$$EPRJ_{\text{new}} = EPRJ_{\text{old}} - \Delta E$$

If the 'new projectile initial energy' is greater than the 'cut-energy', a new iteration is started with  $EPRJ_{\text{new}}$ .  
(ECUTF is DOUBLE PRECISION)

ZO - R $\phi$  - XKT - AMU

ZO is the target atomic number

R $\phi$  is the target density in g/cm<sup>3</sup>

XKT is the target temperature in keV

AMU is the target atomic weight

(all variables are DOUBLE PRECISION)

The whole program has been tested and changed, so that no FORTRAN-rules are violated.

Output of program DEION

ZPRJ , AMU

XKT, R $\phi$ , ZO, AM, XMU, FREEL

Table : AR, ROD (bound electron density), RXX(total electron density), ZEFF

N - Number of bound electrons from oscillator integration

I - Bethe's I from TF model, no shell corrections

XKT, R $\phi$ , EK

EK, I (Bethe's I with shell correction), N(number of effective electrons with shell correction).

BOUND ELECTRONS DEDX USING THOMAS FERMI MODEL EK, XKSUM  
(dielectric function integral), FREE DEDX (free electron contribution)

ZO, ZFREE, ZBOUND

DET $\phi$ T, DEFEL, DEBND

Range and data from range

8.2 Version of the code using atomic physics other than the Thomas Fermi model - DECZI.

This version is different from the regular one in the method of calculating the number of free electrons and in the method of calculating the bound electron contribution to  $dE/dx$ . This version has been specifically used only in the calculations of the stopping power of  $CH_2$ , where the use of the TF model is not convenient.

DECZI routines

MAIN: Controls the calculations and calculates the energy loss in Cold targets. Data for Cold targets provided for:

Aluminium (INDM = 1)  
Copper (INDM = 2)  
Gold (INDM = 3)  
Carbon (INDM = 4)  
 $CH_2$  (INDM = 5)

DETRØ: Controls the calculation of  $dE/dx$ .

Parameters:

XKT - Temperature

$R\phi$  - Density

EK - Projectile energy

DE - Total energy loss

ICØLD - Index used in choosing cold  $dE/dx$  calculations.

ICØLDX - Index determining whether cold target is assumed.

DECLD - Cold  $dE/dx$

INDM - Index defining the target material.

SAHA 1: Solves the SAHA equation for single element targets  
(INDM 1 to 4)

Parameters:

XKT - Temperature

R $\phi$  - Density

ZFREE - Number of free electrons per atom

INDM - Index defining target material

PLDE: Calculates dE/dx due to free electrons (see DEION)

ZFUNC, ZPRIME - see DEION

ELBND: Calculates dE/dx due to bound electrons, using atomic  
shell model, not TF model, as explained in Sec.5.3.

Specific data provided for Al, C, CH<sub>2</sub>.

Parameters:

E - Projectile energy

ZB $\phi$ UND - Number of bound electrons per atom

DESHL - Bound electrons dE/dx

INDM - Index defining target material

IONIZ: Gives fits to approximate Saha calculations, providing  
the degree of ionization as function of density and  
temperature.

Specific data provided for Al (up to Z = 13), Cu (up to  
Z = 20), Au (up to Z = 52), C (up to Z = 6), CH<sub>2</sub>.

(see Sec. 5.3)

Parameters:

RH $\phi$  - Density

TEMP - Temperature

Z - Degree of ionization

DZDT -  $\partial Z / \partial T$

DZDR -  $\partial Z / \partial \rho$  } for use in other equation of state applications

Important parameters in program DECZ 1

XKT - Temperature (keV)  
RØ - Density (g/cm<sup>3</sup>)  
EK - Projectile energy (per nucleon) (keV)  
ZO - Atomic number  
ZFREE - Number of free electrons per atom  
DEFEL - dE/dx by free electrons (keV/g/cm<sup>2</sup>)  
DEBND - dE/dx by bound electrons (keV/g/cm<sup>2</sup>)  
DETØT - total dE/dx  
INDM - Target material index  
APRJ - Projectile atomic weight  
ZPRJ - Projectile charge number  
EPRJ - Projectile energy  
ENP - Projectile energy per nucleon

Input to DECZ 1

IC $\phi$ LDX - If 1 - cold target is assumed

INDM

APRJ

ZPRJ

NSP - Number of projectile data

NR - Number of target data

R $\phi$

XKT

Data for cold target stopping (vector AE) have to be provided in MAIN

Ionization potentials have to be provided in SAHA (vector EE)  
Number of electrons in each sub-shell (vector NN), principal quantum number of each sub-shell (vector XN) and binding energies in keV (vector EB) have to be provided in ELBND.

Output

ICOLDX, INDM, APRJ, ZPRJ

Values of projectile energies ENP (1)

R $\phi$ , XKT

For each value of ENP a table is provided giving:

1 - number of atomic shell

ZEFF - Effective Z for calculating the binding energy in shell I

HBAR - Excitation energy for shell (keV)

XJ - Stopping number for shell

XX - number of electrons in shell I

DES - shell contribution to energy loss

DE - cumulative energy loss

This table is printed for the case of an unionized target and for the case of the real target. In the case of CD<sub>2</sub> the tables are for the carbon component only.

Also provided are:

RA - density in units of 10<sup>24</sup> atoms (molecules)cm<sup>-3</sup>

ZF - Number of electrons per atom (molecule)

H - Debye length in the plasma

DeBroglie wave number for the electrons

DXK1 -

DXK2 - steps in k-integration

DXK3 -

XKCRIT-1 (Debye length)

XKR2 - Intermediate k value in k-integration

XKMAX - maximum wave number in calculation

XNI - Ion contribution to screening

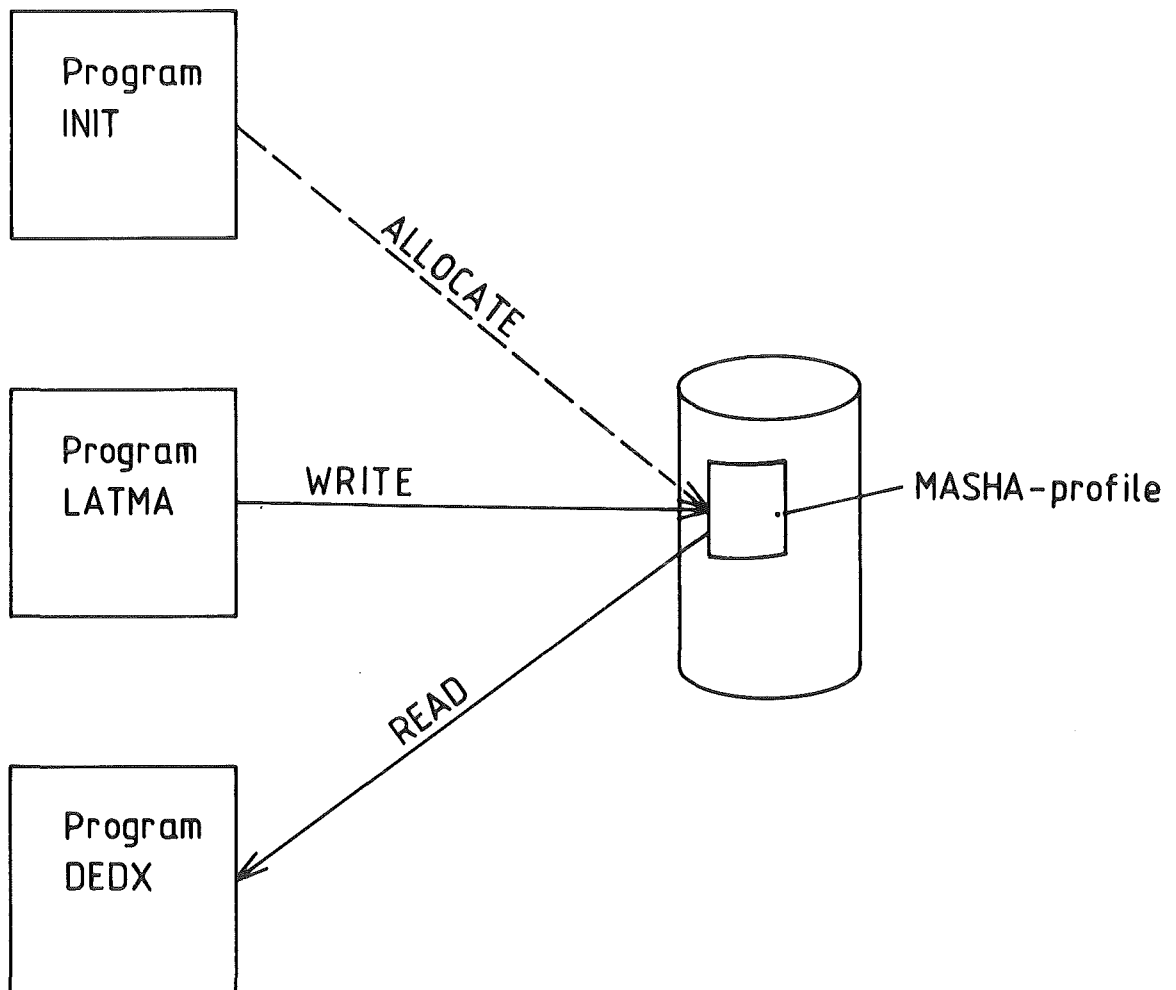
ALPHA - Electron thermal velocity  
EK - Projectile energy per nucleon  
XKSUM - Stopping number due to free electrons  
DEDX - Free electrons  $dE/dX$

If there are no bound electrons in equilibrium, a message is printed.

ZO - atomic number (6 for  $CD_2$ )  
ZFREE - Free electrons per atom (carbon for  $CD_2$ )  
ZB $\phi$ UND - bound electrons per atom (carbon for  $CD_2$ )  
BDEUT - Bound electrons in D (for  $CD_2$ )  
ZFRET - Total number of free electrons (for  $CD_2$ )  
DET $\phi$ T - Total  $dE/dX$   
DEFEL - total  $dE/dX$  due to free electrons  
DEBND -  $dE/dX$  due to bound electrons (in carbon for  $CD_2$ )  
DEDEUT -  $dE/dx$  due to bound electrons in D for  $CD_2$

## 8.3 Flow charts

Fig.13: Connection between the 3 programs and the MASHA - profile



Program INIT allocates a new MASHA -profile

Program LATMA writes his results to this dataset

Program DEDX reads the data produced by LATMA

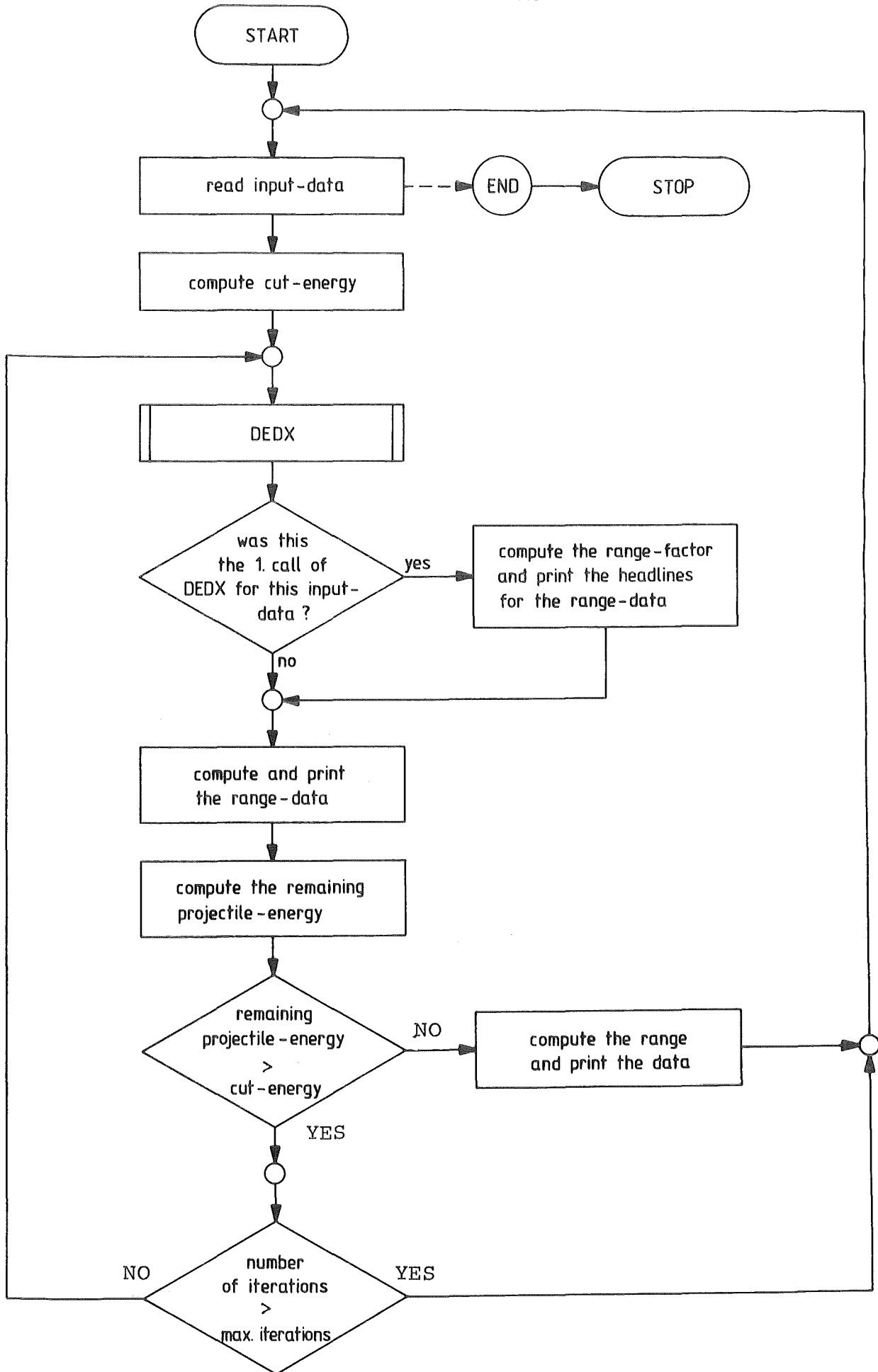


Fig.14

# GENERAL FLOW CHART OF GORGON CODE

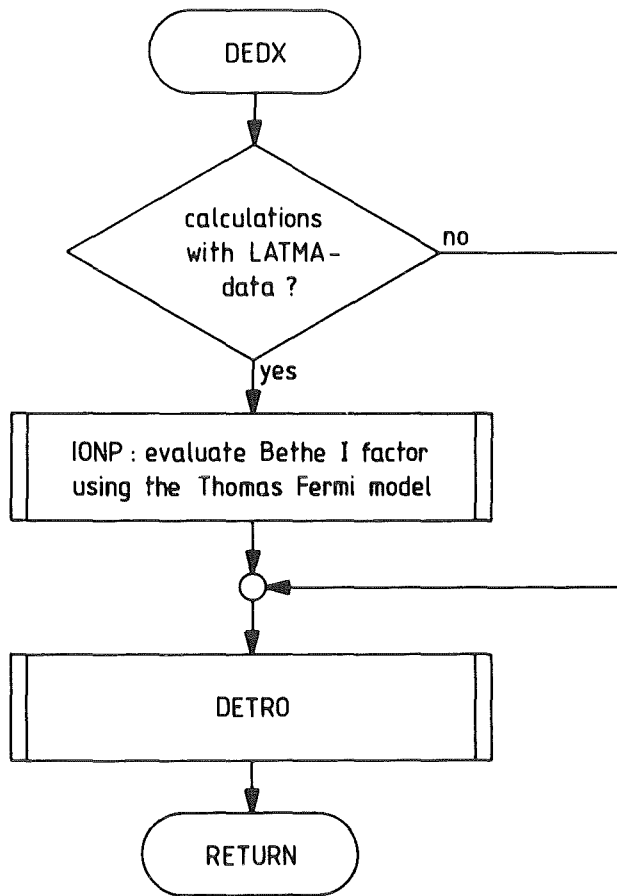


Fig.15 FLOW CHART FOR DEDX

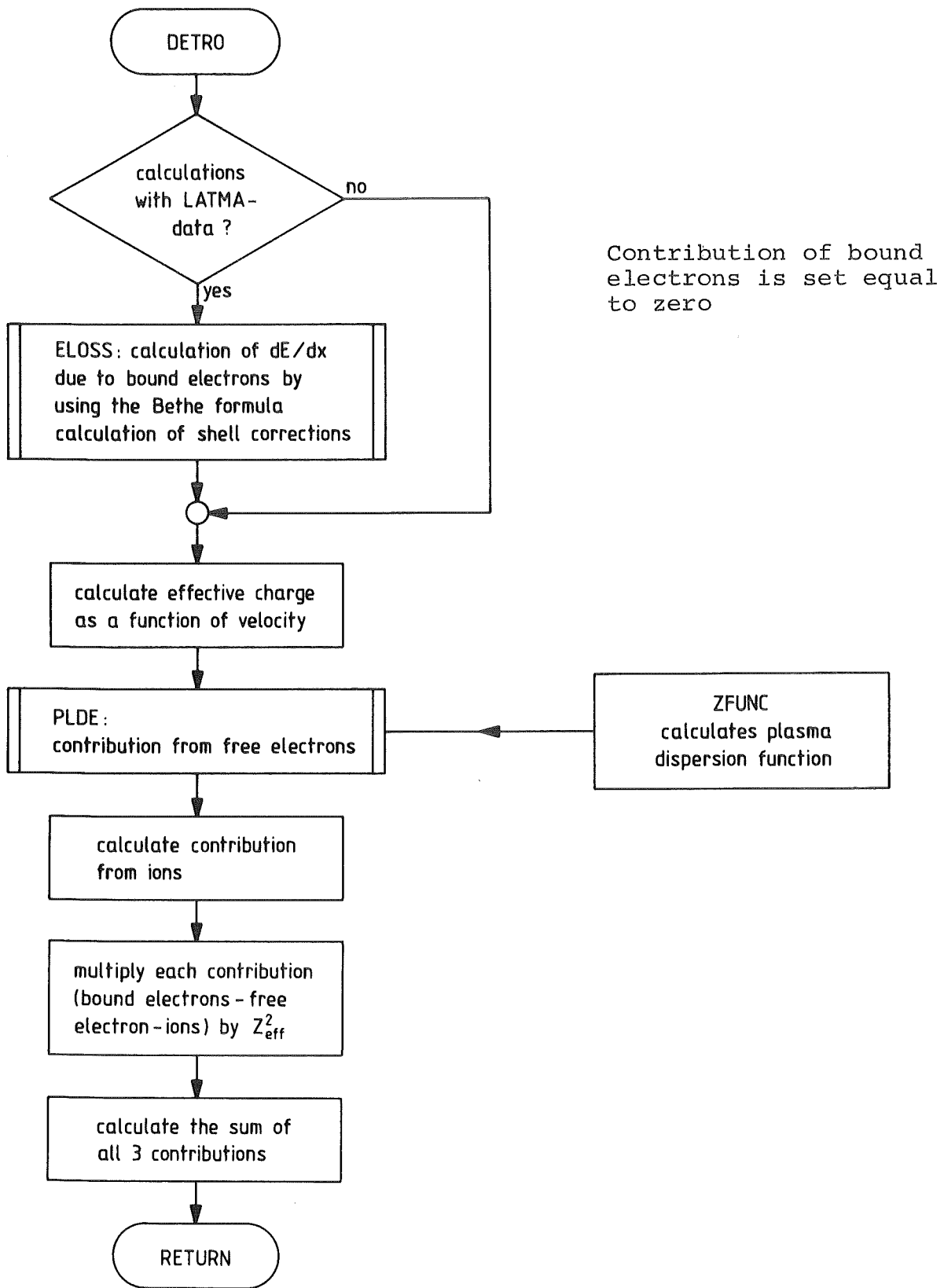


Fig. 16

# FLOW CHART FOR DETRO

#### 8.4 Description of Subroutines

The LATMA code essentially integrates the Thomas Fermi equation (3.18) and has a very linear structure. On the other hand the code GORGON which calculates the energy loss using data from the LATMA code is more complicated in function and structure. It is useful therefore to regard the LATMA code as providing the input data for the main energy loss program. At the present time for each  $dE/dX$  run at a constant density and temperature, the Thomas-Fermi model is solved and the data is stored on a tape. This information is then recalled when needed by the energy loss program. It would be clearly much more flexible if the codes were directly coupled. Then if the density and temperature remained the same, only one LATMA calculation need to be done, but if the density and temperature changed then the LATMA program would be recalled. It is clear that the first method can save time if one continually calculates with one density and temperature or a set of densities and temperatures, but in general it is not possible to set up files for all the materials densities and temperatures that are needed.

The energy loss program GORGON is controlled by the subroutine MAIN. This sets the cut-off energy below which the program does not calculate. Then it calls the  $dEdX$  subroutine which controls the calculation of the total  $DEDX$ . It then calculates the loss of energy in this step using the range factor which has either been given as input or is calculated from the first  $dEDX$  value. This is repeated until the energy drops below the cut-off energy. At the same time the total range is computed. The subroutine  $DEDX$  controls the use of various options and then calls IONP which calculates the Bethe I factor and DETRO which controls in more detail the energy loss calculation. This subroutine calculates the effective charge as a function of the velocity of the projectile and the temperature of the plasma. It calls ELOSS which calculates the energy loss due to bound electrons, PLDE which calculates the free electron contribution and the ion contribution. All of these contributions are

multiplied by the effective charge squared. The total value of  $DE/DX$  is then evaluated.

In the subroutine PLDE the energy loss due to free electrons is calculated. It tests whether the plasma is degenerate or non-degenerate and calculate accordingly. It evaluates the dielectric function integral in the stopping power formula for free electrons (4.14), and also calculates the ion contribution to the stopping power. The subroutine ZPRIME calculates the plasma dielectric function.

IONP calculates the value of the Bethe I parameter using the solution of the Thomas Fermi model obtained from LATMA.

The subroutone ELOSS then uses this value to calculate the energy loss due to bound electrons.

## 9. Results of a Sample Problem

### 9.1 Description of Sample problem.

The sample problem chosen was used in actual pellet calculations /30, 33,34,60/. It is the case of a 10 GeV  $\text{Bi}^{++}$  ion slowing down in solid density lead at a temperature of 200 eV. In the first step of the calculation the LATMA program is run in order to calculate the Thomas-Fermi data (chemical potential, electron density etc.) of solid lead at 200 eV. This data is then stored in a MASHA profile. The DEDX program reads this data and from it, and calculates the Bethe Parameter. For this case the output of the DEDX program is given and the results obtained are discussed in 10.6.

## 9.2 Sample Problem : Method of operation and physics input

A DEDX-run is done in 3 steps.

- 1.) Initialisation of a MASHA-profile dataset (Fig.1)
- 2.) Execution of a LATMA-run to calculate the chemical potential and the electrons density  
(Fig. 18 , Fig. 19, Fig. 20, Fig. 21)
- 3.) Execution of a DEDX-run  
(Fig. 22, Fig. 23, Fig. 24, Fig. 25)

In this sample problem we have Bi-projectiles and Pb-target-material.

Projectile atomic number	ZPRJ = 83
Projectile atomic weight	AM = 209
Projectile initial energy	EPRJ = 10 GeV

Target atomic number	ZO = 82
Target density	RØ = 11.2 g/cc
Target temperature	XKT = 200 eV
Target atomic weight	AMU = 207

```

//INR67020 JOB (0670,101,POD7N),MORITZ,MSGLEVEL=(1,1),REGION=1024K,      000100
// NOTIFY=INR670                                                            000200
//*****                                                                    000300
//**                                                                           000400
//**      THIS JOB INITIALIZES A MASHA-PROFILE FOR A LATMA-RUN.              000500
//**      I U M A S H IS A FORTRAN-UNIT-NUMBER, TO WHICH THE PROFILE IS      000600
//**      ALLOCATED. FOR THIS FORTRAN-UNIT-NUMBER THERE MUST BE A DD-CARD    000700
//**      IN THE G-STEP.                                                       000800
//**      IN THE SPACE-PARAMETER ON THE DD-CARD, THE NUMBER OF BLOCKS       000900
//**      MUST BE EQUAL TO THE VARIABLE I R E C N O, WHICH CONTAINS THE     001000
//**      NUMBER OF RECORDS IN THE DATASET.                                   001100
//**      THE INITIALIZATION IS DONE BY WRITING THE TEXT 'PROFILE-END'     001110
//**      INTO THE FIRST RECORD OF THE DATASET.                               001120
/*                                                                           001200
// EXEC FHCLG                                                                001300
//C.SYSIN DD *                                                                001400
    REAL*8 PEND(2)                                                            001500
    DATA PEND/'PROFILE-', 'END'      '/'                                    001600
    IUMASH=10                                                                    001700
    IRECNO=62                                                                    001800
    CALL DEFI(IUMASH,IRECNO,4HU      ,3200,IVAR)                               001900
    WRITE(IUMASH'1)PEND(1),PEND(2)      002000
    STOP                                                                           002100
    END                                                                           002200
/*                                                                           002300
//G.FT10FOO1 DD DSN=INR670.MASHA20.PROFILE,DISP=(NEW,CATLG),UNIT=DISK,    002400
// VOL=SER=BAT00C,SPACE=(12800,62)                                          002500
//                                                                           002600

```

Fig. 17

Job to initialize a MASHA-profile dataset.  
 The name of the dataset is INR670.MASHA20.PROFILE  
 and it contains 62 Blocks (see SPACE-parameter and variable  
 IRECNO). This job produces no output-messages.

9.3 Sample Problem : Input for LATMA

```

//INR670LA JOB (0670,101,POD7N),MCRITZ,MSGLEVEL=(1,1),REGION=1024K, 000100
// NOTIFY=INR670 000200
//*MAIN LINES=10 000300
// EXEC FHG,NAME=LANEW2 000400
//STEPLIB DD DSN=INR670.ZION.LOAD,DISP=SHR 000500
//G.FT06FOO1 DD SYSOUT=R 000600
//G.FT10FOO1 DD DISP=OLD,DSN=INR670.MASHA20.PROFILE 000610
//*****000700
//** 000800
//** INPUT FOR PROGRAM LATMA 000900
//** ----- 001000
//** 001100
//** 1. CARD: IUMASH IRECNO IMESHP 001200
//** N. CARD: ZO RO XKT AMU 001300
//** 001400
//** IUMASH UNIT-NUMBER OF THE MASHA-PROFILE (INTEGER) 001500
//** IRECNO NUMBER OF RECORDS IN THE MASHA-PROFILE (INTEGER) 001600
//** FOR EACH INPUT-CARD WITH THE DATA 'ZO-RO-XKT-AMU' , 001700
//** 3 RECORDS ARE NEEDED IN THE MASHA PROFILE. 001800
//** 1 ADDITIONAL RECORD IS NEEDED FOR THE END-RECORD 001900
//** EXAMPLE: IF YOU HAVE 7 INPUT-CARDS ==> N=5 002000
//** 1 CARD WITH THE DATA 'IUMASH-IRECNO-IMESHP' 002100
//** 6 CARDS WITH THE DATA 'ZO-RO-XKT-AMU' EACH 002200
//** IRECNO MUST BE MIN. (N-1)*3 + 1 002300
//** IMESHP NUMBER OF MESH-POINTS (INTEGER) 002400
//** 002500
//** ZO TARGET ATOMIC NUMBER (DOUBLE PRECISION) 002600
//** RO TARGET DENSITY (DOUBLE PRECISION) 002700
//** XKT TARGET TEMPERATURE (DOUBLE PRECISION) 002800
//** AMU TARGET ATOMIC WEIGHT (DOUBLE PRECISION) 002900
//**-----003000
//** 003100
//** BEFORE A LATMA-RUN CAN BE STARTED, THE MASHA-PROFILE MUST BE 003200
//** CREATED. THIS CAN BE DONE WITH THE JCL IN THE MEMBER INIT. 003300
//** THE 'NUMBER OF RECORDS' (2. PARAMETER IN THE INPUT FOR THIS JOB 003400
//** - IRECNO), MUST BE THE SAME AS IN THE MEMBER INIT. 003500
//** ALSO THE UNIT-NUMBERS IUMASH MUST BE THE SAME. 003600
//** 003700
//*****003800
//G.SYSIN DD * 003900
 10 62 115 004000
 82.0D+0 11.2D+0 0.1D+0 207.0D+0 004100
 82.0D+0 11.2D+0 0.2D+0 207.0D+0 004200
 82.0D+0 11.2D+0 0.3D+0 207.0D+0 004300
 82.0D+0 11.2D+0 0.4D+0 207.0D+0 004400
 82.0D+0 11.2D+0 0.5D+0 207.0D+0 004500
 82.0D+0 11.2D+0 0.6D+0 207.0D+0 004600
/* 006100
// 006200

```

Fig. 18

- JCL to start a LATMA-run.
- This job calculates the chemical potential and the electron density for 6 temperatures (100eV,200eV.....600eV).
- The material is Pb with a density of 11.2 g/cc.

### 9.4 Sample Problem : Output of LATMA

```

INITIAL DATA:      ZO = 0.82000D+02      RO = 0.11200D+02      XKT = 0.20000D+00      AMU = 0.20700D+03

ARO = 0.19425D+01      PHIO = 0.30416D+01      A = 0.65221D+02

XMU      = -0.41000D+01
PHI1     = -0.40640D+01      PHI2     = -0.40640D+01
XIO      = 0.14602D-01      XII      = 0.14602D-01      DXI      = -0.60997D-04
P(NN-1)  = 0.12641D-03      Q(NN-1)  = 0.12531D-03

XMU      = -0.39271D+01
PHI1     = -0.38926D+01      PHI2     = -0.38926D+01
XIO      = 0.17340D-01      XII      = 0.17340D-01      DXI      = -0.85922D-04
P(NN-1)  = 0.15011D-03      Q(NN-1)  = 0.14880D-03
IX       = 2
PHIO     = 0.30416D+01      DEL      = 0.82393D+00
OLDXMU   = -0.39271D+01      XMU      = -0.27860D+01      OLDPHI   = 0.41159D+00      PHIB     = 0.53552D+00
DELPHI   = 0.17369D+01      DMU      = 0.17294D+00      DPHI     = 0.26323D+00      DEL1     = 0.65698D+00

XMU      = -0.27860D+01
PHI1     = -0.27614D+01      PHI2     = -0.27614D+01
XIO      = 0.53500D-01      XII      = 0.53507D-01      DXI      = -0.80648D-03
P(NN-1)  = 0.46316D-03      Q(NN-1)  = 0.45913D-03
IX       = 3
PHIO     = 0.30416D+01      DEL      = -0.32831D+01
OLDXMU   = -0.27860D+01      XMU      = -0.33061D+01      OLDPHI   = 0.53552D+00      PHIB     = 0.13027D+02
DELPHI   = -0.14547D+01      DMU      = 0.11411D+01      DPHI     = 0.31916D+01      DEL1     = 0.35754D+00

XMU      = -0.33061D+01
PHI1     = -0.32770D+01      PHI2     = -0.32770D+01
XIO      = 0.32076D-01      XII      = 0.32079D-01      DXI      = -0.29234D-03
P(NN-1)  = 0.27769D-03      Q(NN-1)  = 0.27527D-03
IX       = 4
PHIO     = 0.30416D+01      DEL      = 0.35672D+00
OLDXMU   = -0.33061D+01      XMU      = -0.31850D+01      OLDPHI   = 0.13027D+02      PHIB     = 0.19566D+01
DELPHI   = 0.44117D+00      DMU      = -0.52010D+00      DPHI     = -0.18958D+01      DEL1     = 0.27434D+00

XMU      = -0.31850D+01
PHI1     = -0.31570D+01      PHI2     = -0.31570D+01
XIO      = 0.36145D-01      XII      = 0.36148D-01      DXI      = -0.37060D-03
P(NN-1)  = 0.31291D-03      Q(NN-1)  = 0.31019D-03
IX       = 5
PHIO     = 0.30416D+01      DEL      = 0.85647D-01
OLDXMU   = -0.31850D+01      XMU      = -0.31542D+01      OLDPHI   = 0.19566D+01      PHIB     = 0.27811D+01
DELPHI   = 0.89539D-01      DMU      = 0.12103D+00      DPHI     = 0.35163D+00      DEL1     = 0.34419D+00

XMU      = -0.31542D+01
PHI1     = -0.31265D+01      PHI2     = -0.31265D+01
XIO      = 0.37259D-01      XII      = 0.37263D-01      DXI      = -0.39364D-03
P(NN-1)  = 0.32256D-03      Q(NN-1)  = 0.31975D-03
IX       = 6
PHIO     = 0.30416D+01      DEL      = -0.71984D-02
OLDXMU   = -0.31542D+01      XMU      = -0.31565D+01      OLDPHI   = 0.27811D+01      PHIB     = 0.30635D+01
DELPHI   = -0.71726D-02      DMU      = 0.30819D-01      DPHI     = 0.96711D-01      DEL1     = 0.31867D+00

XMU      = -0.31565D+01
PHI1     = -0.31287D+01      PHI2     = -0.31287D+01
XIO      = 0.37176D-01      XII      = 0.37179D-01      DXI      = -0.39188D-03
    
```

Fig. 19

$$P(NN-1) = 0.32184D-03 \quad Q(NN-1) = 0.31903D-03$$

$$\text{NUMBER OF ELECTRONS} = 0.82568D+02$$

$$\text{NUMBER OF BOUND ELECTRONS} = 0.56975D+02$$

$$\text{CORRECTED NUMBER OF BOUND ELECTRONS} = 0.56583D+02$$

$$\text{CORRECTED NUMBER OF FREE ELECTRONS} = 0.25417D+02$$

$$\text{FREERO} = 0.82787D+24$$

1	0.59857D-32	0.28418D+33
2	0.14947D-03	0.25260D+32
3	0.59787D-03	0.59534D+31
4	0.13452D-02	0.21941D+31
5	0.23915D-02	0.10218D+31
6	0.37367D-02	0.54820D+30
7	0.53808D-02	0.32314D+30
8	0.73239D-02	0.20361D+30
9	0.95659D-02	0.13481D+30
10	0.12107D-01	0.92712D+29
11	0.14947D-01	0.65705D+29
12	0.18086D-01	0.47708D+29
13	0.21523D-01	0.35377D+29
14	0.25260D-01	0.26613D+29
15	0.29296D-01	0.20326D+29
16	0.33630D-01	0.15712D+29
17	0.38264D-01	0.12272D+29
18	0.43196D-01	0.96715D+28
19	0.48427D-01	0.76827D+28
20	0.53958D-01	0.61454D+28
21	0.59787D-01	0.49461D+28
22	0.65915D-01	0.40026D+28
23	0.72342D-01	0.32550D+28
24	0.79068D-01	0.26585D+28
25	0.86093D-01	0.21797D+28
26	0.93417D-01	0.17933D+28
27	0.10104D+00	0.14800D+28
28	0.10896D+00	0.12246D+28
29	0.11718D+00	0.10157D+28
30	0.12570D+00	0.84414D+27
31	0.13452D+00	0.70271D+27
32	0.14364D+00	0.58574D+27
33	0.15305D+00	0.48874D+27
34	0.16277D+00	0.40806D+27
35	0.17278D+00	0.34081D+27
36	0.18310D+00	0.28463D+27
37	0.19271D+00	0.23762D+27
38	0.20462D+00	0.19823D+27
39	0.21583D+00	0.16521D+27
40	0.22734D+00	0.13751D+27
41	0.23915D+00	0.11429D+27
42	0.25125D+00	0.94846D+26
43	0.26366D+00	0.78595D+26
44	0.27636D+00	0.65047D+26
45	0.28937D+00	0.53787D+26
46	0.30267D+00	0.44461D+26
47	0.31627D+00	0.36763D+26
48	0.33017D+00	0.30429D+26
49	0.34437D+00	0.25231D+26
50	0.35887D+00	0.20974D+26

Fig.20

51	0.373670+00	0.174900+26
52	0.388760+00	0.146380+26
53	0.404160+00	0.123010+26
54	0.419850+00	0.103810+26
55	0.435850+00	0.879940+25
56	0.452140+00	0.749100+25
57	0.468730+00	0.640390+25
58	0.485620+00	0.549640+25
59	0.502810+00	0.473500+25
60	0.520300+00	0.409300+25
61	0.538080+00	0.354870+25
62	0.556170+00	0.308490+25
63	0.574550+00	0.268760+25
64	0.593240+00	0.234560+25
65	0.612220+00	0.204960+25
66	0.631500+00	0.179240+25
67	0.651080+00	0.156770+25
68	0.670960+00	0.137080+25
69	0.691140+00	0.119750+25
70	0.711610+00	0.104430+25
71	0.732390+00	0.908340+24
72	0.753460+00	0.787300+24
73	0.774840+00	0.679130+24
74	0.796510+00	0.582230+24
75	0.818480+00	0.495100+24
76	0.840750+00	0.416600+24
77	0.863320+00	0.345630+24
78	0.886190+00	0.281380+24
79	0.909360+00	0.223000+24
80	0.932830+00	0.169910+24
81	0.956590+00	0.121490+24
82	0.980650+00	0.772820+23
83	0.100500+01	0.368150+23

XMU = -0.631300+00

WRITING DATA ON MASHA PROFILE WAS FINISHED, NEXT RECORD IS 23

SUM = -0.3945740+03  
WSUM = 0.5711480+02

Fig. 21

---

Fig. 19 to Fig. 21 the output of a LATMA-run for Pb with a density of 11.2 g/cc and a temperature of 200eV.

9.5 Sample Problem: Input and Output for GORGON

```
//INR670DX JOB (0670,101,P0D7N),MCRITZ,MSGLLEVEL=(1,1),REGION=1024K, 000100
// NCTIFY=INR670,TIME=10 000200
//*MAIN LINES=99 000210
//*****000300
//** 000400
//** INPUT FOR THE PROGRAM GORGON 000500
//** ----- 000600
//** 000700
//** ==>THE INPUT-CARDS CAN BE REPEATED SEVERAL TIMES<== 000800
//** 000900
//** IUMASH IRECNO IURANG RFINO 001000
//** IDLEV IUTEST IDVERS MAXIT 001100
//** ZPRJ AM EPRJ FREELI ECUTF ZBEFI 001200
//** ZO RC XKT AMU 001300
//** 001400
//** IUMASH UNIT-NUMBER OF THE MASHA-PROFILE (INTEGER) 001500
//** IRECNO NUMBER OF RECORDS IN THE MASHA-PROFILE (INTEGER) 001600
//** IURANG UNIT-NUMBER OF A OUTPUT-DATASET WHICH WILL CONTAIN THE 001700
//** DATA OF THE RANGE (INTEGER) 001800
//** RFINO IF POSITIVE ==> INDEX TO COMPUTE THE RANGE-FACTOR 001900
//** RANGE-FACTOR = EPRJ/(DE/DX*RFINO) 002000
//** IF NEGATIVE ==> VALUE = RANGE-FACTOR 002100
//** (DOUBLE PRECISION) 002200
//** 002300
//** IDLEV TESTLEVEL-IDENTIFIER (INTEGER) 002400
//** = 0 ==> NO TEST-PRINTOUT 002500
//** = 1 ==> TEST-PRINTOUT ON UNIT IUTEST 002600
//** = 2 ==> MORE TEST-PRINTOUT ON UNIT IUTEST 002610
//** IUTEST UNIT-NUMBER OF A OUTPUT-DATASET WHICH WILL CONTAIN THE 002700
//** TEST-PRINTOUT (INTEGER) 002800
//** (ONLY NEEDED , IF IDLEV .EQ. 1 , OTHERWISE 0) 002900
//** IDVERS IDENTIFIER FOR THE VERSION, WITH WHICH THE 003000
//** CALCULATIONS SHOULD BE DONE (INTEGER) 003100
//** = 1 ==> STANDARD-VERSION 003200
//** = 2 ==> VERSION WITHOUT LATMA-DATA 003300
//** MAXIT MAX. NUMBER OF ITERATIONS TO BE EXECUTED (INTEGER) 003400
//** 003500
//** ZPRJ PROJECTILE CHARGE STATE (DOUBLE PRECISION) 003600
//** AM PROJECTILE ATOMIC WEIGHT (DOUBLE PRECISION) 003700
//** EPRJ PROJECTILE INITIAL ENERGIE IN KEV (DOUBLE PRECISION) 003800
//** FREELI NUMBER OF FREE ELECTRONS/ATOM (DOUBLE PRECISION) 003900
//** (ONLY NEEDED , IF IDVERS .EQ. 2 , OTHERWISE 0.0D+0) 004000
//** ECUTF FACTOR TO COMPUTE THE CUT-ENERGY (DOUBLE PRECISION) 004100
//** ECUT = EPRJ/ECUTF 004110
//** IF THE PROJECTILE ENERGY IS LESS THAN THE CUT-ENERGY, 004120
//** THE JOB IS TERMINATED 004130
//** ZBEFI INPUT VALUE FOR EFF. CHARGE (DOUBLE PRECISION) 004140
//** = 1.0D+0 ==> THIS VALUE IS ONLY TAKEN, IF THE COMPUTED 004150
//** 'ZBEF' IN SUBROUTINE DETRC IS LESS THAN 004160
//** 1.0D+0 004170
//** > 1.0D+0 ==> THE VARIABLE 'ZBEF' IN SUBROUTINE DETRC IS 004180
//** SET TO THIS VALUE 004190
//** 004200
//** ZO TARGET ATOMIC NUMBER (DOUBLE PRECISION) 004300
//** RO TARGET DENSITY IN G/CC (DOUBLE PRECISION) 004400
//** XKT TARGET TEMPERATURE IN KEV (DOUBLE PRECISION) 004500
//** AMU TARGET ATOMIC WEIGHT (DOUBLE PRECISION) 004600
//** ----- 004700
//** 004800
```

Fig. 22

```
/** BEFORE A DEDX-RUN CAN BE STARTED, A MASHA-PRCFILE MUST BE          004900
/** CREATED BY THE PROGRAM LATMA.                                       005000
/** THE INPUT-VARIABLES ZO RO XKT AMU AND IUMASH MUST HAVE THE SAME     005100
/** VALUES AS IN THE LATMA-RUN.                                         005200
/** IN THE G-STEP FOR THIS JOB THERE MUST BE ONE DD-CARD FOR THE       005300
/** MASHA-PROFILE ON UNIT IUMASH (PARAMETERS ON THE DD-CARD MUST BE     005400
/** THE SAME AS IN THE LATMA-RUN) AND ONE DD-CARD FOR UNIT IURANG,     005500
/** WHICH SPECIFIES THE OUTPUT-DATASET FOR THE RANGE-DATA AND ONE      005600
/** DD-CARD FOR UNIT IUTEST, WHICH SPECIFIES THE OUTPUT-DATASET FOR    005700
/** THE TEST-PRINTOUT.                                                  005800
/** THE PARAMETERS FOR THE LAST 2 DD-CARDS SHOULD BE:                   005900
/** FT..FOO1 DD SYSCUT=A,DCB=(LRECL=133,BLKSIZE=3857,RECFM=FBA)       006000
/**                                                                      006100
/*******006200
// EXEC FHG,NAME=CENEW2                                                006400
//STEPLIB DD DSN=INR670.7TON.LOAD,DISP=SHR                             006500
//G.FT10FCO1 DD DISP=OLD,DSN=INR670.MASHA20.PRCFILE                   006600
//G.FT20FOO1 DD SYSCUT=A,DCB=(LRECL=133,BLKSIZE=3857,RECFM=FBA)     006700
//G.SYSIN CD *                                                         006900
    10          62          20          80                             007000
    0           0           1          150                           007100
    83.0D+0    209.0D+0    1.0D+7    0.0D+0    1000.0D+0    1.0D+0    007200
    82.0D+0    11.2D+0    0.2D+0    207.0D+0                             007300
/*                                                                      007480
//                                                                      007500
```

Fig. 23

Fig. 22 and Fig. 23 is the JCL to start a GORGON-run

VERSION-IDENTIFIER IS 1 TESTLEVEL-IDENTIFIER IS 0 CUT-ENERGY IS 0.100000+05 INPUT FOR EFF. CHARGE IS .100000+01

PROJECTILE CHARGE STATE = 0.830000+02  
PROJECTILE ATOMIC WEIGHT = 0.209000+03  
PROJECTILE INITIAL ENERGY = 0.100000+08

PROFILE GIVEN BY: TARGET ATOMIC NUMBER = 0.820000+02  
TARGET DENSITY = 0.117000+02  
TARGET TEMPERATURE = 0.200000+00  
TARGET ATOMIC WEIGHT = 0.207000+03

MASHA PROFILE FOUND: CHEMICAL POTENTIAL = -0.631300+00  
FREE ELECTRONS = 0.254170+02

PROJECTILE ENERGY = 0.100000+08

NO SHELL EFFECTS ASSUMED:  
-----

BOUND ELECTRONS = 0.561930+02  
BETHE'S I = 0.145740+01

SHELL CORRECTIONS:  
-----

EFFECTIVE ELECTRONS = 0.545900+02  
BETHE'S I = 0.123920+01

DE/DX BY BOUND ELECTRONS USING THE THOMAS FERMI MODEL = 0.352030+04

DIELECTRIC FUNCTION INTEGRAL = 0.376590+01  
FREE ELECTRON CONTRIBUTION = 0.276530+04

NUMBER OF FREE ELECTRONS/ATOM = 0.254170+02  
NUMBER OF BOUND ELECTRONS/ATOM = 0.565830+02

DE/DX BY TOTAL ELECTRONS = 0.329410+03  
DE/DX BY FREE ELECTRONS = 0.145510+03  
DE/DX BY BOUND ELECTRONS = 0.183900+03  
DE/DX BY ION SCATTERING = 0.0

I

II

Fig. 24

PROJECTILE CHARGE STATE = 0.83000D+02  
 PROJECTILE ATOMIC WEIGHT = 0.20900D+03  
 PROJECTILE INITIAL ENERGY = 0.10000D+08

PROFILE GIVEN BY: TARGET ATOMIC NUMBER = 0.82000D+02  
 TARGET DENSITY = 0.11200D+02  
 TARGET TEMPERATURE = 0.20000D+00  
 TARGET ATOMIC WEIGHT = 0.20700D+03

RANGE-FACTOR = 0.37947D-02

	ENERGY(KEV)	DELTA E(KEV)	DE/CX BY TCTAL ELECTRONS
1	0.10000D+08	0.12500D+06	0.32941D+08
2	0.98750D+07	0.12575D+06	0.33138D+08
3	0.97493D+07	0.12651D+06	0.33338D+08
4	0.96227D+07	0.12729D+06	0.33543D+08
5	0.94955D+07	0.12808D+06	0.33752D+08
6	0.93674D+07	0.12890D+06	0.33969D+08
7	0.92385D+07	0.13009D+06	0.34202D+08
8	0.91084D+07	0.13203D+06	0.34792D+08
9	0.89764D+07	0.13290D+06	0.35023D+08
10	0.88435D+07	0.13377D+06	0.35292D+08
11	0.87097D+07	0.13468D+06	0.35492D+08
12	0.85750D+07	0.13561D+06	0.35737D+08
13	0.84394D+07	0.13656D+06	0.35988D+08
14	0.83028D+07	0.13753D+06	0.36243D+08
15	0.81653D+07	0.13852D+06	0.36504D+08
16	0.80268D+07	0.13955D+06	0.36776D+08
17	0.78872D+07	0.14207D+06	0.37439D+08
18	0.77452D+07	0.14315D+06	0.37725D+08
19	0.76020D+07	0.14426D+06	0.38016D+08
20	0.74577D+07	0.14539D+06	0.38314D+08
21	0.73123D+07	0.14655D+06	0.38620D+08
22	0.71658D+07	0.14773D+06	0.38932D+08
23	0.70181D+07	0.14895D+06	0.39253D+08
24	0.68691D+07	0.15050D+06	0.39661D+08
25	0.67186D+07	0.15300D+06	0.40320D+08
26	0.65656D+07	0.15434D+06	0.40672D+08
27	0.64113D+07	0.15568D+06	0.41025D+08
28	0.62556D+07	0.15709D+06	0.41396D+08
29	0.60985D+07	0.15854D+06	0.41790D+08
30	0.59400D+07	0.16155D+06	0.42573D+08
31	0.57784D+07	0.16311D+06	0.42983D+08
32	0.56153D+07	0.16471D+06	0.43404D+08
33	0.54506D+07	0.16635D+06	0.43837D+08
34	0.52842D+07	0.16957D+06	0.44687D+08
35	0.51147D+07	0.17134D+06	0.45154D+08
36	0.49433D+07	0.17316D+06	0.45633D+08
37	0.47702D+07	0.17506D+06	0.46133D+08
38	0.45951D+07	0.17848D+06	0.47035D+08
39	0.44166D+07	0.18051D+06	0.47569D+08
40	0.42361D+07	0.18270D+06	0.48145D+08
41	0.40534D+07	0.18630D+06	0.49093D+08
42	0.38671D+07	0.18855D+06	0.49686D+08
43	0.36786D+07	0.19238D+06	0.50697D+08
44	0.34862D+07	0.19476D+06	0.51325D+08
45	0.32914D+07	0.19876D+06	0.52379D+08
46	0.30927D+07	0.20283D+06	0.53452D+08
47	0.28898D+07	0.20551D+06	0.54157D+08
48	0.26843D+07	0.20966D+06	0.55250D+08
49	0.24747D+07	0.21391D+06	0.56371D+08
50	0.22607D+07	0.21816D+06	0.57491D+08
51	0.20426D+07	0.22086D+06	0.58203D+08
52	0.18217D+07	0.22344D+06	0.58882D+08
53	0.15983D+07	0.22566D+06	0.59468D+08
54	0.13726D+07	0.22738D+06	0.59920D+08
55	0.11452D+07	0.22831D+06	0.60167D+08
56	0.91693D+06	0.22797D+06	0.60077D+08
57	0.68895D+06	0.22536D+06	0.59387D+08
58	0.46360D+06	0.21765D+06	0.57355D+08
59	0.24595D+06	0.19160D+06	0.50490D+08
60	0.54357D+05	0.92141D+05	0.24282D+08

RANGE = 0.22389D+00

Fig.25

Fig. 24 and Fig. 25 is the output of a GORGON-job.

Part I in Fig. 24 is printed only one time.

Part II in Fig. 25 is printed for every energy, for which the GORGON-run was started.

If a GORGON-run has finished for one energy,  $\Delta E$  is subtracted from the energy and new run is started with the remaining energy

Fig. 25 shows the results of a calculation of the range.

## 9.6 Discussion of Results of test Problem:

The test problem is chosen to be that of a Bismuth ion travelling through lead. Therefore, the projectile atomic number is 83, the atomic weight is 209 (more accuracy than this is not justified) and the initial energy is 10 GeV. In the target material the atomic number is 82, the target density is 11.2 g/cc (solid density) and the target temperature is 200 eV, and target atomic weight is 207. Diagram 24 shows the output that is typically produced for each energy during its step by step reduction due to the energy loss. This output is reasonably self-explanatory. In Fig. 25 column 3 gives  $dE/dX$  (Total) in  $\text{KeV}\cdot\text{cm}^2/\text{gm}$  and column 2 gives the energy lost as the particle travels a distance of one range factor. Column 1 then gives the next energy. The total range is printed at the bottom and the calculated range factor is shown at the top.

Fig. 26 shows the calculated results for Bismuth ions (10 GeV) /30/ slowing down in lead for 200 eV all at solid density. They show the typical effect of range shortening due to ionization of electrons. The stopping power of free electrons is greater than /58/ that due to bound electrons. The deposition profiles also become more peaked as the temperature rises. This is an effect of the effective charge which is greater in the hot plasma. The deposition profile for heavy ions in cold materials is often constant. This is because the increase due to  $E^{-1}$  term in the Bethe formula is compensated by the decrease in  $Z_{\text{eff}}^2(V)$  as the velocity of the ion decreases. However due to the ionizing effect of the free electrons the  $Z_{\text{eff}}^2$  in a plasma remains reasonably high even when  $V$  decreases towards zero. Therefore Bragg peak familiar from light ion (proton) deposition curves reappears. A full discussion of the results obtainable by the code and the scope of results obtainable will be given in another report.

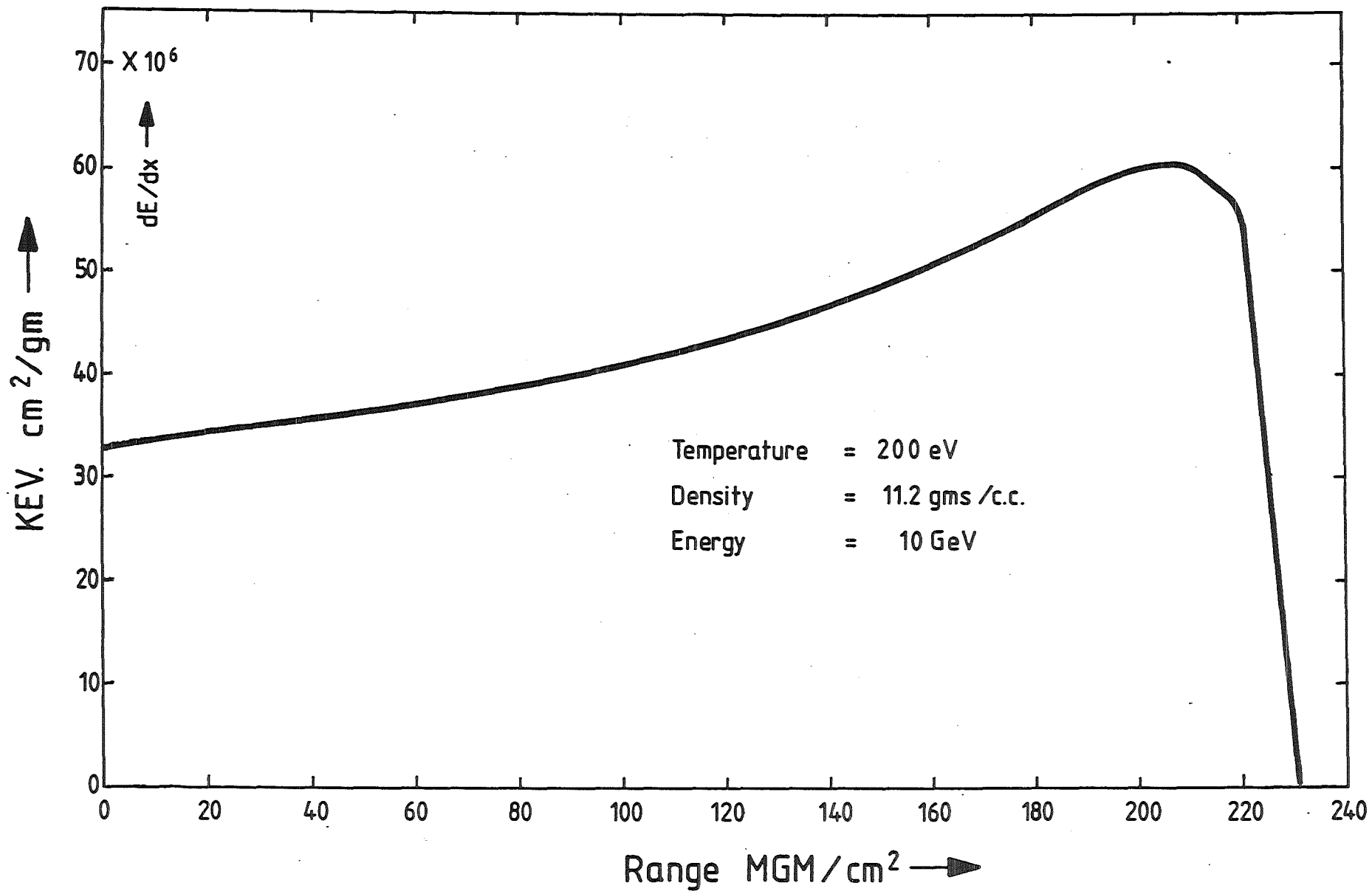


Fig.26: Stopping power of bismuth ions on lead

## 10. Conclusions

The GORGON code has been shown to be capable of calculating the stopping power of heavy and light ions in materials of any nuclear charge  $Z$ . The code in its present state can also calculate the stopping power of  $\alpha$ -particles,  $D^+$  and  $T^+$  ions in hot DT plasmas which are typically produced during the burn of ICF pellets. The code can thus be used to solve a large number of problems concerning the interaction of charged particles with matter in ICF pellet simulations

It has been already noted in various parts of this report that the physics in the code could be improved in various ways to make the calculation more accurate and to extend the codes range of validity.

In particular in very dense strongly coupled plasmas which one often has in laser or ion beam fusion it is likely that other theoretical approaches should be used. Further one needs a truly dynamic approach to the problem of calculating the effective charge on the ion which is losing energy. Also the treatment of slowing down in degenerate electron systems needs to be improved. The first two problems require a fairly large amount of work for their solution. In fact the first problem is still an unsolved problem as the theory of strongly coupled plasmas with partially ionized atoms is still far from being solved. Simple models such as the OCP (one component plasma model) are to an extent understood, but there has been little work on the problem of the stopping power in such systems, and in any case this model may be too oversimplified even to do accurate calculations in DT. The second problem has been treated, but involves the solution of time dependent rate equations. The third problem is easier to solve because there exists simple but reliable theories within the R.P.A. However if the electron plasma is a strongly coupled plasma there exists no well established model.

Finally the code running time is too long for a direct coupling to a sophisticated ion beam fusion code such as MEDUSA-KA. However it can be used to calibrate a simpler but very much faster

code (to be developed) which can be coupled efficiently to MEDUSA-KA. This joint code can then be used to study the interaction of ion beams with plane targets and the implosion and burn of ion beam driven targets.

### Acknowledgements

This work was originally undertaken in connection with the HIBALL reactor study directed by Professor Dr. G. Keßler. The authors would like to thank Dr. R. Fröhlich for reading the manuscript and making valuable comments. We would also like to thank Dr. Z. Zinamon for valuable conversations and help with some of the extensions to the code. Finally the authors would like to thank Frau F. Timke for typing this manuscript.

11. List of symbols used in report

(Code variables are discussed in sections dealing with each part of the code)

<u>Symbol</u>	<u>Description/dimensions</u>	<u>Page</u>
$\alpha$	$\alpha = \mu/kT$	25
$\bar{\alpha}$	$\bar{\alpha} = (9\pi/4)^{-1/3}$	51
$\beta$	$\beta = (kT)^{-1} \text{ ergs}^{-1}$	53
$\delta(x)$	Dirac delta function	36
$\Delta V$	Small volume element $\text{cm}^{-3}$	26
$\Delta N$	Small number of electrons	26
$\Delta \bar{w}_i$	Fluctuation in velocity of plasma particle perpendicular to ion beam, $\text{cm/sec}$	82
$\Delta \bar{w}_{//}$	Fluctuation in velocity of plasma particle parallel to ion beam $\text{cm/sec}$	82
$\epsilon$	Energy of an electron state, ergs.	24
$\hat{\epsilon}$	Dielectric function operator	36
$\epsilon(q, w)$	Wave vector and frequency dependent dielectric function	36
$\epsilon_F$	Fermi energy, ergs	51
$\epsilon_p$	Energy of electron with momentum $p$ , ergs	42
$\epsilon_p^{ex}$	Exchange contribution to single electron energy, ergs	43
$\epsilon_{max}$	Maximum energy transfer to atomic electron, ergs.	77
$\epsilon_p^{HF}$	Energy of electron in the Hartree-Fock approximation, ergs.	76

<u>Symbol</u>	<u>Description/Dimensions</u>	<u>Page</u>
$\zeta$	$\zeta = r/\lambda$	27
$\zeta_0$	$\zeta_0 = r_0/\lambda$	27
$\zeta^*$	Value of $\zeta > 0$	27
$\eta_{\underline{p}}$	Infinitesimally small real number Positive for $ \underline{p}  > p_F$ , negative for $ \underline{p}  < p_F$	49
$\eta$	Infinitesimally small positive real number	50
$\theta()$	Scattering angle-radians	68,76
$\theta(x)$	Heaviside function, $=1, x > 0,$ $=0, x < 0.$	46
$\bar{\theta}(x, iy)$	Function, (4.117).	63
$\theta_1$	Scattering angle corresponding to momentum transfer $g_1$ , radians.	74
$\theta_{max}$	Maximum angle of deflection of ion in collision with an atomic electron, radians.	77
$\lambda$	$\lambda = \lambda(T)$ , (3.19), cm.	27
$\bar{\lambda}$	Screening length in Thomas Fermi approximation, (4.80), cm.	55
$\Lambda_{free}$	$\ln \Lambda_{free}$ is the Coulomb logarithm for electrons	86
$\Lambda_i$	$\ln \Lambda_i$ is the Coulomb logarithm for ions	85
$\mu$	Chemical potential, ergs.	24
$\bar{\mu}$	$\bar{\mu} = \cos \theta$ . Angle between wave vector $\underline{k}$ and velocity of ion $\underline{v}$	24
$\mu_1$	$\mu_1 = 2m\mu$	53
$\mu_E$	Chemical potential of electrons in TF model, ergs.	53
$\mu_0$	$\mu_0 = m^2/n4\pi^2$ , gm.cm <sup>3</sup> .	38
$\tau$	Collision time, sec.	34
$\nu(v)$	Velocity dependent phenomenological collision frequency, sec <sup>-1</sup>	62
$\xi$	Complex variable	63
$\rho_0$	Solid density, gm/cc.	17
$\rho$	Density of material, gm/cc.	19
$\rho(\underline{x}, t)$	Charge density (operator) as a function of space and time, esu/cm <sup>3</sup> .	44
$\rho_{ext}(\underline{x}, t)$	External (to the system) charge den- sity, esu/cm <sup>3</sup> .	44

<u>Symbol</u>	<u>Description/Dimensions</u>	<u>Page</u>
$\rho_{\text{IND}}(\underline{x}, t)$	Induced charge density, esu/cm <sup>3</sup> .	44
$\rho_{\text{tot}}(\underline{x}, t)$	Total charge density, esu.	44
$\rho(\underline{q}, w)$	Fourier transform of charge density (esu/cm <sup>3</sup> )	45
$\phi(\underline{x})$	Error function (4.104)	61
$\bar{\phi}(\underline{x})$	Function, (6.7)	82
$\phi'$	$\phi' = \underline{g} / P_F$	53
$\phi(\underline{r}, t)$	Scalar potential of electric field	35
$\chi(\alpha)$	Function, (3.7)	25
$\chi'(\alpha)$	$\chi'(\alpha) = d\chi(\alpha)/d\alpha$	25
$\chi^0(\underline{q}, w, \beta)$	Fourier transform of susceptibility function for free electron gas.	52
$\chi$	$\chi^2 = e^2 / \pi \hbar v_F$	51
$\bar{\chi}$	deflection angle due to scattering, radians.	81
$\psi(\underline{r})$	Total potential inside a quasiatom in the Thomas Fermi model, ergs.	25
$\psi_E(\underline{r})$	Electron contribution to $\psi(\underline{r})$ , ergs.	25
$\psi_N(\underline{r})$	Nuclear contribution to $\psi(\underline{r})$ , ergs.	25
$\psi_{\underline{p}}(\underline{r})$	Plane wave function of a particle with momentum $\underline{p}$ .	67
$\psi_0(\underline{r})$	Ground state wave function of an atom	67
$\psi_n(\underline{r})$	Excited state wave function of an atom	67
$\psi_E^*(\underline{r})$	Electron part of Thomas Fermi potential excluding self energy, ergs.	31
$a$	interatomic distance $\sim 10^{-8}$ cm.	35
$a_n$	$n = -\infty, \dots, \infty$ . Coefficients in series expansion, (4.74).	54
$a_{\underline{p}}^+$	2nd quantization creation-operator for momentum state $\underline{p}$ .	46
$a_{\underline{p}}$	2nd quantization destruction operator for momentum state $\underline{p}$ .	46
$\bar{a}_0$	Bohr radius, cm.	41
$A$	Atomic weight.	34
$A_0$	constant, (6.6)	82
$A_1$	Atomic weight of ion which is slowing down.	85
$A_2$	Atomic weight of plasma ion in stopping medium.	85

<u>Symbol</u>	<u>Description/Dimensions</u>	<u>Page</u>
B	Isothermal compressibility = $(\partial U / \partial \rho)_T$	12
$b_n$	$n = -\infty, \dots, 0, \dots, +\infty$ , Expansion coefficients	54
$B_1$	First Bernoulli number	53
C	Constant	33
c	velocity of light cm/sec.	85
$\bar{c}$	Real number, $0 < \bar{c} < 1$	54
$C_k$	Constant, (3.61).	
d	Symbol denoting increment in variable.	34
$D^+$	Deuterium ion.	19
$d\sigma = d\sigma'$	$d\sigma = 2\pi \sin\theta d\theta$ , element of solid angle radians.	67
$d\sigma(n)$	Probability of a collision in which an electron is scattered into a solid angle $d\sigma$ and the atom enters the $n^{\text{th}}$ excited state.	68
$d\tau$	$d\tau = dV_1 \dots dV_{Z_b}$ . Element of configuration space of $Z_b$ the $Z_b$ bound electrons in an atom, $\text{cm}^3 Z_b$ .	67
$d\bar{\tau}$	$d\bar{\tau}$ is an element of momentum space, $\text{erg} \cdot \text{sec}^{-1}$ .	24
$dE(\Omega)$	Mean energy loss of particle scattering into $d\sigma$ about $\Omega$ , erg.	67
$dE(q)$	Mean energy loss for all collisions in which momentum transfer does not exceed $q$ , erg.	72
$dE/dX$	Energy loss per unit path length, erg/cm	5
$\rho^{-1} (dE/dX)$	Energy deposition per gm for cross section of $1 \text{ cm}^2$ , $\text{ergs} \cdot \text{cm}^2 / \text{gm}$ .	5
$d^3p$	Volume element in momentum space, $\text{erg} \cdot \text{sec}^{-1}$ .	50
$d^4p$	Volume element in energy-momentum space, $\text{erg}^2 \cdot \text{sec}^{-1}$	49
dV	Element of Volume, $\text{cm}^3$	67
$d_x$	$d_x = e \int x_a$ Dipole moment of atomic electrons, esu.cm.	73
$(d_x)_{on}$	Matrix element of $d_x$ between energy states of atom.	72
$dw(n)$	Transition probability for scattering of particle from momentum $p_i$ to $p'$ when the atom undergoes a transition from the groundstate to the $n^{\text{th}}$ excited state	66

<u>Symbol</u>	<u>Description/Dimensions</u>	<u>Page</u>
$E$	Energy of ion, erg.	19
$\underline{E}(\underline{r}, t)$	Electric field vector, Volts/cm.	36
$\bar{E}_0$	$\bar{E}_0 = e^2/2\bar{a}_0$ , erg.	41
$E_{bi}$	Binding energy of ith electron, erg.	79
$E^{EX}$	Exchange energy, erg.	43
$E_F$	Fermi energy, erg.	43
$\underline{E}_k$	$k^{th}$ Fourier component of electric field, Volt.cm <sup>-1</sup> .	36
$E_0$	Energy of ground state of atom, erg	66
$E_n$	Energy of nth excited state of atom, erg	66
$ E(t)\rangle$	State with energy E at time t	46
$E^{TOT}$	Total energy per particle (electron), erg.	43
$e$	charge on electron, esu.	25
$F$	Free energy /atom, ergs.	33
$F_E$	Electron contribution to Free energy ergs.	33
$F_k$	Nuclear contribution to Free energy ergs.	33
$\bar{F}$	Distribution function in Boltzmann equation (non equilibrium) $\bar{F}(\underline{r}, \underline{v}, \underline{t})$	62
$\underline{F}$	Force Vector, dynes.	37
$f$	Arbitrary quantum mechanical operator	71
$f^+$	Operator adjoint to f.	71
$\dot{f}$	Time derivative of f.	71
$f_{on}$	Matrix element $\langle \sigma   f   n \rangle$ of f between atomic states.	71
$f_{p\sigma}$	Occupation probability of a state with momentum $\underline{p}$ and spin $\sigma$ for the Fermi Dirac model of an electron gas.	43
$f_{\underline{p}}^- \equiv f_{\underline{p}}$	Same as above, when probability is independent of spin	50
$f_{\underline{p}}^+$	$f_{\underline{p}}^+ = (1 - f_{\underline{p}}^-)$	50
$f(\epsilon), f(\epsilon_{\underline{p}})$	Same as for $f_{\underline{p}}$ but for state with energy $\epsilon_{\underline{p}}$ or $\epsilon$ .	53

<u>Symbol</u>	<u>Description/Dimensions</u>	<u>Page</u>
$f_1(u, \bar{z})$	Function (4.65)	51
$f_2(u, \bar{z})$	Function (4.66)	52
$f_0(\underline{v})$	Maxwell-Boltzmann distribution function.	61
$f_1(\underline{r}, \underline{v}, t)$	Non-equilibrium perturbation part of distribution function.	62
$g_0$	$g_0 = \pi^2 \bar{a}_0 / 16 m e^2 p_F^2$ , (4.82).	55
$G(\ )$	Function (6.8)	82
$G_E$	Gibb's Free energy, erg.	34
$h$	Planck's constant, erg.sec.	24
$\hbar$	$\hbar = h/2\pi$ , erg.sec.	37
$H$	Hamiltonian operator for interacting electron gas, ergs.	41
$H_{ext}$	Part of Hamiltonian describing the interaction between the external charge and the electron gas (4.32), ergs.	44
$H_{TOT}$	Total Hamiltonian, (4.36), ergs.	45
$I$	Bethe parameter, ergs.	73
$i$	$i = \sqrt{-1}$	
$k$	Boltzmann's constant ergs/K	24
$\underline{k}$	Wavevector, $cm^{-1}$ .	
$k$	$k =  \underline{k} $ Magnitude of wavevector, $cm^{-1}$ .	36
$K_e$	Electron thermal conductivity , $erg.cm^{-1}.sec^{-1}.K^{-1}$ .	12
$K_i$	Ion thermal conductivity, $erg.cm^{-1}.sec^{-1}.K^{-1}$ .	12
$K_R$	Radiation thermal conductivity , $erg.cm^{-1}.sec^{-1}.K^{-1}$ .	12
$k_c$	Cut-off wave vector (4.15), $cm^{-1}$ .	37
$K(T)$	Function (3.22)	27
$l$	Neutron mean free path in DT.cm.	19
$L$	Stopping number per target atom (4.121).	64
$L_0$	Stopping number/electron in a uniform, electron gas.	65
$l_f$	Defined in (6.9), cm.	82
$M$	Mass of ion, gm.	11
$m$	Mass of electron, gm.	24
$m_1$	Mass of ion which is slowing down, gm.	86
$m_2$	Mass of ion in plasma, gm.	86

<u>Symbol</u>	<u>Description/Dimensions</u>	<u>Page</u>
$m_p$	Proton mass, gm.	85
$m_{12}$	Reduced mass (6.2).	81
$M_a$	Mass of atom, gm.	75
$N_o$	Avagadro's number.	85
$\bar{N}$	Number of atoms/unit vol. $\text{cm}^{-3}$	77
$N_{on}$	Oscillator strength (5.36).	73
$N$	Total number of electrons in volume V.	24
$\bar{n}$	Density of nuclei in a plasma, $\text{cm}^{-3}$	23
$n$	Density of electrons, $\text{cm}^{-3}$	24
$n_E(r)$	Density of electrons as a function of radius in a quasiatom, $\text{cm}^{-3}$ .	25
$N_B$	Number of bound electrons in an atom.	78
$n(w)$	Number of bound electrons per unit frequency around frequency $w$ .	78
$P$	Total pressure. Dynes. $\text{cm}^{-2}$ .	12
$P_E$	Electron pressure, Dynes. $\text{cm}^{-2}$ .	32
$P_k$	Pressure of nuclei, Dynes. $\text{cm}^{-2}$ .	32
$p$	$p =  \underline{p} $ , magnitude of momentum $\text{erg}\cdot\text{sec}^{-1}$ .	32
$p$	Magnitude of Fermi momentum, $\text{erg}\cdot\text{sec}^{-1}$ .	41
$\underline{p}_F$	Fermi momentum vector, $\text{erg}\cdot\text{sec}^{-1}$ .	41
$\underline{p}_F$	Momentum vector, $\text{erg}\cdot\text{sec}^{-1}$ .	41
$\underline{p}'$	Momentum vector, $\text{erg}\cdot\text{sec}^{-1}$ .	41
$\underline{p}_i$	Momentum of particle $i$ , $\text{erg}\cdot\text{sec}^{-1}$ .	41
$P_o(q, w)$	Defined by (4.55).	49
$P(q, w) \equiv \bar{P}$	Polarization propagator.	48
$P_o^R(q, w)$	Defined in (4.59).	50
$\underline{p}_o$	Defined in (4.81).	55
$\underline{p}$	Impact parameter, cm.	81
$\underline{p}_o$	Impact parameter for a deflection angle of $\pi/2$ , cm.	81
$P_n$	Concentration of ions with $n$ electrons ionized.	80
$Px_a$	$x$ component of momentum of electron in an atom, $\text{erg}\cdot\text{sec}^{-1}$ .	73
$\underline{q}$	Momentum vector. Momentum transfer in scattering process, $\text{cm}^{-1}$ .	42 67

<u>Symbol</u>	<u>Description/Dimensions</u>	<u>Page</u>
$q$	$q =  q , \text{ cm}^{-1}$	
$q_{\min}$	Minimum value of $q$ (5.16), $\text{ cm}^{-1}$	69
$q_1$	Value of momentum, $\text{ cm}^{-1}$ .	72
$q_{\max}$	Minimum transfer of momentum, $\text{ cm}^{-1}$ .	72
$q_0$	Intermediate value of momentum, $\text{ cm}^{-1}$ .	72
$\underline{r}$	Position vector, cm.	36
$r$	$r =  \underline{r} $ , magnitude of $\underline{r}$ , cm.	25
$r_0$	radius of quasiautom, cm.	25
$r_s$	radius of sphere of volume $V/N$ measured in units of $\bar{a}_0$ (Bohr radius), cm.	41
$r_n$	$r_n^2 = a_n^2 + b_n^2$ , $n$ an integer.	54
$\underline{r}_a$	Position vector of electron in an atom, cm	68
$r_{\max}$	Radius at which electrons are free electrons, if they have enough energy to move beyond this radius, cm.	78
$s$	Complex variable	52
$\hat{S}$	$\hat{S}$ Matrix in scattering theory, (4.49).	47
$S$	Total entropy, erg/K.	12
$S_E$	Entropy of electrons, erg/K.	34
$S_k$	Entropy of nuclei, erg/K.	34
$R$	Distance ion has travelled, cm.	13
$R_0$	Range of ion in a material, cm.	13
$t$	time, sec	46
$T_H$	Temperature of hot electrons, K.	12
$T_e$	Electron temperature, K.	12
$T_i$	Ion temperature, K.	12
$T$	Temperature, K.	14
$T_f$	Temperature in plasma, K.	83
$T_R$	Radiation temperature, K.	12
$T^+$	Tritium ion.	19
$\hat{T}$	Time ordering operator	47
$T_f$	Plasma temperature, K.	83
$U_E$	Total electron energy, ergs.	24
$U_K$	Kinetic energy of nucleus, ergs.	30
$U_{E, \text{KIN}}$	Electron kinetic energy, ergs.	30
$U_{EK}$	Interaction energy of nuclei and electrons, ergs.	30
$U_{EE}$	Electron-electron interaction energy, ergs	30

<u>Symbol</u>	<u>Description/Dimensions</u>	<u>Page</u>
$U_{E,POT}$	Electron potential energy, erg.	31
$U_{KIN}$	Total kinetic energy, erg.	33
$U_{POT}$	Total potential energy, erg.	33
$u$	$u = w/qv_F (4.62)$ .	51
$\bar{u}$	Relative speed between a projectile ion and plasma electrons, cm.sec <sup>-1</sup> .	86
$U$	Internal energy, erg.	12
$U(\underline{r})$	Atomic potential, erg.	67
$v'_r$	$v'_r = v_r/c$ , cm.sec <sup>-1</sup> .	89
$V$	Volume, cm <sup>-3</sup> .	24
$v$	Particle velocity, cm.sec <sup>-1</sup> .	35
$v_o$	Average velocity of an atomic electron, cm.sec <sup>-1</sup> .	36
$\underline{v}$	Velocity vector, velocity of ion cm.sec <sup>-1</sup> .	36
$v_t$	Average electron thermal velocity cm.sec <sup>-1</sup> .	38
$V(\underline{x})$	Coulomb potential, erg.	42
$V(q)$	Fourier transform function of Coulomb potential, erg.	42
$V_i(\underline{r})$	Pair potential of an ion and an atom, erg.	65
$V(r)$	Thomas Fermi potential of an atom, erg.	79
$V_F$	Fermi velocity, cm.sec <sup>-1</sup> .	51
$V_r$	Relative velocity, cm.sec <sup>-1</sup> .	89
$w$	Frequency, sec <sup>-1</sup> .	36
$w_o$	Average revolution frequency of electrons, sec <sup>-1</sup> .	35
$w_q(\underline{p})$	$w_q(\underline{p}) = \epsilon_{p+q} - \epsilon_p$ , erg.	50
$w_{pl}$	Plasma frequency, sec <sup>-1</sup> .	58
$w(r)$	Revolution frequency of an atomic electron at radius $r$ in the Thomas-Fermi model, sec <sup>-1</sup> .	78
$w_l$	Velocity of light particle, cm.sec <sup>-1</sup> .	81
$w_i$	Revolution frequencies (classical) of electrons in the Bohr model of the atom, sec <sup>-1</sup> .	78
$x$	Position, $x =  \underline{x} $ , cm.	42
$\underline{x}$	Position vector, cm.	42

<u>Symbol</u>	<u>Description/Dimensions</u>	<u>Page</u>
$x_{ij}$	Distance between two electrons, cm.	41
$x_1$	$x_1 = \mu_1 + Y_1$	53
$x_2$	$x_2 = \mu_1 + Y_2$	53
$\bar{x}$	$\bar{x} = q/2p_F$	55
$x_a$	x coordinate of electron a in an atom, cm.	70
$Y(\zeta)$	Function defined by (3.26).	28
$Y_1, Y_2$	See eqn.(4.30) for definition.	53
$Y_i$	Defined in (7.2).	85
$\bar{Y}_1$	Defined by (7.8),	86
$Z$	Charge on nucleus of an atom, esu.	25
$Z_{eff}$	Effective charge of an ion moving through a plasma, esu.	11
$\bar{z}$	$\bar{z} = q/2p_F$ (4.62).	51
$\bar{z}$	Complex variable.	52
$z'$	$z' = kT/\epsilon_F$	53
$Z(\xi)$	Function defined by (4.105) to (4.107).	62
$Z_1$	Charge on moving ion, esu.	77
$Z_2$	Charge on ion in plasma, esu.	81
$Z_{free}$	Average number of free electrons per atom, esu.	80
$\bar{z}$	Degree of ionization, (Number of free electrons/atom).	80
$Z_B$	Equilibrium charge on ion in target material, esu.	9
$\bar{z}_b$	Number of bound electrons in an atom.	67

## References

1. E.Nardi, E.Peleg, and Z.Zinamon,  
"Energy deposition by fast protons in pellet fusion targets". Phys. Fluids 21, 574, (1978).
2. K.A.Long, N.A.Tahir,  
"Energy deposition of ions in materials and numerical simulations of compression, ignition, and burn of ion beam driven inertial confinement fusion pellets.  
KfK-3232, Kernforschungszentrum Karlsruhe (1981).
3. E.Nardi and Z.Zinamon,  
"Charge state and slowing down of fast ions in plasmas",  
Phys. Rev. Lett. 49, 1251 (1982)
4. D.Bailey, Y.T.Lee and R.M.More,  
"Ab initio calculations of the charge state of a fast heavy ion stopping in a finite temperature target",  
Proceedings of the Symposium on Accelerator Aspects of heavy ion fusion", Gesellschaft für Schwerionenforschung, Darmstadt Report, GSI-82-8, p571, (1982).
5. S. Chandrasekhar,  
"Principles of stellar dynamics";  
Dover, p251 (1960)
6. D.Pines  
"Elementary excitations", Benjamin, New York (1965)
7. R. Bangerter,  
"The beam-target interaction in heavy ion fusion",  
Proceedings of the heavy ion Workshop, Argonne, Sept. 1978,  
ANL-79-41, p415, (1979)
8. T.A.Mehlhorn,  
A finite temperature model for ion energy deposition in ion driven ICF targets",  
SAND80-0038, (1981)

9. T.A.Mehlhorn,  
"A finite material temperature model for ion energy deposition in ion driven inertial confinement fusion targets".  
J. Appl. Phys. 52, 6522, (1981)
10. J.Lindhard, M.Scharff, H.E. Schiøtt  
Notes on atomic collisions II: The ranges of heavy ions of low velocity  
Kgl. Danske, Videnskab. Selskab, Mat. Fys. Medd. 33, No.14, (1963).
11. R.M.More,  
"Materials at extreme conditions and ICF targets",  
UCRL-84115, Rev.1 (1980).
12. J.Lindhard,  
"On the properties of a gas of charged particles",  
Kgl. Danske., Videnskab. Selskab., Mat. Fys. Medd. 28, No.8, (1954).
13. J.J.Thompson,  
Conduction of electricity through gases, Cambridge University Press, Cambridge, England (1903)
14. See S.P.Ahlen,  
"Theoretical and experimental aspects of the energy loss of relativistic heavily ionizing particles",  
Rev. Mod. Phys. 52, 121 (1980)
15. N.Bohr,  
"The penetration of atomic particles through matter"  
Kgl. Danske, Videnskab. Selskab Mat. Fys. Medd. 18, No.8, (1948).
16. N.Bohr,  
"On the decrease of swiftly moving electrified particles in passing through matter",  
Phil. Mag. 30, 581, (1915)

17. H.A.Bethe,  
"Zur Theorie des Durchgangs schneller Korpuskularstrahlen durch Materie",  
Ann. der Physik (Leipzig) 5, 325, (1936).
18. H.A.Bethe,  
"Quantenmechanik der Ein- und Zwei-Elektronenprobleme",  
in Handbuch der Physik, Springer-Verlag, Vol 24, 273 (1933)
19. N.E.Mott,  
"On the theory of excitation by collision with heavy particles  
Proc. Cambridge Phil. Soc. 27, 553, (1931)
20. F. Bloch,  
"Zur Bremsung rasch bewegter Teilchen beim Durchgang durch Materie", Ann. der Physik, 16, 285, (1933).
21. E. Fermi,  
"The ionization loss of energy in gases and in condensed materials, Phys. Rev. 57, 485, (1940).
22. L.M.Landau and E.M.Lifshitz,  
"Quantum mechanics", Addison Wesley, Reading, Mass. U.S.A.  
(1960).
23. N.A.Tahir and K.A.Long,  
"Target design studies for a heavy ion-beam driven inertial confinement fusion reactor, Atomkernenergie-Kerntechnik 40,  
157, (1982)
24. R.Fröhlich, B.Goel, D.L.Henderson, W.Höbel, K.A.Long, N.A.Tahir,  
"Heavy ion beam driven inertial confinement fusion target studies and reactor chamber neutronic analysis",  
Nucl. Eng. and Design 73, 201, (1982)
25. B.Badger et al,  
"HIBALL - a conceptual ion beam driven fusion reactor study,  
Vols. 1+2 KfK-3202, and UWFDM-450 (1981).

26. Proceedings of the Symposium on Accelerator Aspects of Heavy Ion Fusion, held at Gesellschaft für Schwerionenforschung, Darmstadt, March/April 1982, Edited by D.Böhme, GSI-82-2, (1982).
27. N.A.Tahir and K.A.Long,  
"MEDUSA-KA,"  
KfK-3454 (1983)
28. M.J.Clauser,  
"Ion-Beam implosion of fusion targets," Phys. Rev. Lett. 35  
848 (1975)
29. M.D.Brown and C.D. Moak,  
"Stopping powers of some solids for 30-90 MeV  $^{238}\text{U}$  ions",  
Phys. Rev. B6, 90 (1972)
30. N.A.Tahir and K.A.Long,  
"The numerical simulation and theoretical analysis of the  
implosion, ignition and burn of heavy ion beam reactor-size  
ICF-targets",  
Nuclear Fusion 23, No.7, 887, (1983)
31. K.A.Long, N.Moritz and N.A.Tahir,  
"The dependence of energy deposition profiles and ranges  
of heavy ions on temperature in hot plasmas produced in  
ICF pellets",  
GSI annual report 1981, Studies on the feasibility of  
heavy ion beams for inertial fusion, GSI-82-6 p54,  
(1982)
32. K.A.Long, N.A.Tahir and N.Moritz,  
"The Energy loss of neutron induced knock-on  $\text{D}^+$  and  $\text{T}^+$   
Ions in DT plasmas and its effect on the burn of ICF  
pellets, GSI annual Report, 1982, GSI-83-2, p.54-56, (1983)
33. N.A.Tahir and K.A.Long,  
"Fusion Power from heavy ion beam imploded targets",  
Phys. Lett. 90A, 242, (1982).

34. K.A.Long, N.A.Tahir,  
"Heavy ion beam Fusion: The thermodynamics of ignition  
and the achievement of high gain in ICF targets  
Phys. Lett 91A, 451, (1982).
35. K.Breuckner and S. Jorna,  
"Laser Driven Fusion"  
Rev. Mod. Phys. 46, 325 (1974)
36. B.Goel and D.Henderson,  
"Neutron Fuel Interaction in a HIBALL target",  
GSI Report, GSI-82-8 (see Ref. 26) p626, (1982)  
and private communication.
37. K.M.Case, F. De Hoffmann, and G. Placzek,  
"Introduction to the theory of neutron diffusion,  
Vol 1., Los Alamos Report, (1953)
38. F.C.Young, D. Mosher, S.J. Stephanakis, and S.A. Goldstein,  
T.A.Mehlhorn,  
"Measurement of enhanced stopping of 1 MeV deuterons in  
target ablation plasmas,"  
Phys. Rev. Lett. 49, 549, (1982)
39. N.F.Mott,  
"Metal insulator transitions"  
Taylor and Francis, London 1974
40. W.Geiger, H.Hornberg, and K.H.Schramm,  
"Zustand der Materie unter sehr hohen Drücken und  
Temperaturen" Springer Tracts in Modern Physics Vol. 46,  
Springer Verlag Berlin, Ed. G. Höhler (1968).
41. D.A.Kirznits,  
"The limits of applicability of the quasi-classical equation  
of state of matter",  
Soviet Physics J.E.T.P. 35, 1081 (1959)

42. R. Latter,  
"Temperature behaviour of the Thomas-Fermi statistical  
model for atoms",  
Phys. Rev. 99, 1854, (1955)
43. L.M. Landau and E.M. Lifshitz,  
"Electrodynamics of continuous media",  
Addison Wesley, Reading, Mass. U.S.A. (1960)
44. S. Doniach and E.H. Sondheimer,  
"Green's functions for solid state physicists",  
Benjamin, New York, 1972
45. L.P. Kadanoff and G. Baym,  
"Quantum statistical mechanics",  
Benjamin, New York, (1962)
46. A.A. Abrikosov, L.P. Gorkov and L.E. Dzyaloshinskii,  
"Methods of quantum field theory in statistical physics",  
Prentice Hall, Englewood Cliffs. New Jersey, U.S.A., (1963)
47. J.R. Schrieffer,  
"Theory of superconductivity",  
Interscience, New York, 1965
48. D. Bohm and D. Pines,  
"A collective description of electron interactions III,  
Coulomb interactions in a degenerate electron gas"  
Phys. Rev. 92, 609, (1953)
49. M. Gell-Mann and K. Breuckner,  
"Correlation energy of an electron gas at high energy",  
Phys. Rev. 106, 364, (1957)

50. K.A.Long,  
"The many body theory of ferromagnetic resonance in metals and alloys",  
Thesis, Imperial College, University of London, (1971)
51. K.A.Long,  
"The evaluation of the wave number and frequency dependent susceptibility function at finite temperature",  
Harwell Report (U.K.A.E.A.) AERE/EMR/PR 2277 (2), (1974)
52. C.Goudard and C.Deutsch,  
"Dense electron gas response at any degeneracy",  
Journ. Math. Phys. 19, 32, (1978)
53. L.Spitzer,  
"Physics of fully ionized gases",  
Wiley, New York, 2nd Ed. (1962)
54. B.D.Fried and S.D.Conte,  
"The plasma dispersion function",  
Academic Press 1961.
55. J.A.Barker and D.Henderson,  
"What is Liquid? Understanding the states of matter",  
Rev. Mod. Phy. 43, 587, (1976)
56. G.Befeki,  
"Collective emission processes in unmagnetized plasmas",  
in Plasma physics, eds: C.DeWitt and J.Peyraud, Gordon and Breach, New York, p1, 1972
57. R.H.Ritchie,  
"Interaction of charged particles with a degenerate Fermi-Dirac electron gas",  
Phys. Rev. 114, 644, (1959).
58. K.A.Long, N.A.Tahir,  
"The importance of energy loss of ions in cold materials and hot dense plasmas for ICF pellet dynamics",  
GSI annual Report, 1982, GSI-83-2 p.57, (1983)